A. Pacifico

Manufacturing Laminate-Free PV Modules at Large Scale




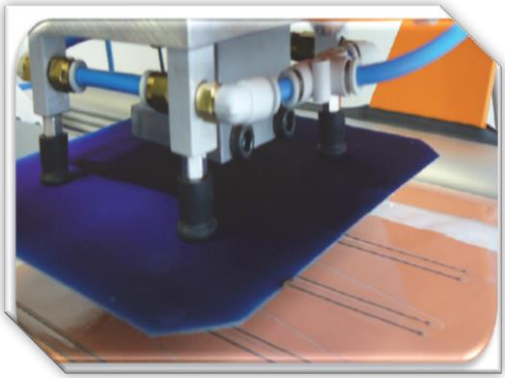


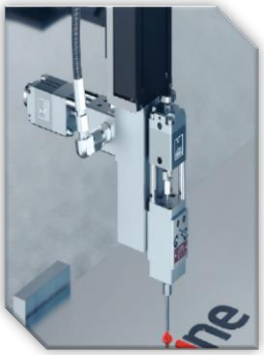



Manufacturing Laminate-Free PV Modules at Large Scale

By

Antonio Pacifico

in partial fulfillment of the requirements for the degree of

Master of Science
in Sustainable Energy of Technology

at the Delft University of Technology,
To be defended publicly on Thursday April 11, 2024 at 11:00 AM.

Thesis Supervisors :	Dr. P. Manganiello
	Prof. dr. A.R. Balkenende
Company Supervisor :	Siemen Brinksma
Project Duration :	May, 2023 – April, 2024
Student Number :	4935675
Faculty :	PVMD, TU Delft

An electronic version of this thesis is available at http://repository.tudelft.nl/

TU Delft Delft University of Technology

BIOSPHERE SOLAR

PVMD Delft University of Technology

Abstract

As photovoltaic (PV) technology enters the terawatt era, reliability, sustainability, and circularity in the solar industry can no longer be optional considerations for manufacturing solar modules. Particularly with increasing resource scarcity, ensuring a sustainable provision of solar energy technology is imperative. However, despite two decades of intense solar manufacturing, the PV industry still predominantly operates within a linear economic structure, characterized by energy-intensive production and limited sustainability practices. One significant challenge associated with crystalline PV modules is the encapsulation process, which occurs within costly and unwieldy laminator machines. While laminating PV modules offers long-term stability and performance, it also imposes significant limitations on disassembly, repairability, and recyclability of valuable materials and components within the module, hindering the closure of loops and extension of product lifespan. The development of sustainable PV designs and manufacturing processes is crucial for transitioning to a circular economy.

In response to this problem, Biosphere Solar, a startup company based in Delft, is actively dedicated to developing a novel solar module design that eliminates the need for lamination. Their research and objectives focus on creating an easy disassembly of solar modules to facilitate subsequent repair and reuse, ultimately achieving fully recyclable PV modules with low-energy input and costs. It is crucial to recognize that transitioning to non-laminated solar modules presents challenges in manufacturing within this new PV module design landscape.

This thesis aims to identify and address barriers encountered in manufacturing laminate-free PV modules. The comparison is made with traditional laminated PV modules, examining two different scales: semi-automated and highly automated production lines. Through both academic and commercial sources, a preliminary literature study was conducted on laminated solar products and their manufacturing processes. Both conventional and innovative assembly methods, such as those based on conductive backsheet technology, were studied. Acquaintance with conventional manufacturing lines provided valuable insights into the challenges and advantages of producing non-laminated PV modules. Subsequently, the focus shifted towards acquiring a thorough understanding and evaluation of a specific module design utilizing back-contact solar cells and conductive backsheet technology, drawing upon insights from Biosphere Solar's approach. The product analysis primarily examines module components, specifications, and materials diverging from classic laminated panels, such as adhesive glue, solder pastes, fluid agents, and edge sealants, assessing their trade-offs and configurations in terms of manufacturability. The analysis of these novel concepts has facilitated the definition of a manufacturing process flow, which is constructed and described based on assembly operations that both align with and diverge from standard PV manufacturing practices. This is complemented by an exploration of adapted and specialized methods for each processing equipment, considering the associated boundary conditions in the assembly process. The main challenges encountered are related to metal paste dispensing, low-temperature soldering, and fluid filling processes, which require multiple units installed in the production line and necessitate specific design and development tailored to this application. The latter, never previously explored at the production scale, is considered non-standard within the solar industry.

Technical results reveal a competitive and positive edge across two different scales of laminate PV lines, particularly evident in larger-scale operations. In the best-case scenario, these have yielded up to a 30% reduction in electrical and air consumption for machinery and up to 50% reduction in required factory floor space. This efficiency stems from the compact work area of the machines and their lower power usage, attributable to the absence of large laminators. Indeed, the electrical consumption of the laminator(s) alone, for production volumes up to 300 [MW] per year, can range between 20% and 50%, with a footprint share up to 10% of the total manufacturing space.

Economically, capital costs also demonstrate promise and have the potential to outperform laminated PV modules, especially in the highly automated setup line. In the best-case scenario, savings between 20-30% for equipment costs and up to 50% for building infrastructure costs are achievable. Nevertheless, the main factors offsetting these mitigated capital costs are the operational expenses associated with the bill of materials and the manpower required to produce this specific laminate-free PV product. In the worst-case scenario, these material expenses can be up to 4-5 times higher than for a standard laminated panel, while up to twice the investment in direct manufacturing labour may be required. This assessment lays the foundation for future research on product-process development and testing, leveraging the trade-offs explored to refine choices and achieve optimal results.

Contents

List of Figures

List of Tables

Acronyms

ABA	acrylonitrile styrene acrylate
ABS	acrylonitrile butadiene styrene
ARC	anti-reflective coating
Ag	silver
Al	aluminium
ASC	anti-soiling coating
IV	current voltage
Bi	bismuth
BB	bus bar
BIPV	building integrated photovoltaic
CTM	cell-to-module
Cu	copper
EL	electroluminescence
EVA	ethylene vinyl acetate
RQ	Research question
Bi	bismuth
Sn	tin
Cu	copper
Ag	silver
Si	silicon
Al	aluminium
PC	polycarbonate
Sn	tin
N_2	nitrogen
SiO_2	silicon dioxide
UV	ultraviolet
TPT	tedlar polyester tedlar
IBC	interdigitated back-contact
LID	light induced degradation
MWT	metal wrap through
ECA	electrically conductive adhesive
PCB	printable circuit board
LTSP	low temperature solder paste
Low-T	low temperature
High-T	high temperature
RPI	rear perforated insulator
P&P	pick & place
PERC	passivated emitter rear contact
TOPcon	tunnel oxide passivated contacts
HJT	heterojunction
MPPT	maximum power point tracker
R&D	research & development
CapEx	capital expenditure
OpEx	operational expenditure
PV	photovoltaic
RRR	repair, refurbish, reuse
CB	conductive backsheet
IGU	insulated glass unit
BoS	balance of system
BoM	bill of material
IG	insulated glass
SA	semi-automated
HA	highly automated
L-	laminated
L-F	laminate-free
STC	standard test condition
G/G	glass-glass
G/B	glass-backsheet
PIB	poly-isobutylene
BC	back-contact
FBC	front-back contact
JB	junction box
TPS	thermoplastic spacers
EoL	end-of-life
Pb	lead
USD	US dollar
c-Si	crystalline silicon
SC	solar cell
PID	potential induced degradation
TCO	total cost of operation
MC	multi-contact
CAGR	compound annual growth rate
IR	infra-red
LED	light emitted diode
NICE	new industrial cell encapsulation
CSP	concentrated solar power
IMC	intermetallic compound formation
SMT	surface mount technology
CPA	compressed dry air
PLC	programmable logic controller
CCD	charged-coupled device
PET	Polyethylene terephthalate

1

Introduction

The introduction chapter of this master's thesis research comprises four sections. Sections 1.1 and Section 1.2 provide an overview of the relevance and introduction of the current context of laminated PV modules, along with its related problem statements and unanswered gaps. Following this, Section 1.3 introduces Biosphere Solar startup company, its purpose, and the innovative solar module structure without lamination. Finally, Section 1.4 discusses the research objectives of this thesis project, including the research questions.

1.1 Global PV Waste and a Linear Model in the Solar Industry

The solar PV industry, particularly over this last decade, is experiencing drastic growth in PV modules installed worldwide, and it is expected to keep expanding [1]. As the PV installation capacity continues to increase, the volume of end-of-life (EoL) modules is also expected to grow, reaching a million-ton scale by 2030, with more than 80% being crystalline silicon (c-Si) modules. The associated PV wastage of decommissioned panels, after their end-of service-life, may also rise. If these materials could be properly or highly recycled, two billion new modules (equivalent to 630-GW capacity) can be manufactured using recycled materials [110] [111]. In a linear economy, raw materials are processed into a specific product, which is then manufactured, used, and ultimately, (most of them) discarded [5].

The development of PV recycling to recover as many materials as possible is already taking place among producers. The bottleneck in recycling is no longer the low yield of a single material but the need to consistently improve the cost-efficacy of the value-recovered process. *Veolia*, a French company, uses a fully automated recycling process, achieving more than 95% overall mass recovery yield [2]. However, the small volumes treated, along with no proper ways to separate recycling materials, make the process considerably expensive, requiring high-energy inputs. Recycled materials should be cheaper than the primary raw materials and considering the current high-energy intensive processes for recovery, this can hardly be achieved at the present time. The recycling processes can achieve high mass recovery, thus reducing the payload in landfills, but may fail to preserve valuable high-quality materials within this economy [2]. The contribution to the panel materials' weight is inversely related to the overall value of the solar panel. For instance, while glass sheets form 75% of the panel weight, they contribute to only approximately 8% of the economic value for the panel (see Figure 1.0) [3].

Figure 1.0 - Material distribution in c-Si solar panels according to weight (**left**) and economic value (**right**). Note that the weight of silver (0,005%) and lead (0,1%) amounts, on the left chart, are so minimal that they are only slightly visible in the graph. Similarly, the economic value of the lead (Pb) and ethylene vinyl acetate (EVA) (encapsulant material of traditional PV modules), on the right chart, was neglected as Pb is only used in minimal amounts and the economic value of the EVA is negligible [3].

EVA also represents a large share of the panel weight (8%). The polymer is demolished during the process of silicon cell separation from the encapsulant, making its recovery extremely difficult. Materials for solar cells and their interconnections, such as copper, silver, silicon (Cu, Ag, Si) are the most valuable within the panel, owning a relatively small amount in weight but requiring complex extractions [3]. In particular, Ag, which is one of the most precious module materials with an estimated market value of approximately $15/troy oz[1]. Full recovery of Ag from

[1] [1] 1 troy oz equals to 31,1 grams

the panel would be attractive since Ag feedstock neither would be purchased nor mined [3]. Moreover, Cu contributes to weight for less than 1% but makes up 8% of the material's economic value. Since Cu usage is forecasted to be the prevailing material for interconnections within solar panels in 2029, a recovery plan should be ensured [3]. On the other hand, lead-free soldered solar cells are predicted to take over and make a large share in the solar market [3].

In 2020, a cost indication of recycling a 1-ton panel was between $600 to $1000 [USD] [2]. Recycling is likely to be economically affordable after reducing the processing costs [2]. Therefore, the recycling processes must be optimized and combined on a large scale and maintained at the highest quality possible [3]. The module recycling can be split into four stages: disassembly, delamination, material sorting, and material extraction. Delamination, the separation of clean materials from the encapsulant (generally EVA), is the key barrier and the most challenging stage due to its process complexity, contamination, and cost [2].

Where there is not yet a commercial scale for PV recycling, the repair, refurbish, and reuse (RRR) schemes hardly exist in the solar market today. Reuse is not an economically feasible option as the panels, when approaching their EoL, lose (some of) their initial quality and efficiency. This is emphasized with the latest module technologies due to their strong increased yield. Hence, the increased efficiency on a product level (lower content of materials for similar performance) can make recycling unappealing and would lead to increased waste and resource loss [3]. Yet, reused modules will inevitably have to cope with their EoL and be recycled after the "n-life" of infield operation. This is mainly due to the organic components, such as polymer encapsulants and backsheet, suffering relatively much for degradation over time. Besides, inorganic parts (e.g. glass, frames) are more robust and usually preserve their good performance longer [3].

As already argued, the very small and relatively fragmented market volumes, with a lack of interest in finding adequate schemes, explain the significant gaps in knowledge and technology related to segments of PV recycling, repair, and second-life PV reliability testing [1]. Materials of the panel cannot be recovered in high-quality value due to the intrinsic limitation of recycling, primarily caused by the delamination issues during the manufacturing process with laminators, leading to waste taking place nonetheless [3].

1.2 The Role of Lamination in Traditional PV Manufacturing Plants

Standard, laminated solar module manufacturing, where solar cells are enclosed between encapsulant foils, is an efficient method for assembling panels due to the minimal amount of required encapsulant material and backsheet, alongside the relatively low cost of glass. The lamination process enhances the optical efficiency of the panel, optimizing electrical connections, panel efficiency, and cost-effective components. However, lamination is a lengthy and highly energy-demanding process, which slows down production line productivity. Additionally, laminator machines occupy a considerable amount of space in production lines, contributing to a large footprint. In terms of economic impact, the operational costs of the laminator(s), along with the significant amount of electrical energy consumed, dominate module manufacturing costs, especially when not considering the PV module's bill of materials (BoM). The high investment cost to purchase a laminator is one of the limiting factors for solar manufacturers, alongside other assembly equipment costs, which can discourage entry into the solar market (Expert Input: *member of Valoe)*.

Laminated (L-) solar modules using c-Si solar cells are the predominant technology used today constituting 95% of cells manufactured worldwide [4]. The modules are designed for rigidity and prolonged exposure to environmental changes, maintaining high initial performance over time. While laminating PV modules offers long-term stability and performance, it poses strong limitations for RRR schemes and full recyclability of high-value components unless a significant amount of energy is expended during recycling to achieve (partial) recovery. Therefore, not only is manufacturing modules energy-intensive, but the process of retrieving a high volume and quality of materials can be even more energy-intensive, particularly considering the degraded performance of components after extended infield operation life. This significantly increases the total cost over the "linear" life of the panel.

Producers should consider RRR options during the design and manufacturing phases to delay reaching EoL and recycling [3]. In the future, if material reserves decrease while resource demand rises, the prices of virgin raw materials will increase, consequently raising the value of recycled material even further [3].

As a result, the solar industry should actively explore sustainable markets that can utilize recycled module materials and enhance recovery/recycling at high values to meet quality requirements at reasonable costs for generations to come. It is crucial to adjust the design of solar panels and manufacturing processes to make this

switch and to ensure repairability, reuse, and eventual recycling [3]. The solar industry should develop innovative PV module designs that simplify disassembly, avoid high costs incurred for recovery/recycling, and eliminate the need for a laminator in manufacturing lines. In other words, a different and thoughtful PV module architecture is necessary if future generations want to have high quality for the recyclability and extended 'second' life of future solar panels.

These measures could inspire the industry to alter panel structures and designs to reflect a holistic view of the product life cycle. The primary goal for the next decade should focus on developing recycling design schemes and manufacturing processes to treat products as a service, which are not only economically but also environmentally beneficial. Abandoning this (linear) model and transitioning to a circular economy within the solar industry would be a significant step toward more sustainable energy production.

1.3 Biosphere Solar Mission and the Manufacturing of Laminate-Free PV Modules: A Circular Purpose

To encourage the production of panels that can be easily repaired and reintroduced into the market, the PV industry should explore the concept of "product as a service" prioritizing highly valued extraction of components for RRR and, as a last resort, for recycling, to close the circular loop [3]. One solution is to adopt a different structural design for the module, eliminating the need for polymer encapsulants, namely, a laminate-free solar module.

Founded in 2020 by a group of TU Delft students, Biosphere Solar, a Dutch startup company, has a mission to promote a commitment to circularity within the PV market and industry. Biosphere Solar's focus is on researching and developing a novel solar module design without lamination. Its strategy involves designing solar panels to be easily disassembled and to facilitate subsequent repair and refurbishment. Aligned with the circular economy standard of retaining products and materials at the highest value-added chain, recycling should be considered the ultimate option. If the panel reaches this stage, Biosphere Solar aims to obtain fully recyclable PV modules with low-energy input and costs.

To avoid lamination, Biosphere Solar's PV modules feature a Laminate-Free (L-F) core structure consisting of a rigid panel in a double glass configuration with an inner frame structure to host and support the solar cells. Their prototypes utilize various types of solar cells, with the most recent PV module design incorporating back-contacted (BC) cell modules and conductive backsheet technology. Further details regarding the solar cell types and PV module version designs are provided in Chapter 4.

Two one-dosing components act as edge sealants with included desiccants to protect internal components and reduce module degradation. Optionally, the interspace volume is filled with a fluid agent to enhance optical continuity and provide active/passive cooling. A schematic of a conventional laminate PV module and Biosphere Solar's L-F module is provided in Figure 1.1.

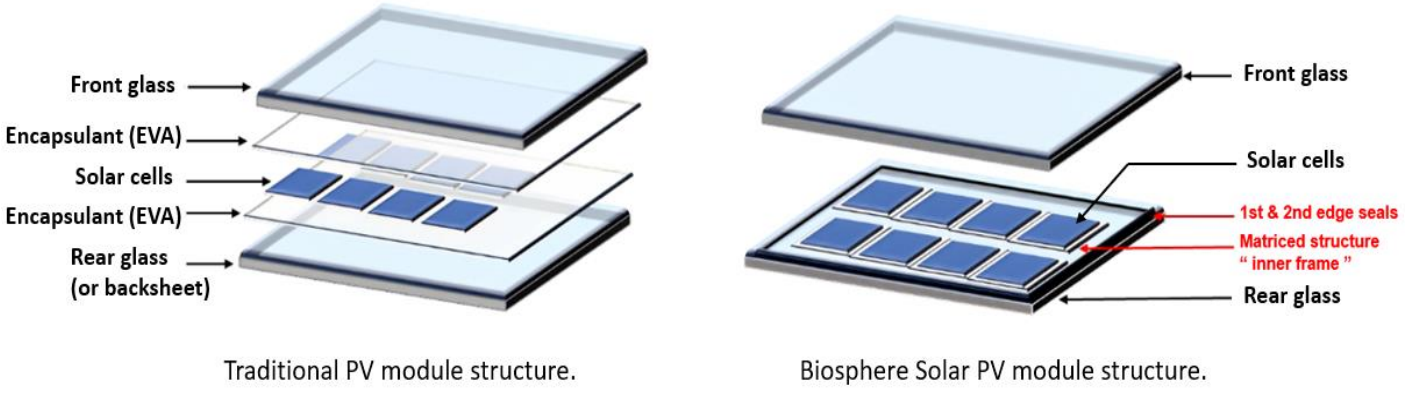

Figure 1.1 - (**left**) Conventional laminate PV module stack and (**right**) laminate-free, glass/glass (G/G) module of Biosphere Solar.

Without lamination involved, this design favours module recovery and recycling and is likely to reduce energy consumption and production costs in manufacturing. As shown later in this report, for production volumes up to 300 [MW] per year, the laminator can utilize between 20% to 50% of the total energy consumed by assembly

equipment and occupies a working space of less than 10%. Economically, its cost share constitutes up to 20% of the total production line investment for equipment, making it a significant portion of initial capital expenditure.

The L-F design enables non-destructive dismantling through RRR, making recycling highly beneficial for material recovery and replacement. As PV technologies continue improving, and the primary resources continue diminishing, RRR and recycling is no longer just an option for PV modules considered waste today. However, the innovative PV module design of Biosphere Solar is likely to encounter gaps and complexities before it can become standardized in the solar industry, especially compared to the already mature technologies of traditional laminated panels. These gaps are expected not only at the product level but also at the process level. If the L-F products have been scarcely investigated before, with only two other L-F product designs developed in the past, as will be introduced in Chapter 4, research on their manufacturing processes does not even exist.

1.4 Thesis Objective and Research Questions

The aim of this thesis project is to identify and address the gaps in the manufacturing of L-F PV modules, especially during the transition from the current prototyping stage to large-scale production. To evaluate these challenges, a comparative analysis is conducted with respect to traditional and mature laminated PV manufacturing lines, to identify potential benefits and drawbacks. To accomplish this goal, the scope and objectives are proposed, along with the following Research Questions (RQ):

1. *What are the barriers encountered in the manufacturing of L-F modules using BC solar cell technology?*
2. *How can these challenges be effectively addressed and what trade-offs exist in both product architecture and manufacturing processes?*
3. *What are the technical as well as economic implications of manufacturing of L-F modules at large-scale in comparison with the conventional laminated PV modules' production lines?*

Given that this study represents the first exploration of manufacturing L-F PV modules of this type, and considering the limited existing literature on the topic, the thesis primarily relies on in-depth desk research, guidance from supervisors, and expert interviews with industrial professionals and PV manufacturers. These interactions are crucial for gathering feedback and insights in the absence of extensive prior research.

2

Literature on Laminated PV Modules

In this chapter, theoretical concepts inherent to laminated PV modules are discussed. The chapter begins by explaining the structure and main components of traditional laminated modules, followed by a roadmap up to the latest solar cells, trends in design formats, and the newest interconnection techniques.

2.1 Conventional, Laminated PV Modules: Layers and Structure

Conventional solar modules are made from high-temperature vacuum-packed solar cells "sandwiched" between thin layers of valuable materials, usually EVA, encapsulated within glass and backsheet (or in a two-glass configuration) to form a monolithic structure. The thin layer made up of solar cells and metal interconnecting materials accounts for approximately 5% of the module's weight but more than half of the value [2]. The solar cell substrate is a highly pure Si wafer (4.4% weight), Ag (0.03% weight) and Al (0.3% weight)) are screen-printed on the cell surface to make electrical contacts. The interconnection materials are mainly composed of Cu (0.8% w), coated by tin (Sn) (0.1% weight), and Pb (0.01% w) [2].

The encapsulated cells are further protected by a highly transparent glass plate at the front side that is resistant to weathering, abrasion, and other physical stresses. The rear protective layer is called a backsheet in a glass/backsheet (G/B) construction configuration. Alternatively, a second glass can be employed in a glass/glass (G/G) or double glass configuration. These, whether to use a backsheet or a second glass plate, act as two pieces of "bread" to prevent physical damage and deterioration to the solar cells and other internal entities during its long life in-field operations [6].

The encapsulated sandwich is usually edged by a self-supporting Al frame (16% w) [2], to protect its internal components from thermal and mechanical tension. It also allows for easy carrying, installation, and maximum safety over time. The frames of the four rails protect PV cells against tough working conditions, guaranteeing a long service life of the panel. Alternatively, a frameless version is available. A single junction box is generally positioned on the rear of the panel to house and protect the electrical connectors, cables, and carry the electrical power to other PV modules or to the outer system.

Different architectures have emerged over the years in standard module design. Nowadays, more and more solutions are available on the market, but the main parts, components, and processes used for manufacturing PV modules have largely remained unchanged [7]. A standardized, laminated solar module, depending on the required power output, is formed between 60 and 72 solar cells, unless customized solutions are applied, with an average efficiency exceeding 15% [7]. An illustration of a standard 60-cell module design is presented in Figure 2.0.

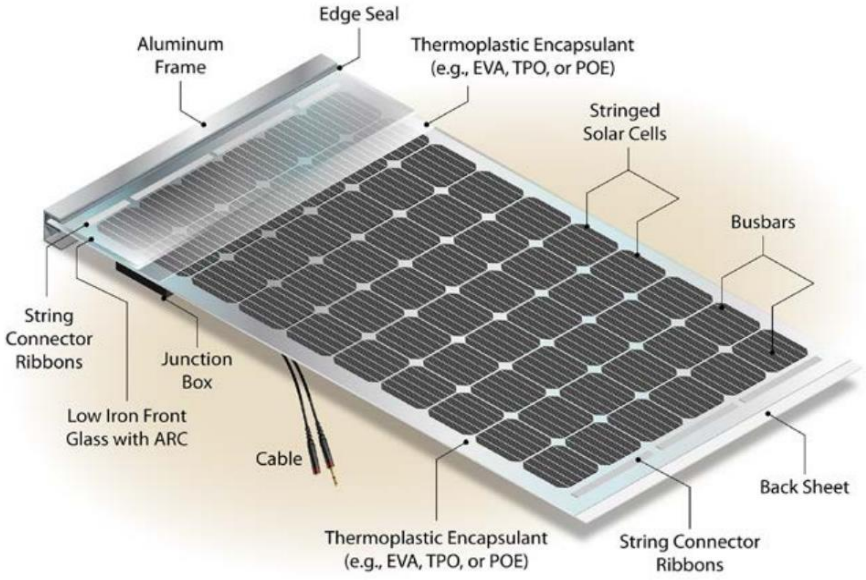

Figure 2.0 - A standard 60-cell silicon module assembly [6]
JB = junction box, **ARC** = anti-reflective coating, **EVA** = ethylene vinyl acetate, **TPO** = thermoplastic polyolefin, **POE** = polyolefin encapsulant

The main components forming the modules are now explained.

SOLAR CELLS: PV cells, composed of semiconductor materials, serve as the core component of the module. These cells capture sunlight and convert it directly into electrical energy through a photoelectric or photochemical effect. This process involves exciting electron-hole pairs within the lattice material, leading to the generation of current. Metal structures are applied to both sides of the cell to facilitate the lateral draining of current for interconnection with neighbouring cells. The current is then transported laterally via fingers to busbars (BBs), resulting in an instantaneous cell voltage and current output when exposed to light. [8].

The predominant type of solar panels currently produced utilizes crystalline silicon (c-Si) cells, which constitute 95% of cells manufactured worldwide in the PV industry [4]. C-Si cells can be either monocrystalline (mono-Si) or polycrystalline (poly-Si), based on their manufacturing process, although this distinction does not significantly impact the PV module production process. Key technical features of solar cells include size, colour, number of BBs, and, most importantly, conversion efficiency, which directly affects the power output of the module [8].

Solar cells made of silicon, commonly referred to as conventional or traditional cells, have been in use since the 1950s and remain the most prevalent type of cells today. Traditional solar cells typically have a wafer thickness ranging from 160 to 190 micrometres (μm). Depending on the type of solar cell employed, the PV module can be either mono-facial or bi-facial, with the latter capable of producing electricity from both the front and back sides of the cell.

GLASS & BACKSHEET: Glass, characterized by its brittle, fragile, ultra-transparent, and colourless structure, is an amorphous non-crystalline material formed by solidifying molten silica (silicon dioxide) along with other chemical compounds such as soda (sodium oxide) and lime (calcium oxide). Incorporating certain inorganic agents during the manufacturing process can enhance its structural integrity, strength, and durability. In most cases, the desirable attributes of glass include aesthetic value, transparency, electrical insulation, rigidity, and its ability to seal out environmental agents. Moreover, its non-reactive nature with most chemicals in the environment makes it an excellent and irreplaceable component of solar panels [9]. The main features of glass sheets used in the solar industry include clear glass made from low-iron content raw materials, Anti-Reflective Coating (ARC) for higher light transmission resulting in a 3% performance boost [10], and Anti-Soiling Coating (ASC). Additionally, Antimony-Free glasses are used for high-value recycling purposes [11].

As previously explained, laminated solar modules can be assembled in a G/B or G/G configuratios. In single glass modules, the front glass plate, typically with a standard thickness of 2 to 4 [mm] [8], serves to protect cells and panels against physical stress and harsh weather conditions, ensuring robustness of the entire structure while maintaining high transparency to allow maximum sunlight transmission. The transmission of sunlight is closely

related to the various interfaces present, which can cause reflection losses. Without ARC, the reflection losses per interface may be higher, thus limiting the efficiency of sunlight capture.

The standard sizes available in the market are 2.25 [m] x 3 [m] and 1 [m]x 2 [m]. The most used standard thickness of the glass is 3.2 [mm] [11]. In a G/B configuration, the backside is typically protected by an opaque layer called backsheet. Made of plastic, its function is to insulate electricity, provide mechanical protection, and shield PV cells from weather and moisture. Generally available in white and sold in rolls or sheets, backsheets vary in thickness, colour, and shielding strength, depending on the materials used [8]. Typical backsheet compounds include tedlar polyester tedlar (**TPT**), polyvinyl fluoride (**PVF**), and polyethylene terephthalate (**PET**).

Recently, the tendency to install glass covers on both sides of a PV module has become a trend. It must be noted that G/G panels are not necessarily bi-facial panels. Benefits and drawbacks of G/G module are highlighted in Table 2.0.

Table 2.0 - Key benefits/drawbacks for G/G solar modules [12], [9], [13].

BENEFITS	DRAWBACKS
Ageing protection: Air, corrosive agents (ammonia, salts), and moisture withstanding. It offers a good cell protection.	***Ageing for cell metallization:*** the glass can trap decomposition products (e.g. acetic acid) from the encapsulant materials, accelerating the rate of ageing
Higher performance through better self-cleaning.	***Significant weight increased:*** the risk of breakage is also higher.
More translucent.	**Additional cost increase.**
Higher safety: *N*on-dripping and passage of fire. No risk of electric shock during installation.	***Non appropriate match with EVA:*** this encapsulant type, in G/G modules can cause degassing, corrosion, and discoloration issues.
Aesthetics and versatile: It can be integrated invisibly into roofs, and building facades and enable control of light transmission and shadowing.	***Risk of higher power loss:*** *this is due to a possible higher module operating temperature due to the additional light absorption from the back side (thermomechanical fatigue of the interconnections).*
Large installed base in industry: a large base of Insulated Glass (IG) industry worldwide.	***Delamination:*** *higher risk due to a higher adhesion loss versus G/Bs.*
Longevity: that is due to the much slower spillage than G/B panels. Its longevity allows clients to run a long-term investment and a stable business plan.	

ENCAPSULANT MATERIAL: One of the most essential materials for assembling a laminated solar panel is the encapsulant. Acting as a binder between the layers forming the solar module and providing structural support, encapsulation offers high transmission, maximum light coupling with cells, mechanical and moisture protection, as well as electrical insulation [14], [8]. The most common material used in conventional panels is EVA, a thermoplastic copolymer resin. Combined with special additives for cross-linking, EVA is heated, thoroughly mixed, extruded, and formed into rolls for storage and packing. Its thickness typically ranges from 0.2 to 0.8 [mm] [15]. This translucent polymer is cut into sheets and deposited between the (front) glass and solar cell, as well as between the backsheet/back glass and cells of the module. This operation is usually performed on manufacturing lines with a cut & place machine. Under the thermal process of vacuum cooking, this polymer becomes similar to a transparent gel housing the PV cells. The quality of the encapsulant can affect light transmission and resistance to yellowing due to ultra-violet (UV) rays [8].

With increasing demand in the solar market and iterative technology, PV encapsulation films are derived from materials with various features to meet different usage needs. Classification methods for PV encapsulation films include colour, structure, pattern, material, process, and cross-linking method. This includes materials such as **EVA**, polyolefin elastomer (**POE**), polyvinyl butral (**PVB**), polyethylene foam film (**EPE**), as well as transparent, white, single-layer, and multi-layer adhesive and casting films [14].

After years of practice, EVA encapsulant has proven to be the most cost-effective, easy to handle, and with the lowest operating costs, guaranteeing long-life PV panels [15].

FRAMES: The entire panel structure, whether in the traditional G/B or newer G/G configuration, is supported by a framework structure that provides additional strength. PV module frames serve to protect the edges of the laminate section containing the solar cells. Typically made of aluminium, these frames ensure robustness and

provide a practical and secure coupling to the solar panel. They are usually around 45 [mm] in height [7]. Along with the frame, a layer of sealant is dispensed on the panel edges to serve as a moisture barrier. Silicone is commonly used for this purpose, although sometimes a special sealing tape may be applied. Special plastic material solutions are also available for specific applications [8].

JUNCTION BOX: A junction box (JB) is an enclosure serving as the interface of a solar module, channeling the power generated by the module externally. One function of the JB is to combine all the sub-strings of the module and connect the bypass diode(s). A standard JB consists of conducting strips from busbar wires, connected by bypass diodes and direct current (DC) polarities. Typically, the single-piece box is attached to the rear middle-side of the backsheet or rear glass plate, either soldered or using a sealant glue, usually silicone gel. The end interconnection of the JB utilizes multi-contact (MC4) connectors to electrically connect solar modules, with cable lengths typically above 1 [m] [118]. Module sub-strings are connected to the JB either through the wet soldering process or by a clamping mechanism. It is crucial to identify and specify these two interconnection methods, particularly for assembly, as the manufacturing scheme may change accordingly, with the use of specific assembly tools or automation modes.

New JB designs are emerging, some incorporating special low-loss or integrated microinverter diodes [8]. Depending on the application, location, structure of the panel, and whether to follow a standardized approach or not, JB assembly can be positioned either at the back of the panel in the middle/bottom position or along the tail edge. Changes in JB design and placement have arisen with the proliferation of bifacial module manufacturing. These newer JB designs are shallower and smaller, aimed at minimizing shading on the module's rear. Furthermore, they enhance heat dissipation and minimize cable length [13].

2.2 From Traditional to Cutting-Edge Solar Cells and Interconnection Methods

This section provides a brief outline of trends in solar cell and module format evolution, as well as the two different interconnection types for PV cells. Our focus is on back metallization contact cells, along with the state-of-the-art cell module interconnection techniques.

2.2.1 Trend in Design Formats for Solar Cells and Modules

The demand for mono c-Si wafers has seen exponential growth over the past two decades, driven by the increased production and sale of PV systems, smartphones, and other electronic devices. The increase in wafer size allows manufacturers to produce more semiconductor material from a single wafer, thereby enhancing productivity and efficiency. Manufacturers have adopted larger cell formats to reduce production costs and increase yield. For instance, small cells measuring 16.6 x 16.6 [cm^2] (M6) are being replaced by larger full square wafers, such as those measuring 18.2 x 18.2 [cm^2] (M10) and 21.0 x 21.0 [cm^2] (G12) [112]. An overview of cell formats is presented in Figure 2.1.

	Unit [mm]
M0	156 x 156
M2	156.75 x 156.75
G1	158.75 x 158.75
M4	161.7 x 161.7
M6	166 x 166
M10	182 x 182 or 200 x 200
M12	210 x 210

Figure 2.1 - (**left**) drawing and metrics of a standard full format cell of standardized M2 wafer, (**right**) full-cut solar cell sizes; (Adjusted from *CETC Solarenergy*).

The current and upcoming generations of standardized cell formats will revolve around full, half, and third-cut sizes M6, M10, G12, and even larger (Figure 2.2 **(right)**). Other options, such as 1/4 and 1/6 cell formats, may be considered as customized. Similarly, standard panel sizes for residential and utility scales are 2.3 [m] x 1.4 [m] and 2.5 [m] x 1.4 [m], respectively [16].

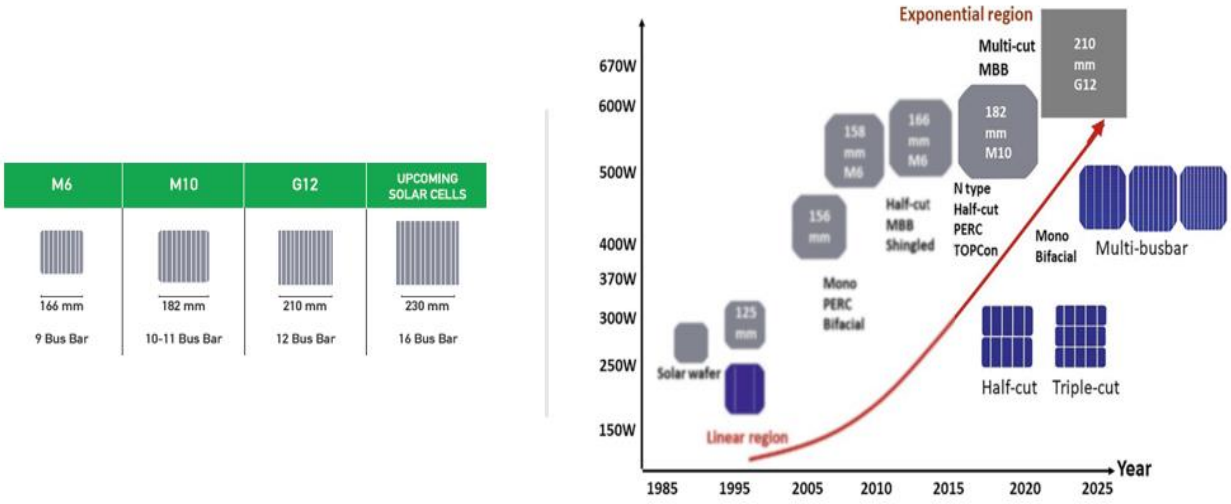

Figure 2.2 - (**left**) Most standardized solar cell formats and number of Bus Bars [16], (**right**) the evolvement of solar cell formats with modules' power outputs [17].

Half-cut cell modules are constructed from conventional cells that are cut in half. This approach reduces the electrical current running in each BB of the cell by half, thereby decreasing resistive power losses and boosting the power output of the module. Consequently, the amount of internal loss for the half-cut module is only a quarter compared to a full-sized cell module [7]. However, achieving this power boost comes at the expense of lower equipment throughput in manufacturing, as twice as many cells must be handled and strung together to make an equivalent-size module. Despite these changes, the basic materials and assembly processes remain largely unchanged [7].

Currently, the main effort in cost reduction is focused on metallization costs. There is potential for reducing the cell metal conductive agents, Ag-, Al-, or Cu-based per cell by increasing the number of busbars per polarity, such as the multi-busbar cell, to 5, 6, or more. This allows for higher finger line resistance, thus reducing the cross-section of the fingers, without affecting cell efficiency [18].

In the past, cell surface area increased from 12.5 x 12.5 [cm^2] to 15.6 x 15.6 [cm^2] (M0), and module size also grew. Innovative cell designs, larger than M0, with low cost and high throughput are emerging, along with module assembly equipment to interconnect these cells [19].

Traditional PV cells are stringed, typically interconnected in series by ribbons [8]. Ribbons are hot-dip tinned conductors, either in tape or flat wire shape, that collect current from the cell. Several PV cells are strung together using ribbon wires, and the generated string is laid up as a matrix array (Figure 2.3). The strings are interconnected via conductive tape or solder to the busbar strips, reaching the JB.

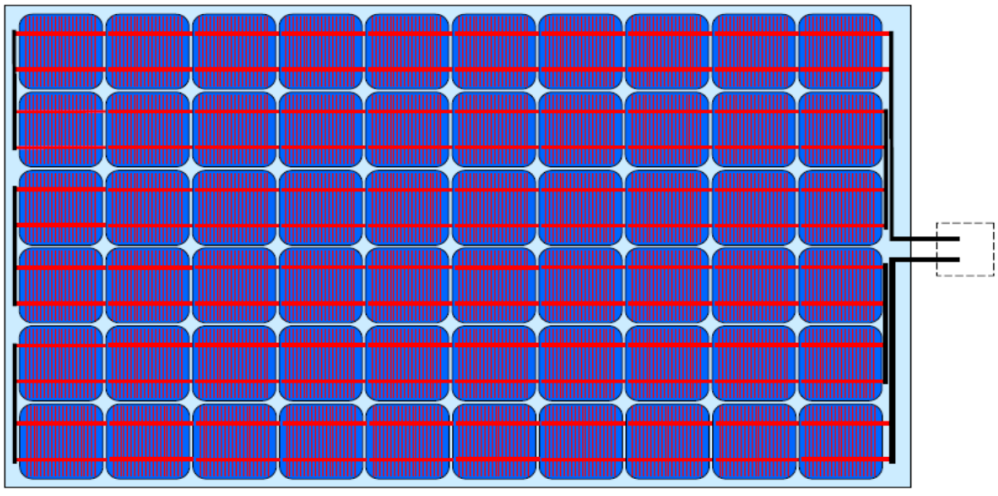

Figure 2.3 - A standard 60-cell module with cells and strings interconnection in a matrix structure: red lines show the cell interconnection with BB strips (in black), which represent the string interconnection reaching the (edge) junction box.

Contact tabbing for conventional solar cells with front-side metallization occurs from the front of one cell to the back of the next one (Front Back Contact – FBC). For cells with only back-sided metallization, they are soldered and interconnected at the back side only (Back Contact – BC). See Figure 2.4 for the two different contact tabbing configurations.

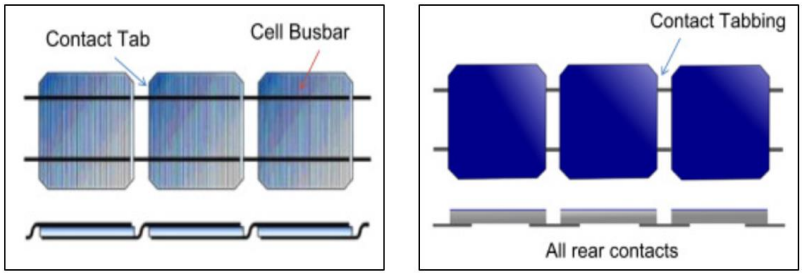

Figure 2.4 - Interconnection of c-Si solar cells to form a module using contacted tabbing and stringing for (**a**) FBC cells and (**b**) BC cells [20].

To complete the module interconnection, flux (Cu) ribbon is cut to size, bent, and aligned with the cell. The ribbon is then soldered onto the front/back bus bars of the cell, repeating the process to form the interconnected string. Soldering can be done manually or automated, using methods such as non-contact Infra-Red (IR) light induction or heated contact [21].

2.2.2 Back-Contacted Cell Modules

The busbar method of stringing is the industry standard, and modules made in this way have performed extremely well for decades. However, running busbars along the front surface of a cell does result in a minuscule amount of shade, causing a slight drop in power output.

Back-contact (c-Si) cells represent an advanced configuration in which interdigitated positive (p-type) and negative (n-type) contacts are placed on the rear surface. The cell interconnections occur at the rear side only. This technology aims for higher efficiencies by minimizing "encapsulation" losses [19]. BC cells eliminate shading losses at the front side, reducing optical and interconnection resistance, and providing a uniform (black or blue) appearance [20].

Compared to mainstream front-metalized cells, BC cell modules offer other benefits, including increased module power output due to reduced resistance and temperature losses, and enhanced module reliability [113]. However, the combination of thin and highly efficient cells poses challenges for the interconnection process. More efficient cells produce higher currents, necessitating wider and/or thicker interconnects, known as tabs, to keep electrical losses low. However, thin cells are more prone to breakage when exposed to high temperatures (>250°C) during the solder process. Moreover, substituting lead in solder pastes increases process temperature by 40÷50°C, leading to yield problems during module manufacturing. Additionally, cracks may develop in the solder, increasing electrical resistance through the interconnection [19], [20].

Front-side non-metallization is an optimal solution for maximum cell efficiency, while rear-side metal contacts and interconnections are simpler. Categories of BC (Silicon) solar cell technologies include Wrap Through (**WT**) Technology, divided into Metallization Wrap Through (**MWT**) (Figure 2.5 (**b**)), and Emitter Wrap Through (**EWT**) technology. This is a new cell technology that increases the conversion efficiency by reducing the busbar-shaded area on the front side with both positive and negative electrodes at the back. The Interdigitated Back Contact Technology (**IBC**) (Figure 2.5 (**c**)), is featured by “fingers” of metal connecting the cell on the back side instead of the front, as described by the name. The IBC includes the ZEBRA cell design technology (Figure 2.5 (**d**)) [22]. To reduce resistance and enhance electrical conductivity to the fingers, ZEBRA cells are available in the market in half-cut format only [22].

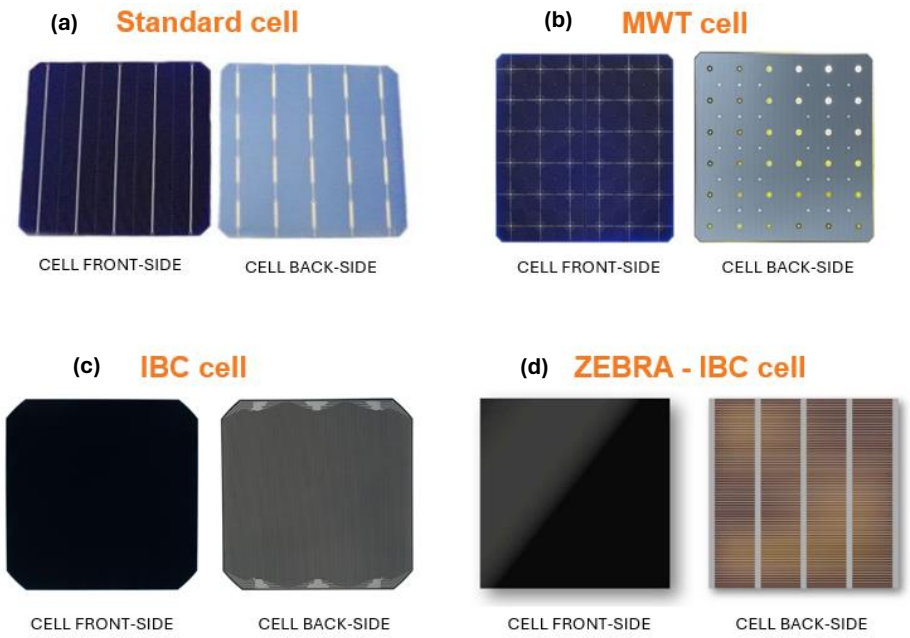

Figure 2.5 - Image of the front and back side of full-cut solar cells: (**a**) Standard cell [10], (**b**) MWT cell (*mpmchybrid.com)* **(c)** IBC cell, (**d**) ZEBRA IBC cell [22].

The market for BC cell modules is forecasted to grow from 4% to 7% of the global PV market. Expectations are for the market to increase from the present ~4GW to ~16GW by 2030, with a +15% Compound Annual Growth Rate CAGR is expected for BC cells (2020-2030), almost twice as high as the total PV installations (8%) [10]. However, processing BC cells at scale could be difficult and expensive. Nowadays, the scale of BC is small and mostly used in distributed-generation projects that run after aesthetics. It has a higher premium compared to a FBC cell, for instance Passivated Emitter Rear Contact (PERC) cell technology. No clear premium index is yet present due to smaller trading volumes and different target markets [26]. There is, though, an accelerated demand for developing automated solutions to produce BC cell panels. An important benefit to BC modules might be the significant reduction in manufacturing process steps as there is no need to interconnect solar cells at their front side.

2.2.3 A Need for Alternative Compounds and Interconnection Methods

In a traditional panel, which constitutes most of the panels on the market, electricity passes through fixed electrical wires soldered to the surface of the cell. For interconnecting solar cells, whether front-to-back or back-contact cells, it is crucial that the solder flows well and results in a good electrical connection.

Traditionally, tin-lead alloy solders were first used in the electronics industry, but concerns over toxicity and broader environmental impacts have limited their use. Two alternatives have since been developed: lead-free alloys, such as Sn, Ag, Cu, and Electrically Conductive Adhesives (ECA), which can be either screen-printable, in a so-called Printable Circuit Board (PCB), or dispensable [23]. The screen-printable method holds the most promise, providing fatigue resistance, plasticity, but it is associated with high processing temperatures. ECAs were also employed initially in the electronic industry to replace lead. They consist of two components: a polymeric resin and a metal filler. The resin provides adhesion and mechanical properties, while the metal filler, in a flake form, ensures optimal electrical conductivity. Additionally, using ECAs also reduces processing steps, which leads to cost savings. However, drawbacks include impacts on electrical conductivity, poor reliability in connections, and reduced impact strength [23]. Another viable alternative is the (lead-free) Low Temperature Solder Paste (LTSP), which is easy to handle and inexpensive compared to ECA. LTSPs, whether containing Pb or not, are widely adopted in the electronic industry, and have a melting point starting from above 100°C [47]. LTSP are classified based on the solder alloy composition and do not contain polymeric compounds. However, the formation of undesired intermetallic compounds may reduce the quality of the soldered metal joints, hence a lowered mechanical stability of the bond [47].

Low-stress interconnection technologies have been developed based on conductive adhesives to facilitate the manufacture of modules using thin cells with a large surface area [24]. Furthermore, these technical innovations on the electrical circuit level of solar cells, help eliminate the need for lead-based ribbons, hence enabling recovering or recycling processes free from hazardous lead waste residues [1].

Besides the processing costs for BC modules compared to PERC or Tunnel Oxide Passivated Contact (TOPCon) cell types, the main difference comes from the metal cost. With a foreseeable increase in PV production and installation, one of the main concerns is the shortage of certain raw materials, particularly Ag, which may not be sufficient to support the growth of future PV production. Ag is a key material used for its conductive oxide and low cost in forming electrodes onto silicon cells [25], [26]. One solution is to replace Ag with alternative materials such as Al or Cu, which are increasingly gaining ground and reducing the amount of Ag per solar cell produced, offering a short-term solution [25]. By using a Cu paste instead of Ag in the screen-printing process, material savings can be achieved. However, Cu cannot be in direct contact with the silicon, so the consumption of Ag can only be reduced to below 5 [mg/W] of cell generation capacity [26].

Improvements in the manufacturing processes and efficiencies are driving a gradual cost reduction for most of the BC technologies. However, a substantial cost drop will require more time. For instance, this concerns the Ag consumption reduction or complete replacement with Cu and Al materials, further improvement to soldering technologies and processes of the cell as well as strings interconnection, along with other advancements in efficiency, throughput, and yield. *Maxeon Sun Technologies*, for instance, has been pursuing such manufacturing improvements for 20 years now [26].

2.2.4 A Novel Interconnection Method for BC Cell Modules: The Conductive Backsheet Technology

In addition to the traditional method of interconnecting cells contacted at both or rear sides, a more advanced technique for module production of BC cells utilizes an alternative IR soldering, employing a thin Conductive Backsheet (CB).

CB technology is a cell-based connection process specifically developed for back-contacted cells, characterized by low mechanical stress on the cells. This technology allows for the interconnection of even the thinnest and most fragile solar cells available today, such as ZEBRA IBC cells, to a structured metal foil using conductive adhesive, seamlessly integrating them into a module [27]. A key feature is the integration of BC cells into a CB, which minimizes Cell-To-Module (CTM) losses, resulting in higher module efficiency and power density [10].

The CB is designed to conduct current from cells up to the JB while also protecting the module from external threats. To prevent any potential current leakage and short-circuiting, a Rear Perforated Insulator (RPI) film is employed. This film separates the cells from the CB through small, precise perforations that isolate positive and negative contact points. By connecting the CB with cells using a conductive paste or adhesive via these perforations, the CB can guide current from cell to cell until it reaches the JB (Expert input: *member of Valoe*).

Differences in the layered structure between conventional module technology using FBC cell interconnection via tabbing and stringing, and an example of back-contact cell module technology combined with CB, is illustrated in Figure 2.6.

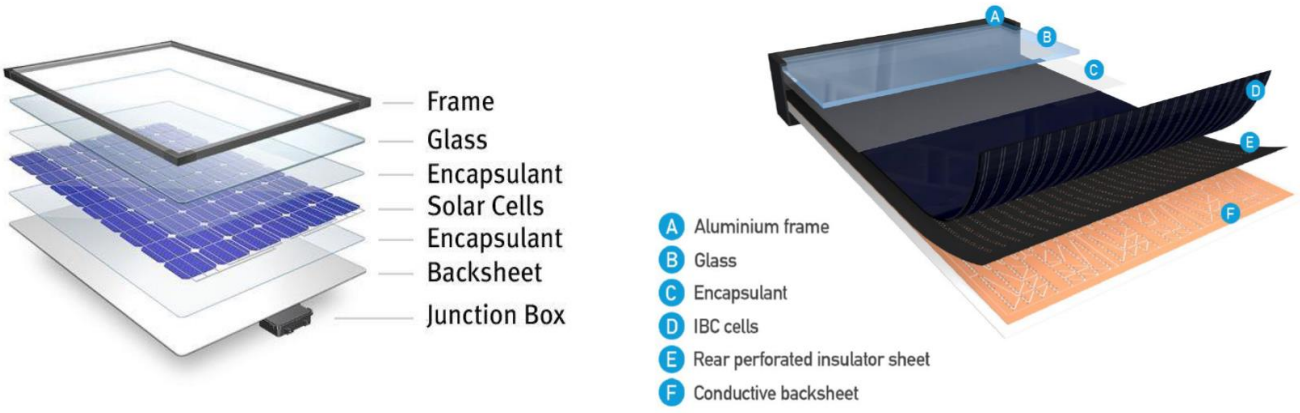

Figure 2.6 - (**left**) Exploded view of the conventional module technology, (**right**) stratification of the back-contacted module with CB technology, [10].

Electrical conductors can be applied to solar cells through printing, plating technologies or applied in the module by metal foils. Using metal foils is nearly two orders of magnitude less expensive than applying metallization directly to a solar cell [24].

A basic structure of an electro CB comprises a laminate of a metal foil, such as Cu and/or Al, to provide electro-conduction, an adhesive layer (epoxy resin), and at least one polymer layer, such as PET [28]. The metal foil is patterned, which can be achieved through known patterning technologies such as mechanical milling, chemical etching, laser ablation, or die cutting. The metal layer may have a thickness ranging from 20 to 100 [µm]. The polymer layer is provided as a single (monolayer) or multilayer backsheet. In a single-layer configuration, it consists of at least one layer of polypropylene with a melting point of at least 140°C, connecting the metal layer via the adhesive layer [28]. The foil is similar to a standard TPT backsheet foil but with an additional layer (metal sheet) [24]. Since shadowing losses no longer play a role, the metal layer in the backsheet foil can be designed to be much wider than the width of a busbar in conventional cells. The conductive sheet is patterned to match the contact points, divided into p- and n-type contacts at the rear of the BC cell, resulting in a series interconnection of cells on the foil. The patterned metal foil, its placement and metallization drawing are illustrated in Figure 2.7.

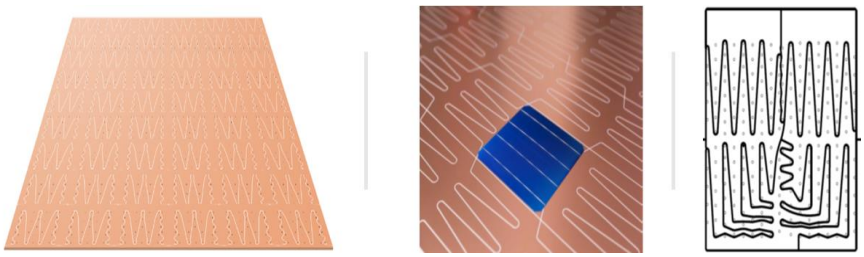

Figure 2.7 - (**left**) electronic CB foil [113], (**middle**) cell placement on the patterned copper foil, (**right**) patterned metallization drawing of the backsheet, [10].

The cell-to-cell connection occurs on the back side of solar cells within the module segment, eliminating the stress caused by adjacent cells' front-to-back ribbon interconnection in conventional modules and avoiding reliability issues such as hidden cracks [29].

Cell-CB contacting is achieved by filling the holes across the insulator film using a (lead-free) ECA or alternatively a LTSP (Figure 2.8) [10]. Additionally, the cell electrical interconnections are simplified and accomplished using the heat from the laminator (Figure 2.8 (**right**)). This is achieved during the lamination process by utilizing three-dimensional interconnected patterns or conductive adhesives or conductive backplane technology.

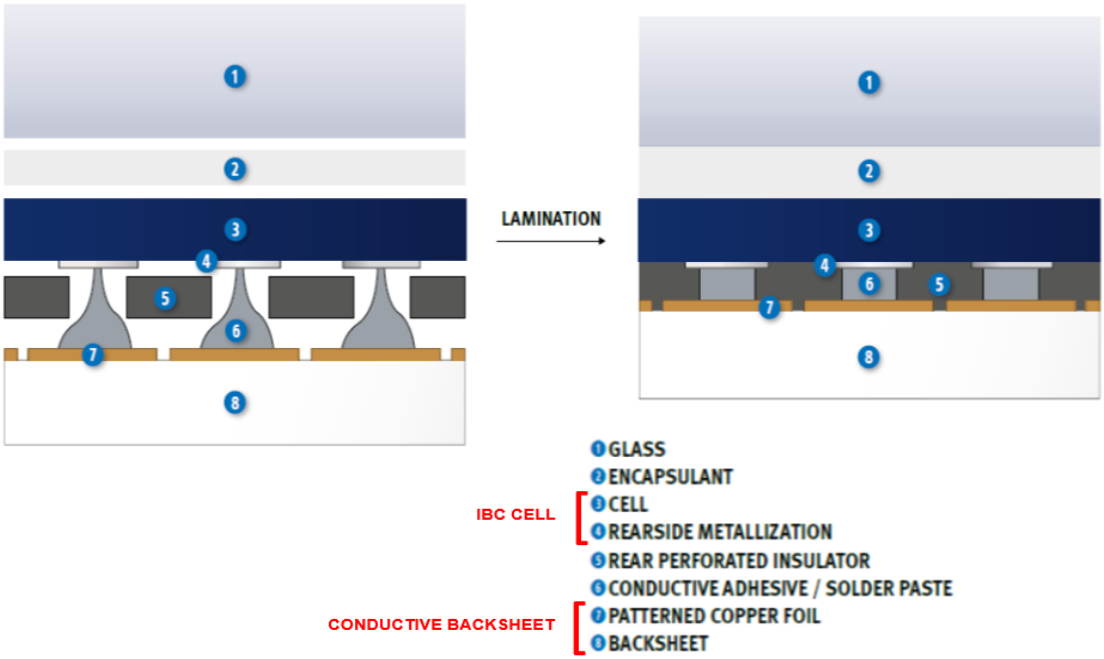

Figure 2.8 - Schematic of the IBC cell interconnection occurring prior (**left**) and in the laminator (**right**). Parts are numbered from top of the module (glass) to the bottom (backsheet) *(Adjusted from* [10]).

Regarding heat dissipation, due to the good thermal conductivity of the CB's conductive metal sheet, the operating temperature can be at least 4°C lower than other conventional modules under the same conditions [29].

The flat and dimensionally stable CB allows lower nominal operating temperature for the cell and module during manufacturing. Additionally, cell thicknesses can be reduced to less than 100 [µm], thanks to integration into the flat and dimensionally stable CB, allowing for minimal cell handling and low-stress heat dissipation during manufacturing [29]. However, this innovative technology encounters drawbacks related to the UV resistance of the polymer PET layer. Additionally, the screen-printed metal layer may (partly) damaged the backsheet during the patterning process, resulting in a deterioration of its electrical insulation properties [28].

2.2.5 Interconnection via Cell's Edge Connectors: Dog-Bone Contact Wire Technology

One of the latest technologies for electrical interconnection is through cell edge connectors, known as "Dog-Bone" connectors (Figure 2.9 (**left**)). Solar cells are interconnected along their edges using a soldered dog-bone wiring technology. This method requires specific solar cells compatible with the dog-bones. To establish a series connection, each dog-bone contains six contact regions that can be soldered, connecting the positively charged side of one cell to the negatively charged side of the adjacent cell [30].

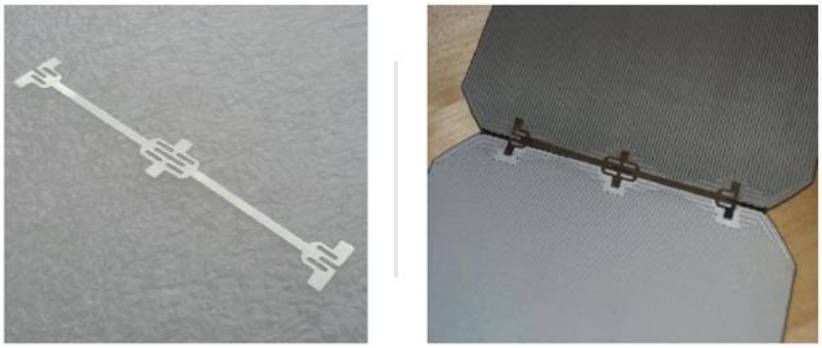

Figure 2.9 - Dog-bone wire (**left**), IBC solar cells interconnected with dog-bone wire (**right**) (*Adapted from* [30]).

One significant challenge of using edge connector technology is to carry all the current to the cell edge, necessitating very high electronic conductivity in the fingers. Therefore, the effectiveness of this method depends on the type and format of cells used. Generally, to minimize conductivity loss, smaller cell formats are preferred, such as half-cut cells, where the dog-bone connection can be very efficient in conducting electricity (Expert input: *Member of Valoe*).

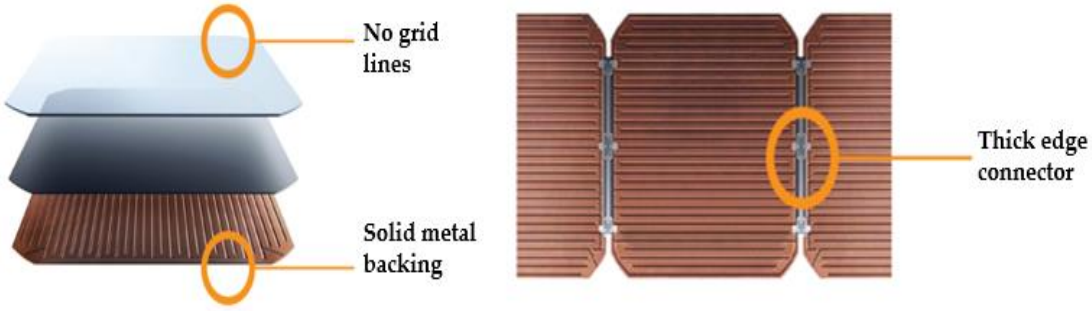

Figure 2.10 - Maxeon cell detail [114].

Thick edge connectors enable cells to expand and contract with daily temperature changes while maintaining a connection without strain [114]. High-quality silicon wafers, IBC cell technology, and robust cell edge connectors can create a good recipe for an excellent solar module.

3

The Process of Manufacturing Laminated PV Modules

This chapter illustrates the general processes for manufacturing conventional, laminated (L-) solar modules. First, an overview of the manufacturing sequences, equipment, and processes for laminated modules' production using the classic cell stringing interconnection method is provided. Later, two turnkey lines of 20 [MW] and 300 [MW] scale of production are presented and discussed in detail. The chapter ends with an overview of the novel assembly technology using the conductive backsheet in laminated PV manufacturing plants.

3.1 Manufacturing Process of a Standard, Laminated PV Module

In this section, assembly steps and equipment descriptions for two scales of complete PV module manufacturing are presented.

3.1.1 Assembly Steps and Line Processing Equipment

Assembling solar cells with the classic IR stringing approach, for either FBC or BC metallization cells, has been the mainstream, cost-effective, and widely available approach for manufacturing solar modules so far. The classic cell interconnection using solder-coated copper flat wire is the current industry standard for producing a cell string that connects the individual cells electrically and mechanically. Processes for laminated panel manufacturing are classified into PRE-lamination, lamination, and POST-lamination stages. Visuals of assembly units and descriptions of block sequences are shown in Figure 3.0.

(a)

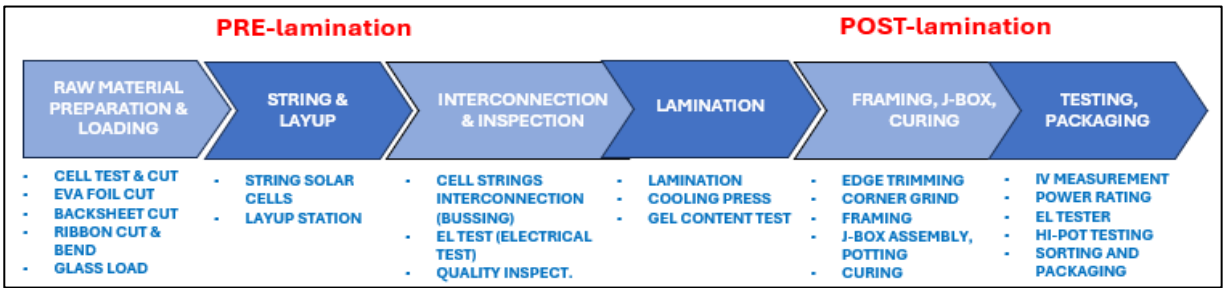

(b)

Figure 3.0 - Assembly process stream: (**a**) block sequence steps, (**b**) visuals of laminated PV module assembly flow (*Adjusted from* [16]).

According to the process flow and visuals of sequence steps of Figure 3.0, a description of the main assembly processes and equipment functionality is now provided.

PRE-lamination

- **RAW MATERIAL PREPARATION AND LOAD:** In this initial phase, raw materials such as solar cells, glass, and encapsulants are prepared and loaded. Glass plates can optionally undergo pre-cutting, washing, drying, and processing. Additionally, for different cell formats, a cutting and testing machine for solar cells (cell scriber) could be adopted along with the preparation of ribbons and bus bars.
- **CELL STRINGING & LAYUP**: Solar cells are soldered to wire or ribbon and electrically interconnected using Bus Bars strips to create cell strings, which are created manually or by the stringer machine. This operation is crucial as the electrical connections of solar cells enable the PV module to transmit electricity and power output. Each string typically consists of 10 to 12 solar cells [33] and is matrixed in the lay-up system to be precisely picked, aligned, and positioned on the glass. The layup is generally performed automatically with an assembly toolset.
- **STRING INTERCONNECTION (Bussing) & INSPECTION:** Multiple strings of solar cells, forming the entire module, are connected in series or parallel to achieve the intended module's power output. Wiring is prepared by cutting or bending it to form a bus across one- or three-hole glasses/backsheet, towards the JB. This process can be performed manually over motorized benches or automated with an automatic bussing machine. The quality of the electrical interconnection process is inspected using the Electro Luminescence (EL) test, which utilizes high-resolution cameras to identify defects such as microcracks, dark areas, finger issues, and short circuits. This thorough quality control allows for monitoring and improvement of the PV panel production process.

Before the lamination process begins, the semi-assembled module still needs to have the encapsulation material and backsheet or second glass covered. The entire assembly relies on the front glass as a mechanical support in a configuration called superstrate assembly, where the front EVA layer is placed first, followed by the solar cells (sunny-side-down), and the rest of the components up to the backsheet or second glass positioning. Alternatively, the assembly chain can lay on the backsheet or second glass plate, known as substrate assembly, up to the front glass cover. The solar cells are then laid up on the rear EVA in a sunny-side-up orientation.

With the top and bottom encapsulation materials and the backsheet/second glass covered, the full structure enters the laminator machine. During this process, both the encapsulant and the conductive adhesive are cured, forming interconnections to create a monolithic body.

Lamination

The PV module is laminated by applying the right temperature and pressure to allow the polymerization process of the encapsulating material, turning from a multilayer structure into a single block unit. This transformation process is a key factor for the durability of laminated solar panels, requiring accurate temperature control across multiple heating zones. An in-depth description and overview of the laminator cycle, types, and capacities are presented in Appendix A.

POST-lamination

- **TRIMMING AND FRAMING:** Trimming the module's edges is a process that removes and cleans the excess encapsulant material overflowed out of the laminator. If operated automatically, the machine efficiently and smoothly removes any surplus remains from the module. Alternatively, to avoid the module trimming process, adhesive tape is dispensed at the module edges before lamination. In the framing process, four rails are assembled around the glass and glued with silicone or other adhesive tapes. The framing technology utilizes aluminium, plastic, or metal corners to fasten the frame and to obtain the right mechanical robustness around the module's edges.
- **JUNCTION BOX ASSEMBLY:** JBs, typically rear-sided in the central position of the module, are fixed either with a pre-set quantity of glue or optionally soldered to the module, thus creating an electronic connection between the ribbon and J-Box's cable. The inner box is potted with the correct amount of silicone to provide long-lasting protection.
- **TESTING:** Solar simulator, Hi-Pot (high potential), and a final EL test are the main inspections carried out during PV module manufacturing. These machines are positioned at the end of the production line and/or along the production chain to maintain the quality and efficiency of PV modules after the most sensitive production phases. The current-voltage (IV) curve measurement is performed by the sun simulator to assess the module's power output, store the measured data, and/or print a barcode label on it. The Hi-Pot machine performs the electrical isolation test on the panel with an eventual quick quality check by an operator. This last test ensures

that the isolation in the product can withstand the maximum voltage it might encounter during operation without breaking down or allowing current output to flow within the panel. To do so, a very high voltage (~1000 V) is applied between various points in the device, usually between conductors and the ground or between different conductors. If any insulating defects occur, such as cracks or weak spots, the high voltage applied causes the current to flow, thus detecting a potential safety risk [105].

- **SORTING & PACKAGING:** In the sorting phase, a selection of modules is made according to the previous tests and quality inspection, thereby packed within different pallet units.

Process steps and assembly equipment as explained above are compatible with both FBC and BC cells, using a classic tabber and stringer for traditional ribbon-based soldered interconnection discussed in Chapter 2. Interconnection via edge connectors requires an adjusted stringer machine for soldering. If using a CB with printing/dispensing deposition method with the metal layer for contacting, the automated stringer and bussing machines would be avoided as the electrical connections take place during the lamination process. In Section 3.2.1, the assembly method using CB technology will be presented.

3.1.2 Turnkey Manufacturing Lines for Laminated PV Module Production

Turnkey module manufacturing lines comprise comprehensive packages of equipment, process technology, and high-level factory control. Details of two different production line scales, utilizing the conventional tabbing and stringing approach for laminated modules, are presented in this subsection.

Typically, a standard solar panel is laminated onto the front glass, serving as mechanical support for the entire structure. With a G/G module configuration, manufacturing may also involve the rear glass plate in a substrate configuration. Whether the module is assembled sunny-side up or down depends on the solar cell technology used and manufacturing layouts. Modules of standard lines generally move on transport systems sunny-side down and with the short side leading [16]. Two different turnkey lines for complete PV module manufacturing are illustrated in Figures 3.1 and Figure 3.2. Assembly operations and related equipment are considered based on 60 to 72-cell G/B modules, with an output of 380 [W/module] and 300-325 working days a year consisting of 3 shifts of 8 working hours a day. These requirements fall within standardized production conditions [34].

Firstly, a semi-automated line reaching a peak output of 20 [MW] per year is illustrated (Figure 3.1). This line is suitable for assembling any type of rigid solar panels using the mainstream technology of multi-busbar FBC solar cells in a G/B configuration. With appropriate integrations, such as a different hardware and mechanical setup of stringer machines and a second glass loading machine, the line would also be compatible with the latest rear-soldered BC cells in a G/G module configuration with classic ribbon-based interconnections. Through appropriate adjustments in the stringer, cell interconnection could also be performed using dog-bone edge connectors, embedded into the stringer. If CB technology is desired for assembly, the manufacturing line will undergo some variations (Section 3.2.1).

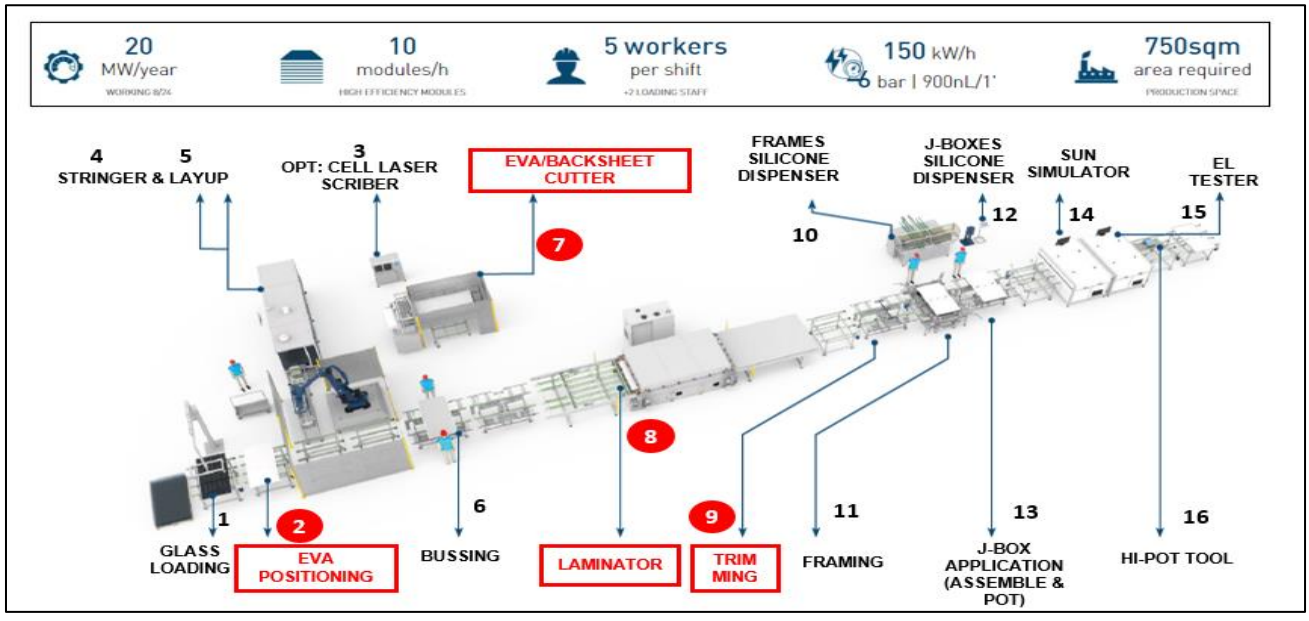

Figure 3.1 –Turnkey line (20 [MW]) for PV module manufacturing and line specs: in red formatting are the assembly operations required only to manufacture laminated solar modules (*Adjusted from* [16]).

In this 20 [MW] line, generally there is no more than one set of equipment for each process. Automated tools such as testing systems, stringers, and layup robots are present, while the remaining processes are carried out manually or semi-manually. Consequently, many precise alignment or centering systems are not included either. The automated tools present are necessary for operations where a higher degree of accuracy is required and do not significantly slow down the production line speed. Other accessories and equipment, such as worktables and centering systems, are included as part of the production line totalling around 20 items.

At the beginning of every line, a glass lifter with vacuum suction cups is typically positioned (Process 1). This lifter allows the lifting of a (front) glass sheet with the assistance of an operator and facilitates safe loading onto the conveyor belt or working table. This operation can be easily integrated into any line and positioned for the 2nd glass layup or at the end of the production line to unload finished panels and accurately place them inside a pallet.

The glass is then moved onto the belt, and the pre-cut EVA encapsulant is manually positioned on it (Process 2). Optionally, in Process 3, a single and precise freestanding laser scriber machine can perform the scribing on any market-available solar cell with the semi-automatic cell basket and loading/unloading system. The machine can cut up to 1500 [cell/h], four cells at a time [16].

In Process 4, a stringer machine solders the solar cells to form strings with the flipper unit on the unloading belt. In lines smaller than 50 [MW] volumes, a single-track IR tabber and stringer machine is employed, compatible with the latest solar cell technologies, full/half/triple-cut cells, and most of the standard format sizes available in the market (M6, M10, M12). The machine could be set for either FB or BC cell stringing process, reaching up to 2100 [cycle/h], which is approximately to 2000 [cell/h]. With a standard 60-72 cell module, the equipment can produce an output of 27-33 [module/h]. Based on the assumptions made earlier for module output and shift per year, the equipment yields an equivalent annual output peak in the range of 70-80 [MW] of solar modules [16].

Strings can either be manually laid up on the glass or interfaced and picked by a three-coordinate system's layup robot/manipulator, either faced-up or down (Process 5). With the use of vacuum suction cups and cameras, the layup machine precisely aligns strings on the glass and encapsulant agent. These machines, for the 20 [MW] lines, can manage up to one stringer machine and handle up to 400 [string/h] made of standard 10-12 full [cell/string] [16].

Once strings are positioned throughout the module area, they must be interconnected by soldering heads with busbars ('bussing') to achieve the desired module power output (Process 6). This operation, in the 20 [MW] line, is carried out manually on a worktable over a motorized bussing station, which is designed to carry out various operations including manual trimming, edge taping, automatic conveyor for JBs, and as a cleaning station. The bussing process, among one of the line's limiting processes, could eventually be operated automatically to avoid further slowing down the production speed, via a bussing machine.

Another standalone operation (Process 7) is performed by the automatic EVA/backsheet foil cutter machine, which keeps the roll straight while cutting it and prepares the incision for the ribbon exit. This process requires an operator to load and unload the material and start the equipment.

When cell strings are electrically interconnected, the encapsulant and backsheet are cut and manually positioned onto the panel, making the whole panel ready to be conveyed into the laminator (Process 8). Insights in Appendix A indicate that laminators for small line capacities usually consist of 3 plate units, housing 3 [module/ cycle] or 'batch,' and depending on the encapsulant type used, their productivity ranges from 9 to 15 [module/h]. The vacuum and curing time can take between 12 and 17 minutes per module [16]. If a minimum of 9 [module/h] is considered with a 3-plate laminator and the assumptions made earlier, the annual peak output is in approximately 27 [MW] production.

Once the module is unloaded from the laminator, its edges are manually trimmed on a working table to clean the extra material that overflowed out of the laminator (Process 9). In place of this, an edge-taping operation could be carried out prior to entering the laminator. In Process 10, a free-standing unit automatically dispenses an even amount of silicone in the frames, eventually drills holes for humidity outlet, and pushes it to the operator. The loading and unloading of frames are performed by an operator who subsequently sets the frames onto the belt for the framing process (Process 11). The next operations are to fix the JB on the rear side of the panel. This operation is performed in Process 12 and Process 13, where silicone is manually dispensed on the JB and subsequently fixed on the inline worktable. The solar module is now ready to be tested.

The first test the module undergoes is the IV curve tracing with the sun simulator (Process 14). The panel is electrically connected with the JB, and an array plate simulates the sun by a flash of light. The test is performed at standard test conditions (STC), namely at 25 [°C], 1 [bar], and 1000 [W/m^2] irradiance. The IV curve of the panel is measured by placing the panel in an open circuit voltage (no current) and measuring it, hence by starting to reduce the voltage, a resistance builds up more and more until the short-circuit conditions (no voltage) are reached, and that maximum current is measured. This operation can be performed in both ways, either from the short circuit and release resistance up to the open circuit condition or backwards. After measuring it, there is a Maximum Power Point (MPPT) tracker that finds the optimal point (P_{max} = V x I) that rates the power of the panel. These tests are generally performed in both configurations explained to detect any mismatches present (Expert input: *member of Soltech*). Sun simulators use light-emitting diodes (LEDs) as a light source with automatic loading/unloading/contacting, with a cycle of ±20 [s/module] and are compatible with all new generation solar modules and new high-efficiency solar cells [16].

The second test performed is the EL test inspection (Process 15). This test, thanks to high-sensitivity cameras and neural network software, allows the user to carry out a thorough quality control of the PV panel by checking single cells and string integrity as well as detecting defects. As mentioned before, the EL test can also be applied along the production chain, mainly before entering the laminator to check over potential uncertain string outcomes, and for easier disassembly. For small lines, where the flow of panels produced is low and the high capital cost for machine purchase is an issue, the panel is usually carried physically across the factory to the EL test machine available. If there is not EL machine present at all, the electrical quality check is performed with a high-resolution camera in dark conditions. Solar cells generate an electric current when exposed to light (containing photons across the entire light spectrum). However, if a current is applied to them, the cells function as a LED in reverse (current and bias voltage), emitting light in the IR spectrum. By using a high-sensitive camera and removing the IR filter, the LED emits a purple colour. The advantage is that when a current runs through that string, the cells will emit an IR light, and this light can be captured with a removed IR filter of the camera in dark environment to check the integrity of the cell string and detect defects.

The last test (Process 16) is the electrical isolation test (Hi-Pot test), with high voltages applied and previously explained.

For increased outputs per year, assembly units must fulfil a higher degree of automation and an increased number of toolsets per process. A high-capacity automated assembly equipment is demanded to achieve maximum uptime, higher throughput as well as line efficiency. An example of a complete solution of a fully automated 300 [MW] line for PV module manufacturing is in Figure 3.2.

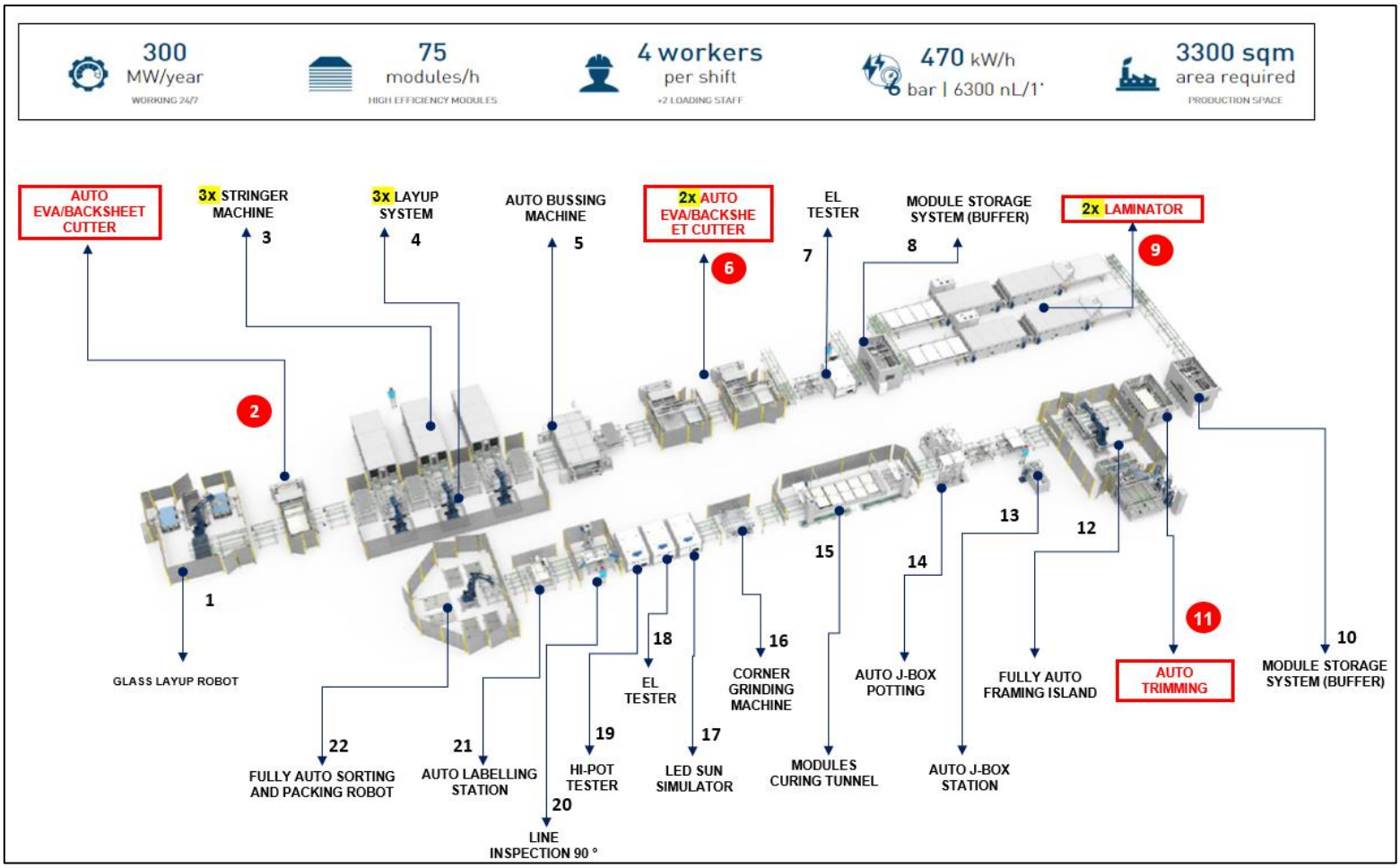

Figure 3.2 - Layout of a highly automated turnkey line of 300 [MW] output power for PV module manufacturing: processes in red format are used to manufacture laminated solar modules only (*Adjusted from* [16]).

In this 300 [MW] line, most of the equipment mode is fully automated, and the labour required is minimal.

The production line starts with the automated loading of the glass plate onto a transport system. Unlike the small line, there are now three two-track tabber & stringer units handled by three layup robots to pick and place the formed strings. Each stringer, with a larger capacity than the 20 [MW] line unit, can generate up to 4000 [cycle/h] and, under the standard assumptions made earlier, can exceed 100 [MW] of annual production.

Automated pick & place (P&P) systems are usually handled by a n-axis robot system in which one unit can manage up to two stringer machines. It is equipped with an auto mechanical arm with vacuum suction cups that minimize cell breakage [34].

The layup robot picks up strings out of the stringer track(s) and turns them before positioning on the glass already on the belt with the first layer of encapsulant. Two units of EVA/Backsheet film cutters prepare the incision for the ribbon exit, automatically cutting, picking, and placing encapsulant foils over the glass or solar cells. Eventually, for G/G panels production, an automated 2nd glass loader must be integrated into the line after Process 6.

Generally, even for small lines with an annual production volume equal to or greater than 50 [MW], the EL test is performed twice. The first test is performed on the panel before entering the laminator phase to check the outcome of the electrical interconnections, as the whole structure here is still not chemically bonded and therefore easily disassembled. A final EL test is carried out at the back-end line before the module is labelled and packed.

Two fully automated double-step laminators are used with a capacity of 5x2 [module/cycle] dividing the cycle into pumping and curing time to double up the production capacity. A pre-heating step generating the vacuum takes place in the first step, and the crosslinking and core part occur in the second step chamber. The last laminator step uses a cooling press system on the discharge belt. The usable area is divided into 5 plates, each of which is

divided into 3 controllable and independent thermal zones to set up a better lamination recipe and achieve better lamination results [32].
Assuming the productivity is 50 [panel/h] under normal curing time, with a double-step 5-plates laminator, an annual yield, under the initial assumptions, is in the range of 150 [MW]. Accounting for the same productivity also for the second laminator, the volume of 300 [MW] is reached. As this represents one of the highest capacity laminators, if a larger scale of line were investigated for this study, another unit would have been added.

Due to the high stream of panel generation, and that the laminator sets the slowest and limiting processing time throughout the line, buffer systems (Processes 8 and 10) are generally positioned before and after the lamination step to balance the incoming and outgoing modules for levelling out the production rate. These systems, using automatic drawers, place and remove modules and can store in the range of 15 to 50 modules for a temporary stockpile [16].

Unlike the 20 [MW] scale, this highly production scale also includes fully automatic trimming and framing stations in which a module is processed with a cycle time of less than 30 [s]. Before being tested, automated JB machines assemble and pot JBs on the rear side of the module, facilitating the conveyance of framed modules into the curing line to ensure proper curing through precise timing. Although the JB operations are performed in automated mode, the assistance of an operator is recommended to inspect the machine work for the correctness of the interconnected cables. The curing station allows time for the single or mixed glue component (Silicone) applied on JBs and frames to reticulate and be transported after complete hardening and curing. Hence, the standard IV measurement, EL and Hi-Pot tests are performed along with an inline optical inspection machine that picks up the panel from the conveyor and turns it 90° so that the operator can quickly inspect the quality of the panel. Additionally, these stations can also be used as a cleaning station before testing.

The line ends with Processes 21 and 22. The first is an automated labelling machine that applies a label on the panel frame based on results from the power curve measurement test to define a panel belonging class. This last operation is quite challenging to estimate exactly due to the various panel thicknesses, panels with coatings on the front, different cell distances, which all can alter the module power output.

The second is a fully automated sorting & packaging station handled by robots with different pallets representing power classes and a horizontal or vertical packaging area with corner covers.

The number of workers in the 300 [MW] line can range from 6 to 8. These are for loading/unloading materials, changing spools of encapsulant cutters, checking if units are working properly, and assisting in the testing and quality inspection of the panel and packaging. Line accessories, including transport and alignment systems, can reach the order of 80 items in total [33].

The choice of investigating these two scales of PV laminated lines comes from the adoption and comparison with laminate-free module assembly which will be discussed in Chapter 5. With greater annual production volumes than 300 [MW], line productivity must be enhanced. This translates into either larger units or a higher degree of automation with more sets of equipment. For instance, two laminators will no longer be sufficient.

A broader overview of production line technical specifications for different scales and solar module manufacturers is presented in Table 3.0.

Table 3.0 - Main production line specifications for different PV module manufacturers (blue) with production line volumes included.

Company Name	Production Volume	Line Throughput	Power and Air Consumption	Floor Area	Labour	Reference
	[MWp/year]	[module/h]	[kW] | [litre/min]	[m^2]	[worker/shift]	
Ooitech Solar	10	16	150/ -	800	12	[31]
Reoo/Abloomax	5 (1shift) – 15 (3 shift)	6	50/ -	600	10	[35]
Eurotron	14	5	-	-	2	[115]
Ooitech Solar	20	32	200/ -	1000	16	[31]
ECOPROGETTI	20	10	150/900	750	8	[16]
Reoo/Abloomax	10 (1shift) – 30 (3 shift)	9	100/ -	1500	> 6	[35]
Mondragon Assembly	50	15	100/1500	600	10	[36]
ECOPROGETTI	60	15	160/1000	900	8	[16]
Eurotron	86	30	-	-	2	[115]
Reoo/Abloomax	30 (1 shift) – 100 (3 shift)	24	200/ -	> 1500	> 8	[35]
ECOPROGETTI	100	25	200/2600	1300	10	[16]
Mondragon Assembly	100	30	150/2000	800	15	[36]
Reoo/Abloomax	100 (1 shift) – 300 (3 shift)	96	300/ -	> 40000	> 12	[35]
Ooitech Solar	120	70 (3 shift)	400/ -	1500	22	[31]
Confirmware	150	45	-	3050	25	[37]
Mondragon Assembly	150	40	200/3000	1800	10	[36]
Eurotron	175	60	-	-	2	[115]
ECOPROGETTI	200	50	360/4600	3000	6	[16]
Eurotron	260	90	-	-	4	[115]
ECOPROGETTI	300	75	470/6300	3300	6	[16]
Confirmware	300	90	-	3700	28	[37]
Mondragon Assembly	300	80	350/4500	2200	15	[36]
Confirmware	450	135	-	4050	31	[37]
Reoo/Abloomax	500	150	450/ -	7000	≥ 35	[35]
ECOPROGETTI	500	100	600/7800	3800	5	[16]
Mondragon Assembly	600	160	700/9000	3600	25	[36]
Confirmware	600	180	-	4250	35	[37]
ECOPROGETTI	1000	180	1200/10300	6000	9	[16]
Mondragon Assembly	1200	320	1750/22500	11000	50	[36]
ECOPROGETTI	2000	360	3000/20600	12700	14	[16]

3.2 Different Assembly Routes for Back-Contact Cell Module Manufacturing

The integration of BC cells into module assembly remains challenging [38]. An alternative and novel manufacturing method aimed at addressing these challenges for BC modules is through screen-printed metal-patterned CB technology. Its manufacturing analysis is explained in the following subsection.

3.2.1 Manufacturing Laminated Solar Modules with Conductive Backsheet Technology

For years, PV component companies have supplied solderable contact surfaces for ribbons, the connections of the solar cells to allow electricity generation, transportation, and dissipation. To fully benefit from the advantages of BC cells during manufacturing, such as avoiding cell-to-cell soldering and gaining in energy yield, an alternative module manufacturing technology is proposed: patterned CB foil technology [27]. The key difference from proven systems involves using a metal foil as a flexible, solderable circuit board. CBs in the solar industry can manufacture high-power back-contacted modules in a process-optimized route (Expert input: *Member of Valoe*).

Today, back-contacted cell modules are beginning to be mass-manufactured worldwide with this novel technology [38]. Replacing conventional soldering, for BC metallization cells, with conductive foil and encapsulation structure proves significant reduction in manufacturing process steps as no stringer and bussing machines are required, thus potential cost reductions [38].

For cell contacting with CB, either screen-printable or dispensable deposition methods can be applied. If LTSP is chosen (see Figure 3.3), an injection system is required to dispense the metal paste or similar conductive

adhesive on the CB for cell contact. The accuracy of cell placement and dispensing system is in the order of ±50 [µm] (micrometer) [38].

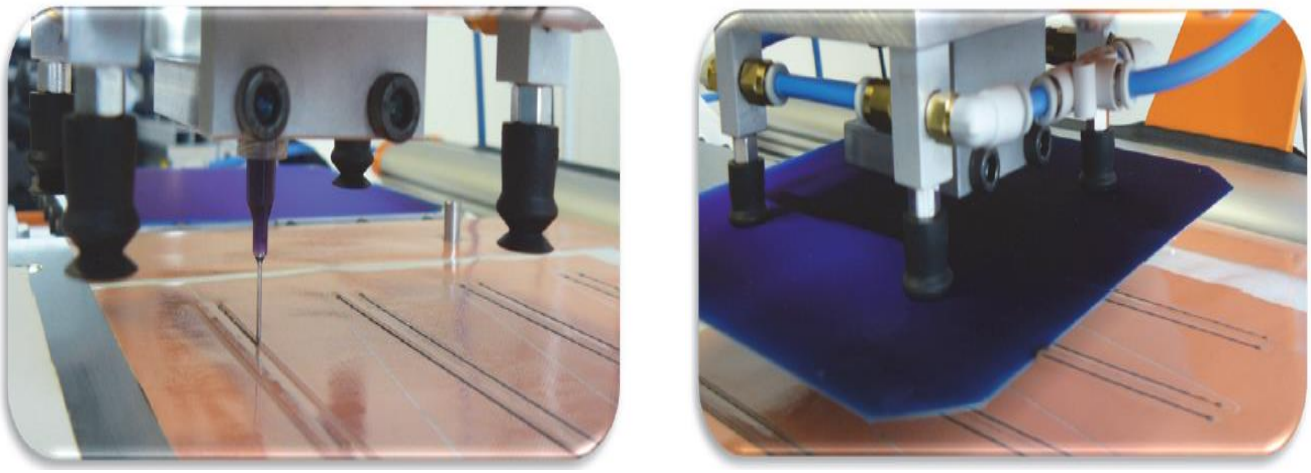

Figure 3.3 - (**left**) Image of a solder paste's injection machine and (**right**) solar cell placement on the CB [38].

Generally, after the cell contacting with solder is settled, the module is flipped before lamination, as lamination is generally performed with the glass facing downward. Alternatively, the entire module could be assembled onto the front glass plate as a mechanical support. The assembly process with LTSP on CB consists of a structured metal paste and a dielectric layer for electrical isolation between the metal sheet and cells. The isolation layer is locally opened to establish cell-backsheet contact. The semi-finished module must be laid upon foils of encapsulant and backsheet before closure with the front or rear glass before entering the laminator [38].

3.2.2 Assembly Flow of a Complete PV Manufacturing Line for Laminated BC Cell Modules with Conductive Backsheet

The basic idea of this novel technology is to view solar cells through the lens of the electronics industry. The PCB serves as a circuit-mounted component, akin to what the electronic industry employs at high speed and efficiency. Similarly, solar cells can be placed with extreme speed and accuracy and at low cost. Although PCBs are not scaled as in electronics industries, the same principles apply to the solar industry's manufacturing process. For high module production volumes, such as those at the scale of 300 [MW], cells are assembled via automated P&P operation onto the PCB layers (Expert input: *member of Valoe*).

Upon the metal layer, structured to form a circuit, cells are picked and placed (P&P). One benefit, unlike for standard rectangular-shaped solar panels, is the flexibility in shapes for the circuit. The panel need not necessarily have straight edges, and cells can be positioned at arbitrary angles. The metal layer of the PCB design eliminates the need for busbars and their placement complexities. Complicated forms would require a complex bussing system with the conventional tabbing-stringing approach. When PCBs are used instead, this operation is eliminated (Expert input: *member of Valoe*).

A complete block sequence of a 300 [MW] production line for BC double-glass panels manufacturing with the conductive sheet screen-printed technology is presented in Figure 3.4.

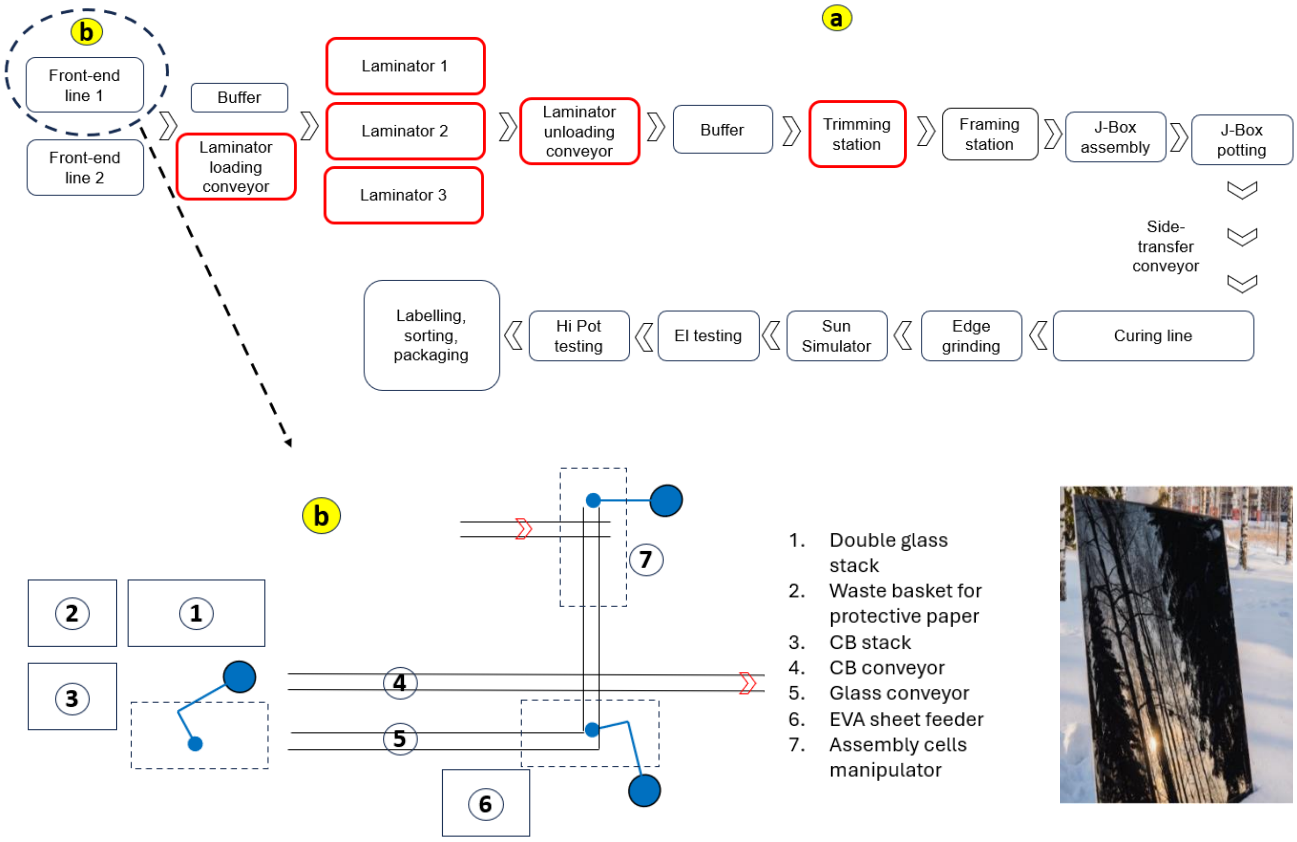

Figure 3 .4 - (**a**) Flow diagram in blocks of a complete manufacturing line for laminated G/G module with CB technology: the red contour of blocks represents processes employed only in L- module manufacturing. (**b**) Schematic of one front end of line for material loading and preparation (Expert input: *member of Valoe*). At the right side is a photograph of a laminated BC solar panel manufactured by using this novel assembly technology [116].

The red contour blocks of Figure 3.4 (**a**) represent units assembling only laminate solar panels, which make up part of the factory footprint. What differs from a conventional plant is the front end of the line (Figure 3.4 (**b**)), where no stringer and bussing systems are present, as the electrical connection is accomplished in the laminator. The front end of the line consists of material loading and preparation zones as well as cell assembly. Glass plates are loaded (block 1), picked up, and placed on the conveyor (block 5), and a robot places the encapsulant sheets from the EVA sheet feeder (block 6). The CB stack and conveyor are independent in blocks 3 and 4.

According to the options in assembly, which can be in a superstrate (from front glass loading), and the whole assembly is carried out layered from the front glass. Alternatively, the assembly is performed in a substrate (from backsheet or rear glass loading) configuration; automated units must be set based on that orientation accordingly. For BC cells, as there are no wires on the front and PCB contacting is at the rear side only, the substrate configuration is preferable; BC cells are laid sunny side up, and the whole assembly uses the rear glass as a mechanical support.

The glass and CB loading hold two autonomous conveyor belts taking the panel to the assembly cell area (block 7). The combined conductive layers include EVA and conductive backsheet. To ensure good contact between cells, a small amount of ECA material is printed on the top of the metal foil of the backsheet to match the electro deposition on the back of solar cells. A 60 full-cell module would require about 2000 dots of conductive adhesive to be printed [24].

In addition, a thin insulating layer, the RPI, is applied parallel to the loading/assembly cells area. This layer ensures there is no risk for short circuit and leakage current. The schematic of the layer stratifications is shown in Figure 3.5.

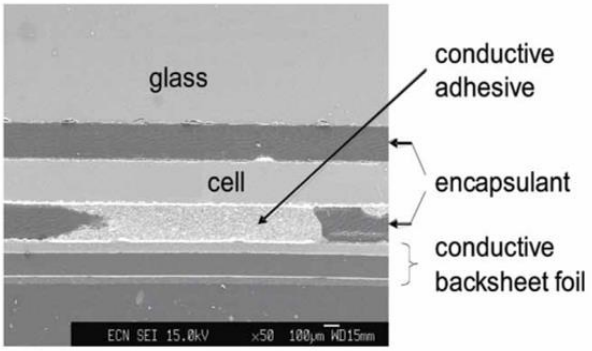

Figure 3.5 - Cross-sectional view of the module with conductive metal layers *(Adapted from* [24]).

To conclude the description of the front end of the line sequences, in block 7, there is a shuttle, a cyber line handling cells via a linear robot or manipulator. This picks cells or strings and places them onto these multiple conductive patterned layers of the module, and acts as a cleaning stage. Since the front contacts and tabs are no longer required, cells can be placed closer together in the module (improved packing density), thus reducing electrical resistance. There is also no need for string interconnection at the top and bottom of the module, which increases the module's output area. With the top and bottom encapsulation materials (EVA) and 2nd glass covered, the full structure goes into the laminator machine while simultaneously forming the interconnections to become a monolithic body. Hence, both the encapsulant and the conductive adhesive are cured. The lamination process thus allows for cell-to-cell interconnection, as the temperature at which the connections are established is approximate to the laminator operating temperature, of approximately 140-150°C [24]. The ECA that is cured during lamination establishes the electrical connection between cells and backcheet foil. Subsequently, a completely standard middle and back end of the process line follows up (Figure 3.4 (**a**)).

However, the reliability of the most used encapsulant type (EVA), besides the assembly methodology used for laminated PV modules, is still to be proved for the long run. Even with the adoption of the novel metal patterned CB technology, the adhesion between encapsulant(s) and polymeric layer may be poor. This is due to the non-uniform pattering areas of metal that may be present, starting to drift during lamination leading to delamination during the lifetime of the module. De-lamination does limit the PV module service life due to for instance an increased water and air/oxygen ingress at the laminated interface [28].

4

The product: Laminate-Free PV Modules

Laminate-free (L-F) modules are the primary focus of this chapter. Firstly, a discussion on the relevance of a circularity model in the solar industry is introduced. Subsequently, various concept designs of L-F modules are presented, alongside the introduction of Biosphere Solar and its module architectures. Emphasis is placed on the L-F PV-Module Version 2 of Biosphere Solar, accompanied by an analysis of its components, specifications, and manufacturability.

4.1 Design for Circularity in the Solar Industry

Solar energy is a renewable, low-carbon energy source with both scalability and affordability. It offers not only environmental benefits but also presents challenges [2]. The solar industry operates within a linear economy, where resources are consumed during production and disposed of at the end of a product's useful life [39]. The importance of sustainability in the PV sector is steadily increasing. Particularly, a sustainable PV module design and manufacturing process is essential for transitioning from a linear to a circular economy.

The idea behind the circular economy is that every material or product can be repurposed for something new at the end of its operating life. This is demonstrated in a linear economy but to a very limited extent [5]. Valued retrieval or high-value recycling treats decommissioned modules as a resource rather than waste, creating added value. Such processes in the PV industry focus on retrieving all valuable components, materials, and their embodied energy, including elements such as Al, Si, Ag, Cu, and glass. This enhances resource efficiency and the material circularity rate of the solar industry (Figure 4.0) [2].

Figure 4.0 - From linear (**left**) to circular (**right**) economy [117].

Closing the cycle involves more than just recycling. Aiming at recycling as the only valid option for EoL modules is short-sighted and would not result in a circular c-Si PV industry [3]. In a circular economy, second-life mechanisms such as part harvesting to repair, refurbish, and reuse play a pivotal role, leading to products being in

use for longer periods and could significantly contribute to closing the loop in the PV industry for c-Si modules. The reflection on whether it is feasible to apply the RRR model when panels reach their EoL (after 20-25 years) is still ongoing [3]. Reparation and recovery, at a different phase than the panel's EoL, for its reuse or refurbishment, may be a viable option. Moreover, outdated technology at EoL could render recovery steps obsolete. This means that the recovered value of components in terms of quality and volume is still high, whereas the cost for disassembly and restoration may likely to remain unchanged. For instance, PID-related issues are predominantly reported within the first 5 years of operation, involving up to 40% of failures, while up to 50% of glasses may break within the first 5 years of life [1].

However, the techniques and business models in the current PV industry are not sufficiently developed to maintain the quality of materials and products [39]. Up to now, several experiments have been conducted by PV manufacturers on L- solar panels for the separation and recovery of various materials at the EoL, but due to the strong bonding applied by the encapsulant(s) EVA with other components, even the recovery of glass and other precious metal components may turn complex and requires extra treatments, which are costly and have a certain environmental impact. There are two different ways to replace the EVA encapsulation. Firstly, alternative materials and recovery processes can be employed. A solution developed while retaining the laminate EVA is to use double-encapsulated modules with a release layer. According to [39], the structure is evaluated with its recyclability, optical characteristics, and degradation rate. A transparent, non-adhesive film placed between cells and EVA is used that does not adhere to the PV cells (Figure 4.1) [39].

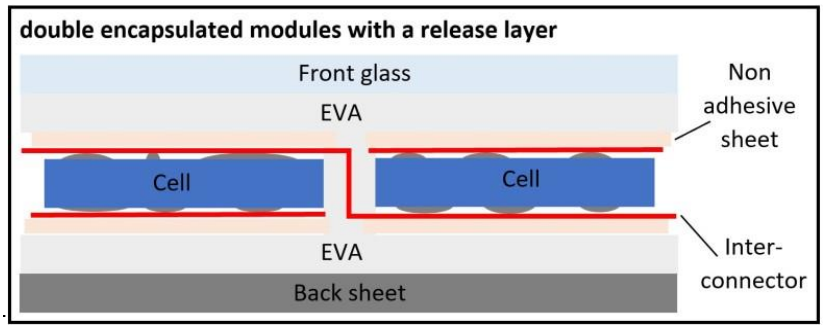

Figure 4.1 - Structure of a double-encapsulated module with a release layer in a G/B configuration [39].

However, the module failed as the additional sheet worsened optical properties. The transmission decreased, and module reflections increased by 3.4–3.7%, with increased resistances [39].

Secondly, the other solution is to completely change the design of the module.

4.1.1 Developing Novel Concept Designs: Laminate-Free PV Modules

A complete change in the structure using L-F PV module technologies has also been proposed to overcome the limitations of laminated encapsulants while reducing material costs and enhancing recyclability. The removal of materials used in the module during disassembly can be easily separated, maximizing the quality of recovery entities.

To overcome the limitations of the state-of-the-art module encapsulation technology based on EVA lamination and cell soldering, Apollon Solar, for instance, has introduced the New Industrial Solar Cell Encapsulation (NICE) technology. This Ag-free and solderless module concept replaces laminated encapsulants with neutral gas filling and edge sealants over the module perimeter [13]. An important feature of the NICE technology is the application of external pressure, making cell interconnections solderless. Creating a depression (vacuum) inside the module establishes the electrical series connection between cell contact lines and metal interconnectors, thus eliminating the need for soldering, the most widely used technology today. This approach reduces embrittlement and minimizes mechanical stress on the cell during processing [13]. The module utilizes an edged air and humidity-tight sealing technology, a concept inspired by the double-glazing industry. This is based on the application of an organic sealing material from the Poly-Isobutylene (PIB) family (Figure 4.2 **(b)**). Key requirements include maintaining a very stable vacuum in the module and ensuring that the rear sheet exhibits excellent gas and humidity tightness. This rear sheet can be formed either from an electrically insulated metal foil or another glass plate.

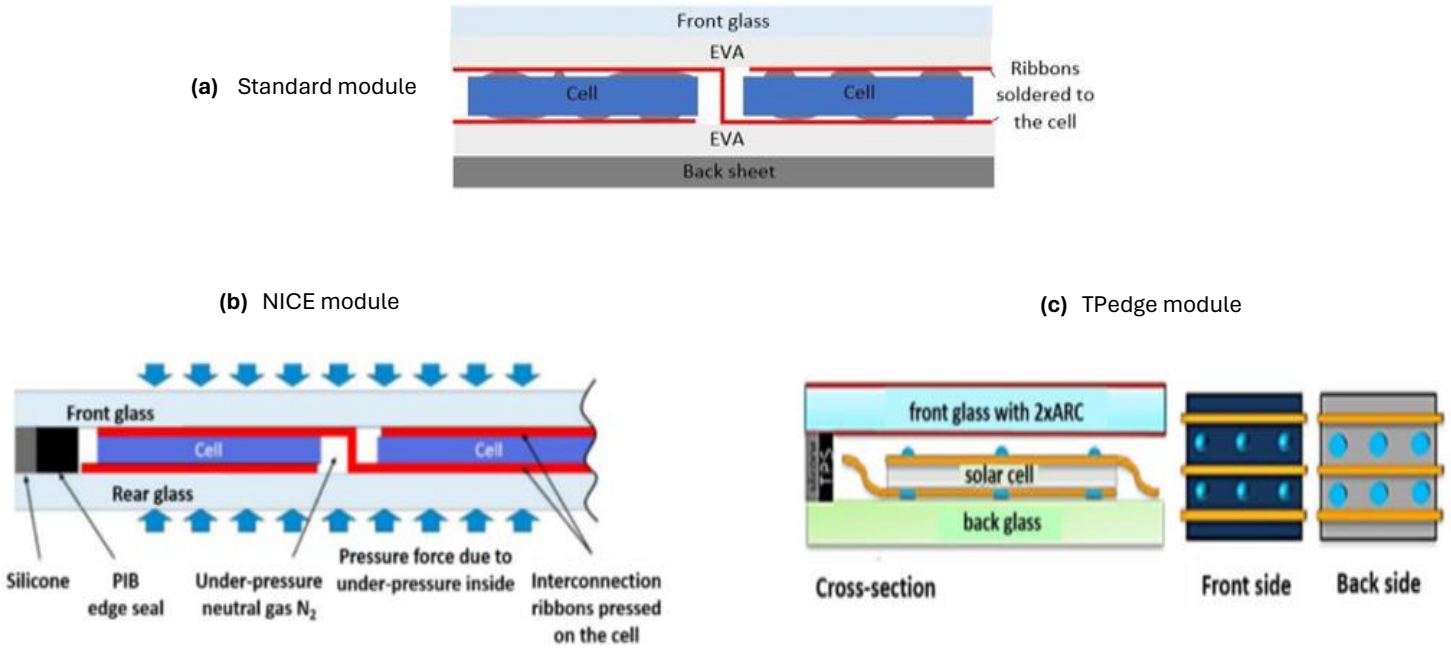

Figure 4.2 - (a) Cross-section schematic of a conventional EVA laminate module [39]; **(b)** N.I.C.E. gas-containing module [13]; **(c)** TPedge module sketch with adhesive pin positions and double-layer edge sealing. Edge seals consist of primary (Thermoplastic spacer) and secondary (Silicone) layers [13].

Replacing EVA with gas in G/G modules reduces parasitic absorption of the encapsulant and avoids drawbacks of polymer encapsulation [13]. Gas encapsulation offers significantly higher added value in terms of recyclability. From a recycling perspective, disassembling a NICE module enables the recovery of entire piece components such a glass, copper tabs, and solar cells at low-cost and with a negligible amount of contamination by other materials, resulting in a clean residue-free surfaces [107]. However, a complete structural change represents a challenge for this novel structure to overcome in the long run and represents a significant investment in terms of changes or new setups in production [39]. Drawbacks are related to stability. The additional film leads to a reduction in stability and diminished optical properties. Although L-F technology may not have optimized optical losses and heat management, making it likely cheaper in €/kW but more expensive in €/kWh, it represents a first step in the direction of a circular economy [39].

Similar to the NICE technology, the "TPedge" module concept applies an edge seal consisting of a thermoplastic spacer (TPS) filled with drying silicates and silicone to a frameless module filled with gas (Figure 4.2 **(c)**), promising good reliability [13]. These modules, despite not having a high-yield design, aim to lower module costs through shorter production times achieved by eliminating the bottleneck lamination step, along with lower module material costs with savings on encapsulation and frame [13].

A similar route, that recalls the design of L-F modules architecture of NICE and TPedge technology, is adopted by Biosphere Solar.

4.1.2 Introduction to Biosphere Solar

Biosphere Solar is a Netherlands-based start-up with the goal of establishing fair and circular standards in the solar industry market. The company is developing a novel and unique design for laminate-free solar modules. Similar to the NICE and TPedge concept designs, the general structure of Biosphere Solar panels consists of dual glass modules with an inner frame supporting the matrixed cell structure and outer edge sealant components. The primary edge seal is made of PIB, while the secondary edge seal is made of silicone, providing module encapsulation and protection.

The core structure, designed to avoid lamination, includes cell encapsulation and edge seals, which are fundamental and common elements in all Biosphere Solar module prototype designs.

Biosphere Solar's mission and strategy focus on disassemblable PV module manufacturing, developing L-F technology through open-source, low carbon footprint, resource-conserving production processes, and ensuring

a reliable and transparent supply chain. As with all early-stage concepts, Biosphere Solar's L-F modules may carry increased vulnerability compared to standard and long-proven laminate panels, despite being the goal for a longer lifetime through re-use and a lower degradation rate. Further, complete circularity is aimed for, with end-of-life options ranging from high-value refurbishment, upgrades, repairs, and reuses to full recyclability, reclaiming all end-of-service-life panels for circular treatment. The vision of Biosphere Solar revolves around three main pivotal drivers: circular economy, fair working conditions, and sustainable standards.

Biosphere Solar modules are designed for various applications, targeting end-users in rooftop segments, field-mounted projects, and utility-scale solar parks. The outer structure, similar to frameless G/G laminate modules, may be adapted for BIPV (Building-Integrated Photovoltaics) due to its aesthetical appeal. While the ins and outs were explained in Chapter 2, a major limitation of a G/G structure is the increased weight, risk of breakage, and installation concerns [13].

4.1.3 Production Roadmap of Biosphere Solar

In the years 2020-21, Version 0 was developed: the very first prototype served as a reference model for future evolutions. In 2023, design Version 1.0 was launched as a compatible product on the market. A fully sustainable solar proposition (Version 2.0) will be released allowing for large scaling and industrialization. From 2025 onwards, research and development will enable the rollout of Biosphere Solar's Version 3, a low-cost lightweight product for global markets. Since the very first module version (V0), different architectures and assembly techniques have been developed as well as tested with continuous improvements, progressing up to the latest Version 2.0, the focus of this report. For each newer version, a series of factors are studied and improved, such as efficiency, energy conversion, rigidity, modularity, aesthetics, thermal and optical continuity, durability, degradation rates, etc. The goal is to revolutionize conventional module technologies, increase sustainability, and reduce costs. Moreover, the development is also related to the DIY (do-it-yourself) kit, which serves as an additional mini panel, acting as an educational tool. This enables individuals without extensive training to safely dismantle the module without compromising critical components. The mini panel is utilized to enhance the design of larger modules through feedback and iterations.

4.2 Biosphere Solar: Laminate-Free PV Module Architectures

This chapter, a core part of the product design, explains the L-F PV module designs developed by Biosphere Solar with a focus and a detailed analysis of the architecture Version 2.

4.2.1 PV Module Architecture: Version 1.0

During the first months, the research focused on understanding the core structure of this version design and its manufacturability, including experience at the production line. It consists of a fully sized G/G module manufactured at the partner factory Soltech in Belgium. The module is intended for pilot and demonstration purposes and will be tracked and maintained by Biosphere Solar throughout the project length. The module uses front metallized mono c-Si Bifacial PERC solar cells. Future iterations of this version module will aim for higher efficiency, lower weight, and cost.

In contrast to L-solar panels, new terms are emerging: cell-bed matrix, joints, string, and edge spacers. The purpose of the cell-bed is to securely hold solar cells in position, offsetting the EVA absence, enhancing recyclability, and avoiding collisions. String spacers are used to maintain the position of cell strings between adjacent strings. Solar cell holders (or joints) stabilize solar cells, alleviating pressure on the soldered busbars connecting two adjacent cells. These are neatly closed into the two slits placed between two cells (Figure 4.4). Several designs of cell-beds were engineered by Biosphere Solar with additional features to enable modular interconnections. Similarly to the glazing industry, the module employs an Insulating Glass Unit (IGU) spacer frame as a mechanical support and security from the outer environment. The IGU bar is secured with corner connectors within which desiccant beads (made of silica gel & oxygen absorber mix) are added as separate cloth sachets into the space bars to prevent moisture ingress and penetration, thus protecting cells and maintaining contact between the front and rear glass. At the module edges, to offer additional encapsulation and protection from weathering, butyl tape serves as a primary seal material and silicone as the second seal, dispensed and pressed into place. Figure 4.3 illustrates a visual depiction of the panel and its encapsulation structure.

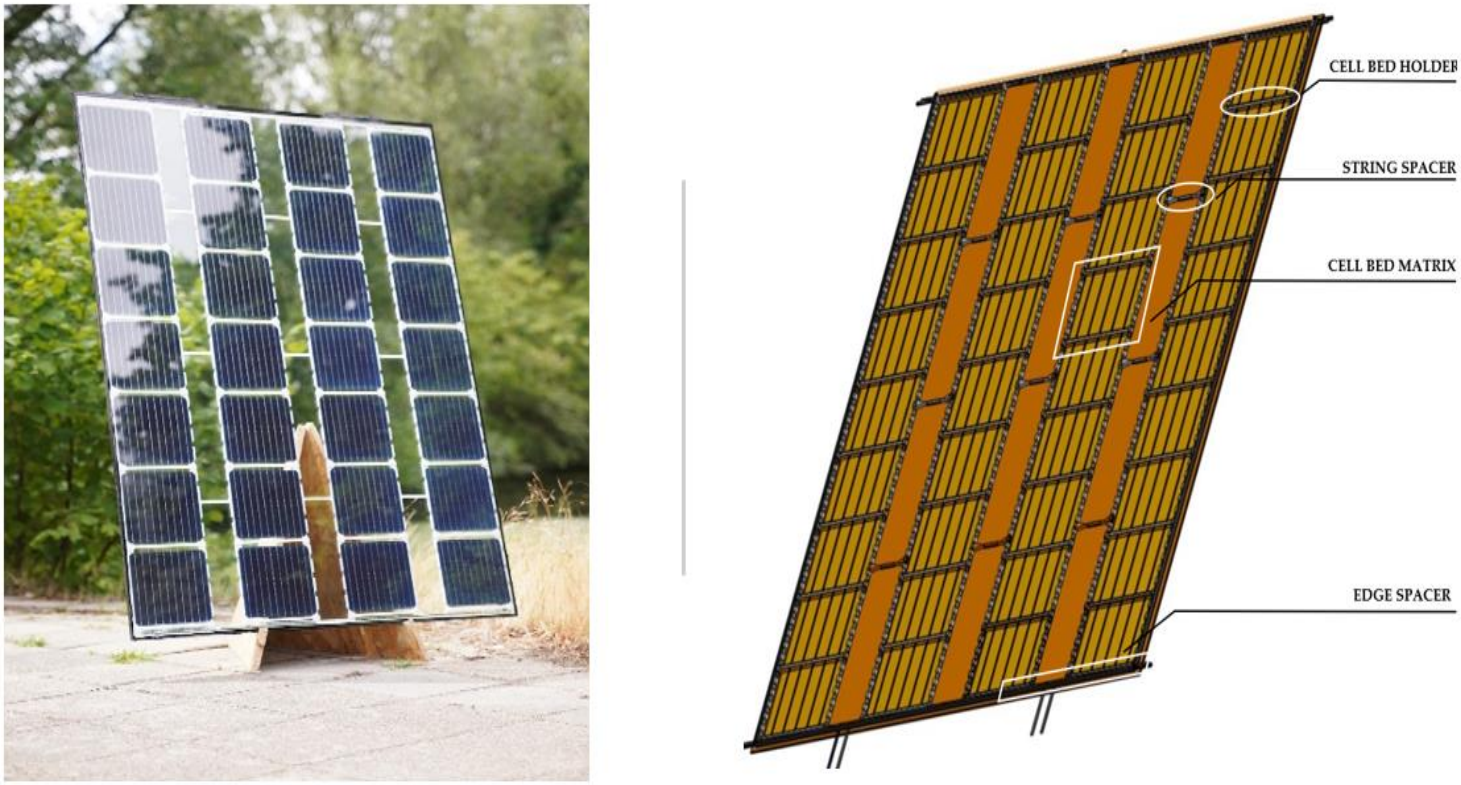

Figure 4.3 - (**left**) Photograph of Biosphere Solar PV module (V1), (**right**) panel cross-section view of the cell encapsulation structure.

The latest manufactured Version is V1.1, designed for pilot projects and testing purposes. The module is composed of 144 or 120 half-cut PERC Bifacial cells, minimal cell spacings, an increased active area, with a theoretical power output of 392 [Wp] (watt peak). The panel comes with a glass/frame clamps mounting system. Biosphere Solar is working towards the creation of a circular product passport labelling with the expectation of a low carbon footprint.

With its uniform appearance, this L-F module provides an edge-seal as well as a polyester film to secure the cells. Alternatively, a PVB lamination[2] could be applied to the front and rear glass panes for enhanced post-breakage performance. However, many aspects of the module are still under research such as thermal profile, IV-curve, fill factor, fire rating, and projected lifetime.

4.2.2 PV Module Architecture: Version 2

The second version, the subject of this thesis, is a rigid and frameless G/G construction type designed for fully disassembly. It is a double edge-sealed, fluid-filled, L-F PV module. It features two glass panes interconnected via an inner frame for mechanical rigidity. The rigid solar module comes in two different designs:

- A minimal transparency version of a 120-cell module, composed of 12 strings
- A 40% transparency version made of an 80-cell module

As the Version 2 modules are in the designing and development stage, subject to potential changes, the 120-cell module is the version considered for this report. Comparisons with the 80-cell module will be made, even though exact string layouts have not been specified yet. Moreover, the 120-version module is a high-packed module with minimal cell spacing and more challenges to be addressed.

Both module designs have standardized dimensions. The solar cell technology employed for this module is the highly efficient ZEBRA-IBC bi-facial in a standard half-cut format M6. Each cell string is aligned and positioned on an electrically conductive backsheet, utilizing this novel technology that employs a PCB with traces onto which a metal solder paste is injected. Solar cells and strings are automatically interconnected using low-temperature (low-T) soldering techniques. The assembly is held in place using an inner frame, a matrix structure of cell spacers

[2] Poly Vinyl Butyral (PVB) is a durable plastic resin used between two panes of glass to bond them together

integrated. The perforated and customized CB foil comes with incorporated cell spacers, and it is fixed onto the glass plate via the built-in adhesive layer either attached on the CB substrate or deposited on the glass plate. The module edges are protected by two extruded single-component sealants. Firstly, a warm edge-spacer film containing PIB with integrated desiccants is deposited between the glass substrates. Subsequently, a silicone component acts as a secondary edge sealant, filling the module and reaching the outer glass edges. The inner volume is filled with a fluid agent intended to provide passive/active cooling, optical continuity, and adequate pressure to keep cells in place towards the CB. Wires are electrically connected to a standard JB, positioned in the middle rear-side of the module with a three-part JB.

The distinct signature of this module arises from all the parts and materials, accentuating its circular characteristics.

The non-transparent version could be targeted, for instance, to fields-applied and integrated PV, while the 40%-transparent version for floating projects and/or agrivoltaics, to exploit the bi-faciality factor of the dual facial cells and where a larger level of direct sunlight is demanded.

The design configurations of the components have been adjusted and developed from the previous designs. For instance, it was previously planned to assemble the panel with front and rear glass substrates embedded together, creating a click-fit between two parts: TOP cell-beds and BOTTOM cell-beds. These are connected to the front and rear glass, respectively, by a UV-cured adhesive dispensed in a pattern.

As illustrated in Figure 2.2 (Chapter 2), the trend for the newest generation of solar cells moves toward higher formats and an increased number of busbars per cell intended to reduce metallization costs. The high-yield, high-quality IBC cells, as previously argued, are powerful and long-lasting commercially available cells but also feature favourable aesthetics due to their uniform dark colour. Furthermore, the rapid growth of IBC cell manufacturers such *as Valoe, Longi, Maxeon* is constantly increasing, even though it is an expensive niche product. Within the IBC solar cells, the ZEBRA technology stands out as a cell type for this study. Since several years of development, the bifacial IBC cell is a concept based on a standard industrial low-cost manufacturing process [18]. The half-cut format does offer benefits, including higher power output, increased modularity, and reduced Balance of System (BoS) costs. However, there are drawbacks connected to the increased manufacturing complexity, susceptibility to microcracks, compatibility issues and limited availability [40].

More importantly, the novel CB technology eliminates the need for expensive cell-to-cell interconnection soldering, quickening the manufacturing process, eliminating the need for EVA encapsulant to fully minimize PID losses as well as refurbishment of the modules, and, ultimately, recyclability. These advantages may be offset by potential complexities in manufacturing and assembly, leading to an increased total cost, given the niche and novel nature of the technology. Furthermore, due to the customized design approach, it may be considered a non-standard concept within the solar industry, limiting availability [18]. By using the screen-printed CB, part of the required electrical conductivity can be transferred from the cell metal grid to the superstrate metal foil material(s), thus reducing paste consumption [18]. More precisely, a dispensable Cu paste can be a potential method applied to the circuited traces of the CB. On the other hand, as seen in Chapter 2, the ECA is a printable high-processing temperature (high-T) soldering, while low temperature (low-T) soldering with injectable paste is a valid alternative for the heat-sensitive cell spacers. This can further reduce electrical consumption in manufacturing and maximizes solar cell recovery and recycling.

Regarding the module construction type, the market share of frameless double glass is projected to increase [13]. The choice of a frameless glass/glass (G/G) configuration stems from the benefit of impeding leakage current pathways, thereby reducing PID impact and eliminating the need for aluminium frames and associated processing. However, considering the necessity for thicker panes than framed laminated panels, these modules are heavier, more prone to glass breakage, and likely feature less rigidity [13].

4.2.3 PV Module Version 2: Componentry and Specifications

The following section investigates module parts and materials, addressing factors relate to manufacturing.

4.2.3.1 Glass Panes and Solar Cells

The glass used in the solar industry is typically a processed low-iron float glass optimized for solar applications. In 2023, available standard thicknesses for glass panes range between 2 to 4 [mm]. According to [112] the expected trend in front side glass thickness is a reduction to 2 [mm]. Thicknesses below 2 [mm] is not expected to have significant market share [112].

The two glass sheets used for this report are coated with durable ARC and ASC, preventing surface dusting and contamination, maintaining consistently high light transmission [41].

The dimensions considered for the glass sheets are 1040 [mm] x 1776 [mm] x 4 [mm] for both front and rear panes. Thinner glasses may be considered, but these are likely to cause issues in the long run due to the lower mechanical rigidity of the module, especially with no frame. Conversely, a 6 [mm] glass would significantly increase the module's weight and no longer falls within the standardization. A 2.5 [mm] glass thickness for both front and rear sheets balance the module's overall weight to be on a par with a 3.2 [mm] laminate G/B [13]. Tempered glasses come ready-to-use with three pre-drilled holes at the back for JB connection and attachment. Conversely, laser drilling after tempering would be an expensive option.

The ZEBRA cell technology is bi-facial cell used to collect all the current at the back side, reaching a conversion efficiency of 23.4 % [42]. The manufacturability and specifications of ZEBRA cells within the structure are disputed in Section 4.2.4.1. If a different BC cell technology were chosen, such as MWT, the change would reflect in manufacturing, specifically in the design of the conductive foil, paste deposition and soldering systems.

For FBC metallization cells, this panel assembly design would hardly be suitable. A different approach for the interconnections would be required. For instance, a classic tabber and stringer or an innovative ECA stringer would be more appropriate as assembly methods.

4.2.3.2 Cell Spacers (Inner Frame)

One distinctive feature of these modules is the inner frame for cell encapsulation, which is made of thermoplastic materials that soften reversibly upon heating and harden when cooled down. The cell module spacers must meet the requirements of impact resistance, module rigidity, and stability.

Acrylonitrile butadiene styrene (ABS) and acrylonitrile styrene acrylate (ASA) materials can fulfil these requirements, constituting core parts of the module structure. ABS is a thermoplastic material with an amorphous polymer. It stays hard even at low temperatures, resistant to impact, abrasion, dimensional stability, and strain [43]. It is a highly versatile type of plastic used in various manufacturing areas. The glass transition temperature of ABS is around 100 [°C] [44]. Similarly, ASA filament is a versatile thermoplastic suitable for many applications, with improved weather resistance, broadly adopted in the automotive industry [45]. Another polymer studied by Biosphere Solar is polycarbonate (PC) with a glass transition temperature slightly higher than ABS, of roughly 150 [°C] [45]. It is a UV non-resistant and impact-resistant polymer used in fields for thermal stability and biodegradability. Cell spacers do not touch the cells' corners to avoid the risk of cell warping and further breakage. Solar cells and spacers analysis, dimensions, and drawings are provided in Figure 4.11 and Table 4.2. Dimensions and configurations of cell spacers will be widely discussed in Section 4.2.4.1.

4.2.3.3 Conductive Backsheet and Adhesive Film Substrate

A conductive backsheet, resembling a PCB commonly used in electronic devices, is typically made of materials possessing conductive properties. These often include metal compounds like Al, Cu, or Ag integrated into a polymer matrix to create a flexible and durable sheet [28]. Standard backsheet thickness for laminate modules is in the range of 0.1 to 0.4 [mm] depending on the type and selected structure design. The customized conductive foil design provided has dimensions of 1010 [mm] x 1746 [mm] (W x L). The CB thickness, seen as an additional layer (metal layer) to the standard laminate panel's sheet, was assumed to be between 0.3 and 0.4 [mm] [7].

To avoid soldering ribbons, a standard CB foil is scribed with metal trace tracks on its superstrate, and a solder mask is applied for the cell and string soldering. The dimension of a printed trace encompassed on one half-cell is 1.05 x 83 [mm] (W x L). The thickness of the printing scribe adopted is 20 [µm]. Higher printing traces are possible but may require multiple screen printing or extrusion steps (Expert input: *member of Copprint).*

The possibility of having freedom in super and substrate architectures, along with the desire to minimize manufacturing time and costs by avoiding additional assembly equipment, this, has led to a customization option design. A top-view drawing is provided as a visual in Figure 4.4.

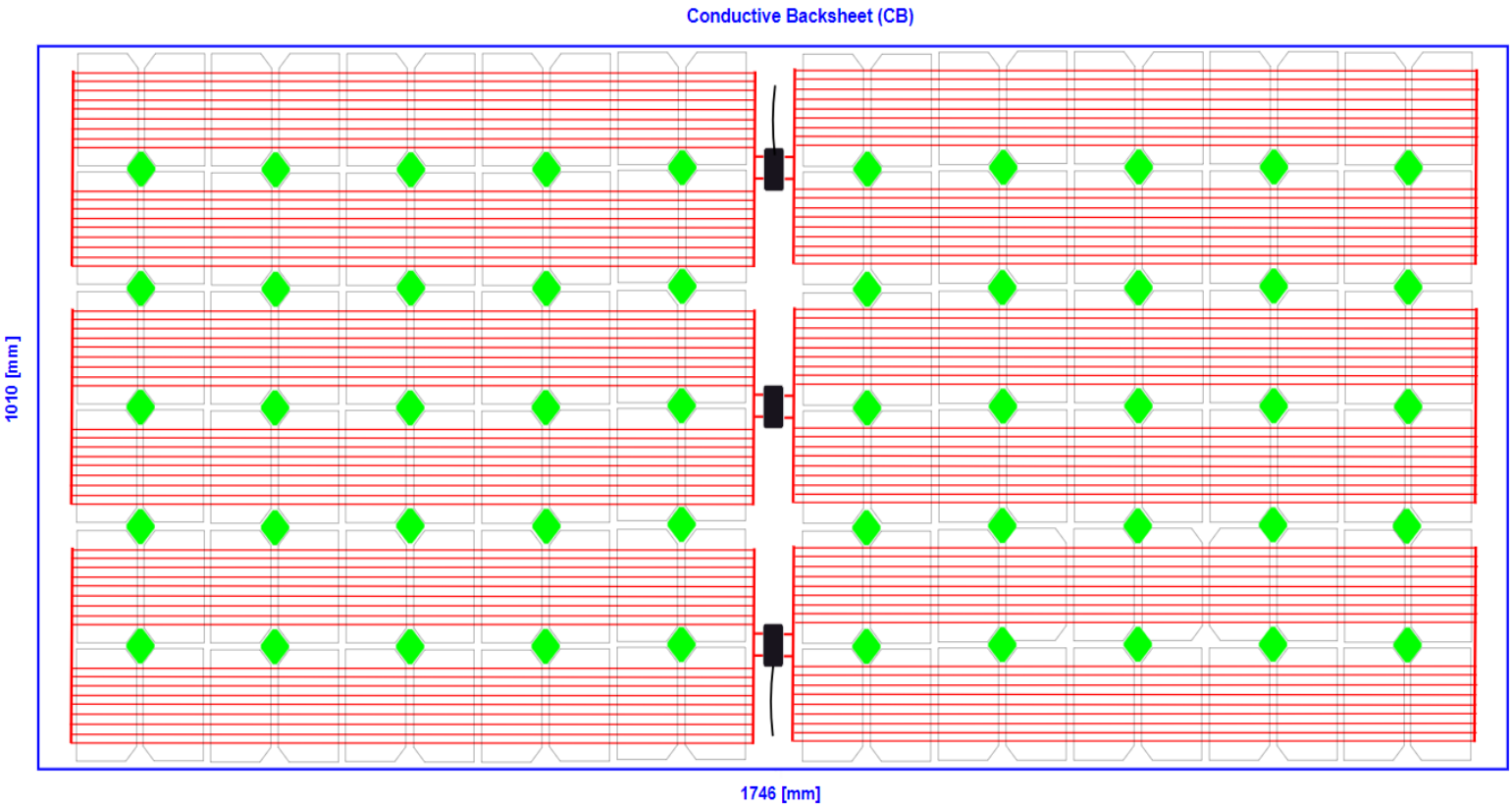

Figure 4.4 - Schematics of the top panel view with trace patterns (red lines), solar cells and cell spacers (in green), three-part JB included. The enclosed blue rectangle represents the CB with W x L dimensions in [mm].

The width of a single BB cell and that of a soldering trace are both 1.05 [mm]. Traces of one string consists of 10 solar cells with a 2 [mm] spacing between two adjacent cells as well as strings; therefore, its length is approximately 0.85 [m]. The total length over the 108 traces (12 strings) including the busbars strips lengths (for string interconnection), reaches 95 [m] per panel.

When sourcing a suitable glue material, requirements should account for its thermal and chemical stability to temperature swings, low shrinkage, high-track adhesion, optical transparency, resistance to thermal cycling, and cost-effectiveness [46]. In particular, the chemical properties are related to resistance to moisture, solvents, and fast curing. Fast curing is essential to allow short processing time in the manufacturing. All these requirements are aimed at the long-term sealing performance. The conditions to meet also include safety, health, and ecological concerns to comply with.

Adhesive materials needs be applied (in a pattern) so that air is not trapped. Usually, silicone dielectric gels are used as they are formulated especially for encapsulation of electronic components and assemblies requiring protection from exposure to high temperatures (Expert input: *member of Gelest*). As the adhesive film is going to be in contact with the liquid filler, this must not be a soft agent preventing significant swelling.

Alternatively, non-adhesive material such as cured silicone gels with adhesion primer may be another option for use, being highly flexible and without any stiffness built into them (Expert input: *member of Gelest*). The use of primer formulation and cure heat would probably be required. Unlike adhesive materials, no air-trapping issues may be encountered when curing the non-adhesive product as it may contain platinum addition cure silicone and do not require moisture or air to cure, which will cure in thin bond lines. This will ease the layup process in the manufacturing.

These products might swell in the presence of a fluid filling agent (such as dimethylsiloxane). For long-term sealing, in the presence of some types of fluids, in aerospace and automotive applications, typically a fluorosilicone or phenylsilicone adhesive/sealant is used (Expert input: *member of Gelest).*

Both adhesives and non-adhesives may have issues related to processing in manufacturing and/or costs. Their application method and processing, for instance, the curing time can take up to hours; therefore, other types of adhesives are also examined.

Another potentially employable category is UV-cured materials. While not standard for PV/solar applications, they are utilized, for instance, as hard coats for optical discs or to enhance display performance. They are generally compatible with a wide range of materials, but it is essential to consider the formulation of the adhesive and properties required for the module. The UV-cured compounds are environmentally safe, have fast processing time, and are formulated in rigid, semi-flexible, and flexible grades. The specific grade varies in viscosity, hardness, thermal, and electrical properties. These blends polymerize when exposed to the proper wavelength/intensity of UV light. For certain types of UV adhesives, such as epoxies, acrylates, urethanes, the cure formulations require no heat and shorten lead times. These products can be dispensed manually/automatically with little manufacturing space [46]. However, additional equipment in manufacturing may be required to achieve the intended grade of curing in a short cycle, such as dedicated UV-curing equipment.

The rigid UV and dual curing adhesives may also be considered as good candidates (Nanosilica, dual UV/heat cure). These are featured in good heat exposures swings, and high optical clarity for the backside light absorption. The product cures on demand for precise alignment between substrates requiring exact positioning. UV-curable hard coats are fit to many chemicals' substrates, including polycarbonates and safety glasses. The curing speed is in seconds to several minutes with a thickness of a few microns to about 3 [mm] [46].

At the initial stage of this research, the designs intended was to bond only the cell spacer's substrate with adhesive. This was achieved by applying a bead of adhesive glue around their perimeter, directly onto the rear glass plate. However, after some considerations, it was decided the potting dimensions to encompass the entire CB area, bonded with an assumed thickness between 0.1 and 0.2 [mm]. Based on this, the total volume of glue required for a single panel is the range of 0.3 to 0.4 [L]. However, the selection of UV-curing agents is very challenging as some formulas would be relatively exothermic, and not intended for large bonding areas. Additionally, they offer a relatively high linear shrinkage (about 1-2 %) which may cause issues such as peeling or curling on a large scale (Expert input: *member of Masterbond.com*)

4.2.3.4 Conductive Metal (Solder) Paste

The metallization scheme, utilizing isolation paste in selected module areas makes back-contact solar cells, particularly emphasized in this study focusing on ZEBRA cell, compatible with module technologies using interconnection by soldered ribbons, as well as those based on electrically CBs. This leads to greater flexibility in the assembly processes [18].

When selecting solder pastes, one of the challenges is to ensure that the parts maintain high quality for the soldered joints and to adapt the paste formula to factors such as processing properties in manufacturing for that specific application. Typical properties of the paste require: excellent joint strength and oxidation resistance, gap-filling ability, and non-leaching characteristics (Expert inputs: *member of, TechconSystem, Rotec)*.

There are properties of the alloy and flux performance that are very important for the selection of both deposition and soldering methods as well as processes. First, it is essential to know whether the alloy should be lead or lead-free and to comply with toxicity regulations. Some applications are exempt from being lead-free because the reflow temperature requirements can only be met with high-lead solder alloys [47]. An illustration of some lead and lead-free alloy formulas as a guide is presented in Table 4.0.

Table 4.0 - Alloy temperature guide for leaded and lead-free types: the two categories include the alloy type, solidus and liquidus state temperatures [47].

LEADED ALLOYS			LEAD-FREE ALLOYS		
Alloy	**Solidus (°C)**	**Liquidus (°C)**	**Alloy**	**Solidus (°C)**	**Liquidus (°C)**
Sn43 Pb43 Bi14	144	163	Sn42 Bi57 Ag1.0	137	139
Sn62 Pb36 Ag2	179	189	Sn42 Bi58	138E*	
Sn63 Pb37	183E*		Sn96.5 Ag3.0 Cu0.5	217	219
Sn60 Pb40	183	191	Sn96.3 Ag3.7	221E*	
Sn10 Pb88 Ag2	268	290	Sn95 Ag5	221	245
Sn10 Pb90	275	302	Sn100	232MP**	
Sn5 Pb92.5 Ag2.5	287	296	Sn99.3 Cu0.7	227E*	
Sn5 Pb95	308	312	Sn95 Sb5	232	240
			Sn89 Sb10.5 Cu0.5	242	262
			Sn90 Sb10	243	257

* Eutectic – Solidus and Liquidus are equal ** MP -Melting Point

The best ability to spread and adhere to the surfaces being joined, known as “wetting”, in soldering is achieved at a peak temperature 15 [°C] or more above the liquidus state [47]. This process occurs when the metal(s) of the paste merge with the metal on the PCB traces, causing the solder to become fluid and flow along components and substrates, thereby creating the necessary solder joint. Therefore, if the lead-free alloy is the selected material, the low melting temperature from solidus to liquidus is limited to Sn and Bi-based compounds. If Cu is desired in the paste composition, the melting temperature should reach 219 °C (3rd row of lead-free alloys) to become liquidus, which may cause cell spacers to deform [47].

Besides the melting temperature, the particle size of the paste elements is also significant for the manufacturing requirements. Using sizes that are too large can cause printing and dispensing difficulties, compromising quality. Conversely, powder grains that are too small come with increased costs.

Another property to carefully consider when sourcing for the right paste is the flux category available, which relates to the activity levels and physical qualities of their residue. The term “activity” refers to the ability to prevention oxidation from metal surfaces during soldering. These can range from a Rosin flux with very low activity, suitable only for easy-to-solder surfaces, up to the “Water Soluble” flux (activators, thixotrope, and solvent) which can range from no activity to extremely high activity levels for soldering even the most difficult surfaces, such as stainless steel [47].

Based on the above, the paste requirements for L-F module manufacturing are to be designed to enable low-temperature surface mount assembly technology with a low melting point, preferably lower or equal to 140 °C [48]. Additionally, a fine grain structure offers better resistance to thermal cycle-based fatigue. The components used for the paste needs to be lead-free to prevent the formation of intermetallic with a low melting point and be compatible with all commonly used lead-free surface finishes [48].

The ability of the filler metal to spread out and be well-joined over conductive substrates is a fundamental feature to achieve good soldering results. To suit different application methods the behaviour of the paste should be accurately designed. Generally, thin-layer application methods like thin printing or spraying require more formulations, whereas dispensing or thick-layer printing requires higher viscosity [49]. Therefore, not only the formula of the alloys and their grades but also the dimensions of the paste compound are essential, as they are correlated to the manufacturing process to be configured. A thicker or wider paste film may require a different assembly method and/or a longer processing time to achieve good solder quality.

Pastes are based on a CB trace’s filler metal selection and solar cell ribbons. Considering 9 traces per string (per polarity) and 12 strings in total, 108 traces must be soldered with appropriate conductive paste (Figure 4.5). Paste alloys such as Cu or Tin/Bismuth/Silver-based (Sn/Bi/Ag) are deposited onto the 108 straight traces via a dispensing/printing method. Similar to the conventional busbars and tab wires' thickness [50], the deposited paste dimension over one trace of half-cell is assumed to be 1 [mm] x 83 [mm] x 0.2 [mm] (W x L x H) The total volume of paste required is about 20-25 [cc] (cubic centimeter) per panel. A detailed evaluation of the required paste is provided in the last section. Further specifics are in Table 4.3, detailing the manufacturing method examined in Chapter 5.

Making wise solder paste selections is fundamental for manufacturing high-quality and durable L-F solar modules.

4.2.3.5 Primary and Secondary Edge Seals

PV modules are consistently exposed to extreme conditions, including heat, cold, moisture, UV radiation, and wind. To safeguard the module components against aging and functional impairment, excellent sealing is imperative. Edge sealing between glass or frames prevents the intrusion of water and other contaminants, drastically reducing gas diffusion [51]. Therefore, their dimensioning is crucial for long-term durability. (Figure 4.5). However, sealants are susceptible to degradation, which can lead to the opening of cracks, facilitating the diffusion of fill gasses. Moreover, they must withstand the internal loads and environmental factors, including atmospheric pressure fluctuations that can cause expansion or contraction on components, including the fill liquid [108].

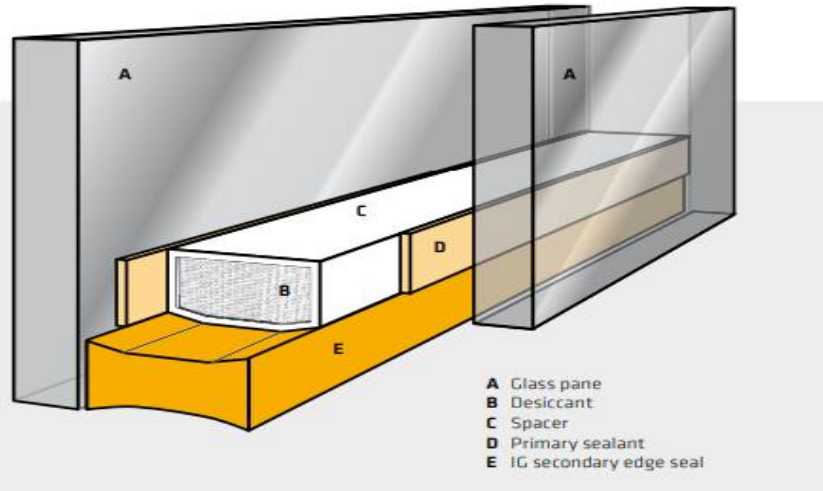

Figure 4.5 - Overview of the warm edge system in the glazing industry [52], [53].

Abundant adhesive materials, available in either single or dual-part components, such as Polysulphide, Poly-Isobutylene, Silicone, are already widely used within the glazing sealing market. These are excellent encapsulant agents also suitable for adoption in L-F solar module production [52]. The high seal spacers for this L-F module architecture are composed of one-part components: the 1st and 2nd edge sealants are hot melt PIB and Silicone, respectively.

4.2.3.5.1 Poly-Isobutylene (PIB) – 1st Edge Seal

Edge sealing using butyl tape has historically been the go-to for manufacturers. However, increased downtimes, lack of flexibility, and material waste that is often overlapped in the corner positions contribute to manufacturing process inefficiencies. On the other hand, the hot melt PIB provides a superior seal against moisture ingress compared to butyl tape used in the prior module version. It is a tried and tested warm edge technology widely manufactured and used for structural glazing in the construction and insulating glass industry (Expert input: *member of Graco*). The product to adopt, either tape or hotmelt, should not be electrically conductive.

The primary edge seal adopted for this report is hot melt PIB, a thermoplastic rubber type with an integrated desiccant for dehydrating the space between the panes [53]. It is heated up to +110 [°C] and 140 [°C] to be processed and dispensed on one of the two glass substrates. It provides stability over a large range of temperatures, and it optimally functions as a spacer as well as a sealant [51] [52]. As a first-level seal, it is featured by an extremely low moisture transmission rate and gas permeation. Additional advantages of this material include improved thermal resistance, and optimal adhesion properties to glass, spacer bars, and silicone-secondary sealant [52], [53].

The lifetime of the PIB edge seal can be estimated through damp heat and other standard certification testing. Studies show the lifetime of an IGU sealing to be roughly 25 years [53]. The NICE module technology featured a 10 [mm] width sealing line, which is sufficient to assure humidity tightness for long-term performance [54]. Similarly to the NICE technology and glazing industry products, the edge spacing left for the PIB in this study is also 10 [mm]

width, meeting the minimum required distance through insulation (DTI) requirements [55]. The total extruded volume, with given dimensions of 10 [mm] x 5532 [mm] x 3 [mm] (W x L x H) is in the order of 160-170 [cc].

4.2.3.5.2 Silicone - 2nd Edge Seal

Silicones have been used as encapsulants since the early days of PV history due to their robust properties, offering significant benefits, especially for space applications. However, during the commercialization process, the material nearly disappeared from the market as EVA became more cost-effective [39] [56]. Silicone gels or films are well-suited as encapsulant agents for the PV industry creating an airtight seal between panes [39]. They offer high resistance to temperature and external influences, durability, and low mechanical stress in modules. Other properties of silicone gel encapsulants for solar panels include inertness, transparency, extended lifespan, recyclability, and cost-effectiveness [56].

This sealant agent is applied at the edge of the panel, between the glass sheets and the outer side of PIB, with the function of bonding and sealing, with a volume shrinkage of only 4% [57]. It is a neutral-curing one-component material with very high mechanical strength, and excellent adhesion to various substrates. Its applications range from the domestic appliances industry to renewable energy for frame bonding, sealing, and potting of JBs [57]. Most importantly, the second sealing is accurately dimensioned to ensure it withstands most loads and secures the primary seal. The dimensions of the silicone around the panel perimeter are 5 [mm] x 5572 [mm] x 3 [mm].

4.2.3.6 Module Filling Agent

The aim of the fluid filler in L-F solar modules is to enhance the panel performance through better cooling, optical coupling, and cell encapsulation.

The output of a solar module decreases as the operating temperature of the cells increases above Standard Test Conditions (STC). Thus, it is desirable to keep the operating temperature of the PV cells around STC. To address this issue, the PV module should be exposed to the entire solar spectrum while heat is extracted by means of circulating gas or liquids [58]. In traditional solar modules, lamination reduces reflection because the encapsulant materials have a refractive index matched to glass, resulting in good ‘optical coupling’. In L-F modules, it is crucial to consider optical coupling and how encapsulation transmission changes during aging by filling the module at the front glass/cells interface [13]. Filling the module with a fluid agent may help address this issue.

In the IG industry, the filling between the two glasses is accomplished with a gas element rather than a liquid. The most common gases used are argon, krypton, or xenon due to their low thermal conductivity, which helps improve the insulating properties of the glazing components. Gas filling agents are already market-proven and tested, especially in the IG industry. Liquids are not used in the glazing field due to their potential to leak, which could compromise the integrity of the only edge seal present and reduce the insulating properties of the module. Moreover, using gas prevents issues such as condensation and keeps the product weight low. Gas-filled G/G modules have an optical discontinuity at the internal glass/air interface. Therefore, they require internal ARCs on the front glass to reduce reflection losses [13]. Simulations in nitrogen (N_2) filled double glass NICE modules, compared to those with EVA encapsulant, reported a 0.6% lower power output due to poor optical coupling, and adding a silicon dioxide (SiO_2) capping layer on the cell was suggested to improve the ARC [13]. Argon increases the temperature, and gas-filled modules are more sensitive to temperature swings, in which the gas may convert into heat and expand. On the other hand, liquid filling increases optical continuity while maintaining thermal stability. Better performance can be achieved when bare c-Si solar cells are immersed in liquids for enhanced heat removal and optical continuity. However, the liquid agent should meet the following requirements to optimize the performance of L-F solar modules [59]:

1. good heat transfer performance
2. match of the sunlight absorption by the liquid (be transparent) with the spectral response range of the c-Si solar cells
3. chemical and thermally stable, also when in contact with other materials of the module
4. non-toxic, non-reactive, non-corrosive, electrochemically neutral
5. heat gain potential, non-flammable
6. low economic cost

Since, neither a set nor a specified fluid filler is provided, the research explores various possible options for the filler. Based on these and their trade-offs, the barriers in manufacturing are to be identified and addressed.

There are several fluids potentially meeting the highlighted conditions, each with its pros and cons.

- Water is readily available and cost-effective with relatively good thermal properties. However, it has limitations regarding freezing point and corrosion potential, especially without additives or in cold climates. De-ionization is necessary to prevent ion formation and current conduction even though may still exhibit electrical resistivity.
- Glycols (ethylene, propylene) are common antifreeze agents mixed with water, possessing good thermal properties but have a certain degree of toxicity, may not be electrochemically stable, and require special care in handling and disposal (Expert Input: *member of TechconSystem*).
- Candidates for liquid fillers may also include molten salts (sodium and/or potassium nitrate), known as solar salt, valued for their thermal stability, used in some concentrating solar power (CSP) systems or prototype stages, and thermal energy storage.
- Other candidates are synthetic fluids (silicone or coconut oils) or dielectric fluids (transformer oils or synthetic esters) used in various industries, including electronics, automotive, and aerospace. For example, silicone oil, known for its thermal stability and resistance to oxidation, is primarily used as a lubricant, coolant, or insulator but is also utilized in PV panels for heat transfer and cooling, demonstrating stability as an encapsulant material for c-Si solar cells [58], [59]. Similarly, dielectric fluids used in some PV panel designs for electrical insulation and heat transfer can be produced in large quantities with straightforward chemical processes, resulting in lower production costs [59]. Moreover, experiments from [58], with a 10 [mm] thick liquid layer, shows that the liquid spectrum filters help keeping the PV module at low operating temperatures, thereby improving the performance. Biodegradable synthetic ester liquids with high fire point act as a dielectric coolant, removing heat from component areas [60].

Cooling properties, which are a complex combination of many factors including viscosity, density, heat capacity, and thermal conductivity, may affect panel performance and the manufacturing process. Additionally, refractive index and viscosity must be accurately considered for optical performance, influenced by cooling performance, and related factors. In particular, the viscosity, crucial for maximizing light transmission in solar panels, depends in turn on factors such as glass and solar cell characteristics, panel design, and environmental conditions.

It should be noted that when light reflects off a surface with a higher refractive index (greater oxygen content), a 180° phase shift occurs, leading to destructive interference. This phenomenon is utilized in ARC glasses. To minimize reflection losses at multiple interfaces (glass/liquid and liquid/c-Si) across different wavelengths, the refractive index of the liquid should surpass that of glass ($n \sim 1.3$). Fluid oils for optical applications are available in a broad range, offering various refractive indices and viscosities. Generally, refractive indices range from 1.3 to 1.7, with products tailored to exact refractive requirements [61]. Similarly, viscosities vary greatly depending on the agent, spanning from a few to several orders of magnitude [61]. Lower viscosity mediums generally exhibit better light transmission efficiency due to improved flow and spreading, minimizing air gaps, and enhancing contact at the medium interface [61]. In manufacturing, less viscous fluids allow for faster filling times and improved efficiency. However, they also present downsides such as more challenging process control and precision.

As there is no specified fluid for filling, the choice depends on the type and its properties, necessitating different settings and/or additional tools for the filling process. For example, under similar cost and material property considerations, an ester oil may be significantly more viscous, up to two orders of magnitude, compared to silicone oil [61]. This would require additional heating to adjust and maintain the working temperature during the process, introducing complexities and constraints in manufacturing.

The exact filling volume for this study remains undetermined, as it needs to account for the geometry of each spacer, cavities within spacers-solar cells, dimensional tolerances, and edge spacing of the CB. An approximate filling volume was estimated to be between 1-1.5 [L] (litre) per panel.

4.2.3.7 Junction Box (JB)

As outlined in Chapter 2, the JB serves as the module's primary exterior component, housing electrical connectors, cabling, and bypass diodes. Typically affixed to the rear side of the module via adhesive or soldering.
While one-piece “or split type” JBs are predominantly used for traditional frame components, split-type JBs are preferred for new dual glass double-sided components. Moreover, advancements in module design, such as half-sized cells, varied internal stringing methods, and multiple bypass diodes, have enabled the adoption of three-point JBs positioned at the centre of the module [13].

The split JB design aims at cost reduction and is continuously refined to optimize performance. It notably reduces the volume of filling and potting required through an optimized shell structure.

The decision has been made to adopt the three-split JB. However, the positioning choice necessitates a trade-off between a standard middle back-sided placement and a smart tail-edged placement. In Table 4.1 the benefits and drawbacks of these two configurations are analysed.

Table 4.1 - Pros (green) and cons (red) of two different JB configurations.

Middle back-sided JB	Tail-edged JB
Largely used in solar industry for standardized and laminated G/G modules (less expensive)	More aesthetically pleasant [13]
Less BB wire resistance for the string interconnection as the travel is halved	No likelihood for solar cell coverage if bi-facial cells are used (no loss in power output)
Simplified string interconnection design (bussing)	Less market availability than standard junction boxes (Expert input: *member of Valoe*)
Reduced cell/CB edge spacing as no solder trace must run through	Increased wire resistance due to the full module surface travel for metal traces
No punching edge seals option	Increasing the trace path: extra cost due to the additional raw materials usage (metal traces, conductive paste), processing time for assembly units to interconnect cell strings
Ease in using the same slits for flooding the module when vacuuming and filling (via an integrated and tailored JB) (Expert input: *member of Valoe*)	Rather thick patterned and room to leave at the CB edges to let the solder traces though
Weakest area to punch the rear glass pane (Expert input: *member of ECOPROGETTI)*	

Based on the considerations made above, the final decision is to adopt a three-point standardized middle back-sided JB, which is already utilized in laminated G/G module manufacturing. This JB configuration involves making two pre-drilled bores on the backside of the module for installation and sealing. To maximize bi-faciality yield, the approach is to position the middle cells ensuring they remain unshaded from the JB, thus minimizing cell power output loss on the rear side. An example of a standard 3-point JB model is depicted in Figure 4.6.

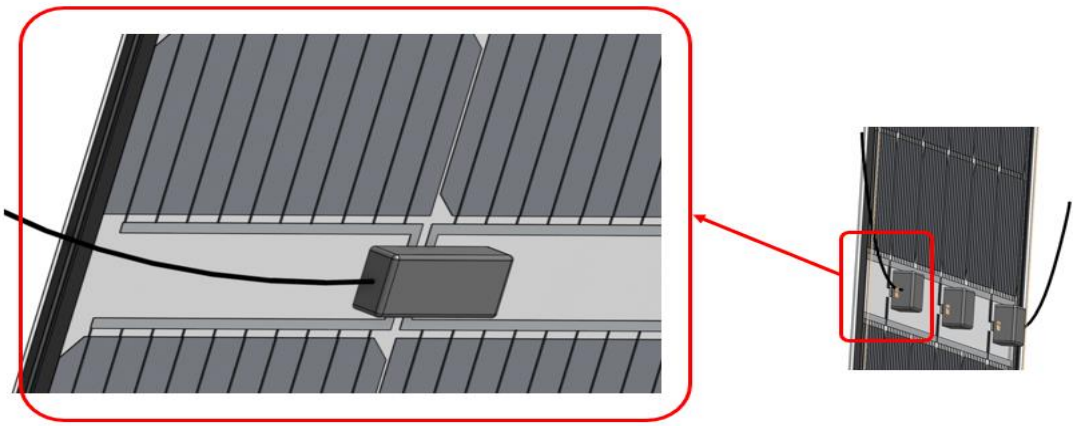

Figure 4.6 - (**right**) Visual and reference template of a 3-point JB and zoomed in (**left**) JB disposed at the middle-back side of the panel with the relative interconnections (Image: *Biosphere Solar*).

With the module assembly using a CB foil, there exists significant flexibility in installing and positioning the JB (Expert input: *member of Valoe*).

4.2.4 PV Module Version 2: Analysis and Manufacturability

In this section, solar cell orientations and cell spacer design options are explored first, followed by an analysis of the module components, specifications, and manufacturability.

The inner frame acts as a matrix of cell spacers, providing uniform support for the overall structure. This approach minimizes stress on the cells and regulates panel pressure. Since glasses typically exhibit slight waviness rather than being completely flat, larger glass sizes may result in increased panel instability. In such cases, the central

section may expand, complicating the mounting process (Expert Input: *member of Ecoprogetti srl*). The two glass sheets are parallel with identical dimensions but may not necessarily have the same thickness. Thicker rear glass may be chosen for stability, establishing a neutral axis for the cells, and reducing stress (Expert Input: *member of Ecoprogetti srl*). The decision has been made to utilize 2 to 4 [mm] glass plates with uniform dimensions, as exceeding a 4 [mm] thickness significantly increases module weight and challenges.

Reflections will be made regarding each half solar cell disposition and cell spacer designs to ensure a more robust structure, particularly in the central part of the module, where greater rigidity is required. These choices are also intended to streamline and enhance manufacturing processes.

4.2.4.1 Solar Cell and Cell Spacer: Configurations

A different solar cell technology is employed to the previous Version 1. This cell format, as depicted in Figure 2.1 and Figure 2.2 in Chapter 2, represents one of the latest generations of highly efficient solar cells (Figure 4.7 **(1)**).

In L-F modules, a compact structure is essential to replace the laminated encapsulant. This necessitates a robust and reliable design of the module components and architectural analysis. The orientation of half-cell strings significantly influences the module and its manufacturability in assembly. For example, changes in the architecture of cell spacers between solar cells correspondingly impact factors such as panel rigidity, raw material usage, perforation processes for the tailored conductive sheet, and positioning onto it. A representation of two different cell string arrangements for the adopted ZEBRA technology is shown in Figure 4.7 **(2).**

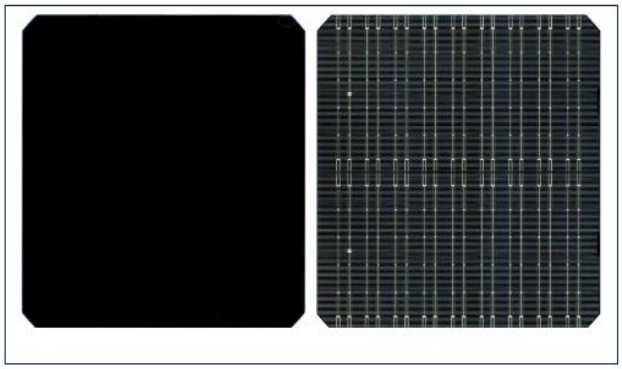

(1) Image of front and rear side of a full cut ZEBRA cell

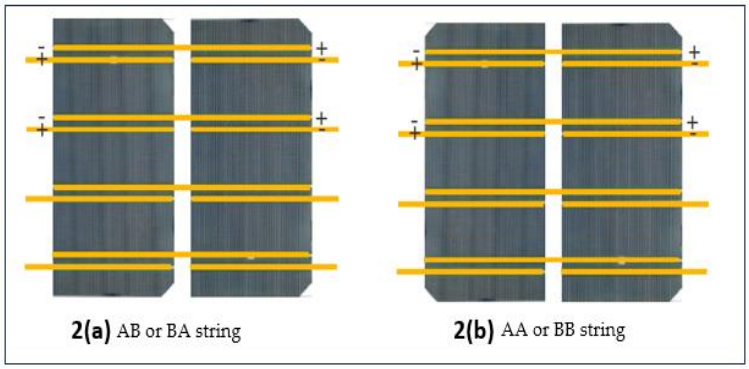

(2) Different cell interconnection orientation of the ZEBRA cell

Figure 4.7 - (1) Front (left) and rear (right) images of a ZEBRA IBC cell M6 and 9 BB format [42]; **(2)** The Half A and Half B cells in two different cell arrangement designs: **2(a)** AB or BA string with 180° cell rotation, **2(b)** two half-cut cells in AA or BB string configuration [43].

Throughout the development of this solar module version by Biosphere Solar, the solar cell orientation **2(a)** has been primarily utilized. However, the alternative of having the half-cell disposition as shown in **2(b)** should not be disregarded. Let us analyse these by illustrating the two different solar cell arrangements (**2(a)** and **2(b)**) along with two cell spacer designs in it (Figure 4.8).

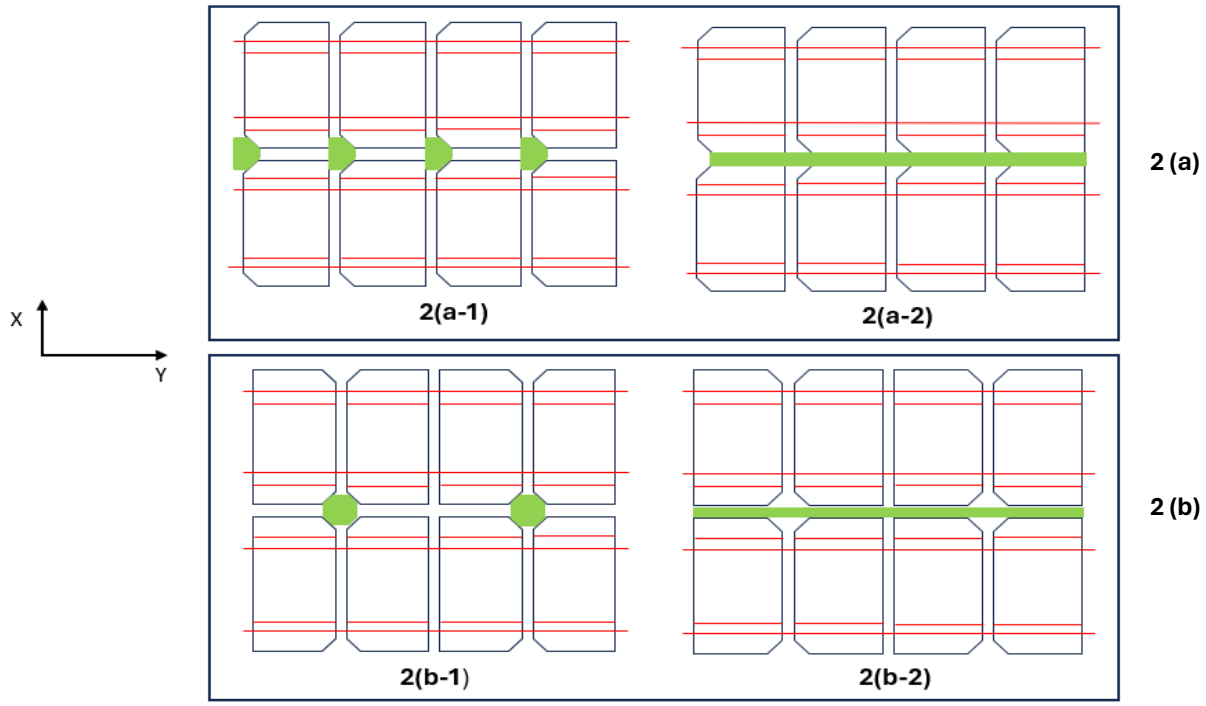

Figure 4.8 - Different half-cell arrangements and cell spacer geometry designs (green) between adjacent cell strings. The **2(a)-** string design refers to AB or BA half-cell configuration, including two different spacer geometries: **2(a-1)** half octagon-shaped, **2(a-2)** long rectangular-shaped. The **2(b)** layout (AA or BB half-cell arrangements) features two different spacer geometries: **2 (b-1)** octagon-shaped, **2(b-2)** rectangular-shaped. For simplicity, the drawing is not to scale with red lines representing BBs at cell edges only. The design is simplified to two strings of four half-cut cells. The drawing is the outcome of this research study.

String spacers are only positioned on the Y-axis (long straight edge) where no BBs run across, avoiding interference with the cell-to-cell interconnection stream. The **2(b)** solar cell arrangement (AA or BB) encompasses all corners of the solar cells, resulting in a larger and more robust structure. Streamlining the manufacturing of half-cells involves avoiding flipping or turning them 180° before the soldering process, as they may already be supplied in AA or BB configuration stacks. This reduces the number of operations required for automated layup systems, thereby reducing cycle time.

From a manufacturing perspective, the octagonal spacer geometry facilitates accurate positioning by the automated toolset due to its similar sides' length. Hence, there is no need to be turned into a specific XYZ coordinate positioning before alignment onto the customized CB. Another significant benefit comes from the number of sets and quantity of material usage. Using the simplified design **2(b-1)**, only two octagonal spacers are required. Over the entire 120-cell module, 50 octagonal sets are necessary rather than 100. This may lead to savings in raw material usage, time, and energy during production (by milling or moulding) and integration. Additionally, the **2(b-1)** geometry enhances module rigidity in the Z-direction, reducing the likelihood of breakage over time, particularly in the middle part of the panel, which may be the weakest.

The 2(b)half-cell orientation may offer superior benefits. Choosing between the **2(b-1)** or **2(b-2)** spacer configurations should consider overall module stability and its correlation with other components. Conversely, the cell spacers' **2(a-2)** and **2(b-2)** design options are unfavourable for stability reasons, manufacturability, and assembly operations due to the minimal distance between two strings in the 120-cell module (of 2[mm]), requiring highly precise tools and alignment systems.

Other spacer geometries were considered and represented in Figure 4.9. However, designs B and D, peaked towards the X-direction with a busbar edge-cell corner spacing of only 2.9 [mm] (panel metrics are illustrated in Figure 4.11), risk of obstructing the solder trace of the conductive foil for cell interconnections. Additionally, the risk is also associated with damaging or melting the heat-sensitive cell spacers during the soldering process, leading to the rejection of these designs.

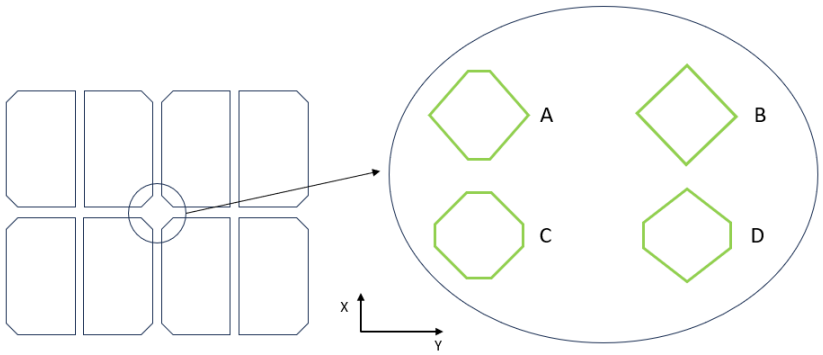

Figure 4.9 - Four different design configurations (**right**) for the AA or BB strings arrangement previously depicted (**left**).

Geometry design A does not obstruct the metal foil traces towards the X-direction but is considered less favourable than design C, as it is constrained in coordinate positioning for layup.

After careful consideration, the half-cell arrangement **2(b)** with spacer design C, featuring full octagonal geometry, is selected as the design choice for this report, offering more benefits to the product and manufacturability. Other geometries, such as cross-shaped spacers between strings or at cell corners, were not considered due to their perceived weakness in maintaining structural integrity over time.

Initially, a design for the inner frame consisted of two spacer pieces, the TOP and BOTTOM cell spacer parts, intended to be glued to the rear glass using UV-cured adhesive, forming a click-fit structure between them. However, this two-piece design would have increased production costs and assembly complexity significantly. Additionally, there were concerns about potential degradation and breakage when in contact with a liquid-filled module, leading to its exclusion as a viable option.

The spacers are attached via adhesive foil on CB, which is in turned glued to the rear glass. Figure 4.10 illustrates the inner structure with two different schematic drawing views.

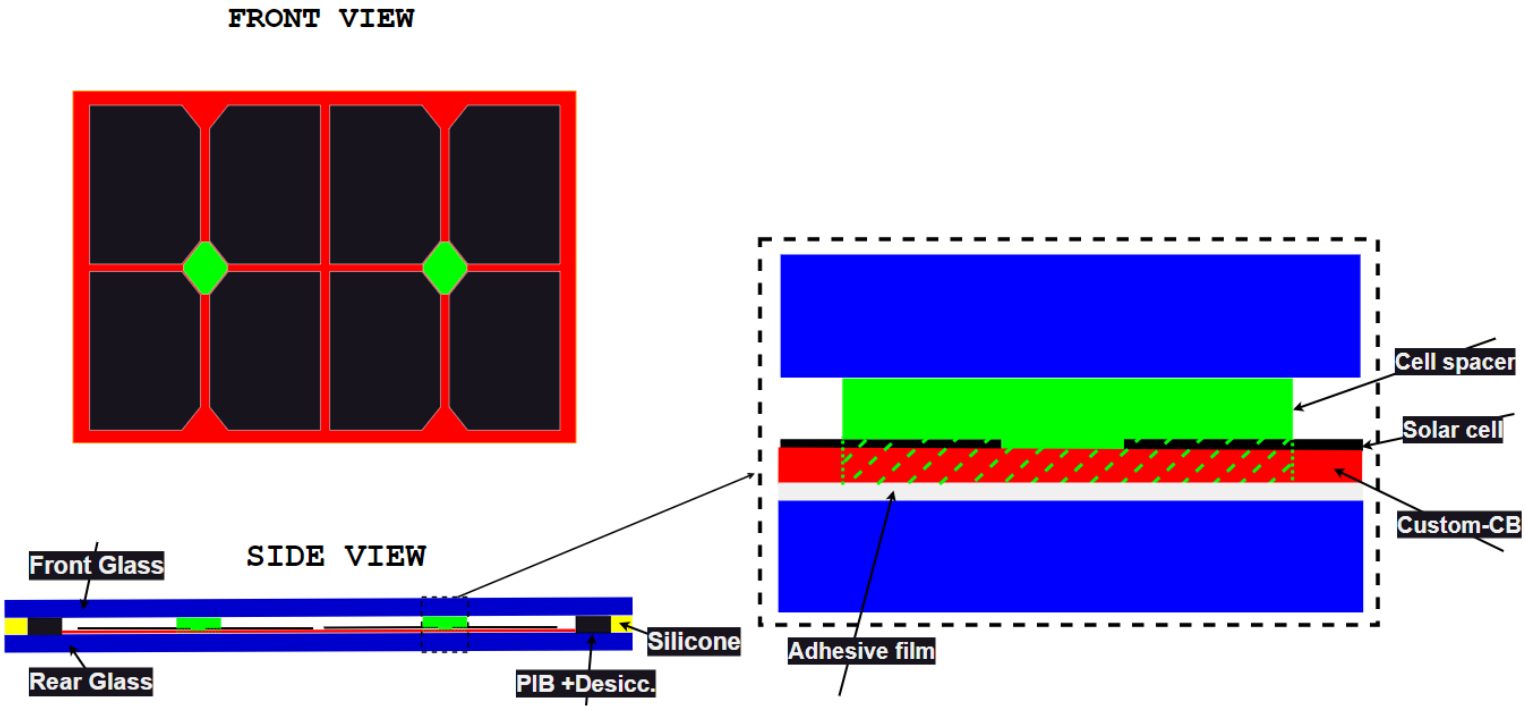

Figure 4.10 - Front and side view drawings of the simplified panel (not in scale). Edge sealants and glass plates are omitted in the top view for drawing clarity.

Solder pastes and metal traces are not included in the drawing for better clarity. A comprehensive list of components, materials, and relative specifications for the 120-cell version of the L-F module is summarized in Table 4.2.

Table 4.2 - Bill of Material (BoM) and main datasheet of the analysed module concept. Unit dimensions are in the XYZ axis (W x L x H)

Component	Category	Functionality	Material	Q.ty/panel	Unit Dimension (WxLxH)	Specifications | Reference
Glass	frame	Module protection and light transmission	Soda-lime	2 [pcs]	1040 x 1776 x 4 [mm^3]	Tempered, low-iron, antimony-free, ARC, ASC, PVT laminated [41]
Solar cell	cells	Convert solar light into electricity	Mono c-Si, Cu, Ag	120 [pcs]	166 x 83 x 0.16 [mm^3]	n-type, mono c-Si. half-cell, Bi-facial M6 Zebra IBC, 24.4%(η), 6.67 Wp (full sized) [42]
Cell spacer	frame	Keep cells in place. Mechanical integrity	polycarbonate	50 pcs	35-55 [mm^3]	(Biosphere Solar)
Adhesive film (CB/glass)	encapsulant	To bond conductive sheet with glass pane	UV-cured adhesive	0.35 [cc]	1010 x 1746 x 0.2 [mm^3]	-
Conductive solder paste	electrical	To solder solar cells & strings onto CB	Tin (Sn), Bismuth (Bi), Silver (Ag)	20-25 [cc]	1 x 83 x 0.2 [mm^3]/ 1BB cell	[48]
Conductive Back Sheet (CB)	electrical	To connect solar cells, bypass diodes and terminals	Tin, Flux, Copper (Cu)	1 pc	1010 x 1746 x (0.3-0.4) [mm^3]	-
1st Edge Seal	encapsulant	Module protection from weathering	extruded PIB + desiccants	110-160[cc]	10 x 5532 x (2-3) [mm^3]	[53]
2nd edge Seal	encapsulant	Module & PIB Protection	Silicone	50-85 [cc]	5 x 5572 x (2-3) [mm^3]	[57]
Filler (liquid)	encapsulant	Cooling, optical continuity	Silicone oils/synthetic esters	1-1.5 [L]	~1010x1746x (0.5-0.7) [mm^3]	[61]
Junction Box with by-pass diodes	electrical	Connection of BB wires and cables	Polymer, Cu, wire,Rubber, Silicone	6 rails / 3 diodes	7.2[cm] x 25 [cm]	[118]
Cables	electrical	Connect solar panel to JB	PVC/PE/PP/Copper	2 [pcs]	1200 [mm] x 4[mm^2]	[118]
MC4 connector	electrical	To connect solar panels	Plastic/Polymer/Rubber	2 [pcs]	5.9[mm] x 4 [mm^2]	[119]
Label	adhesive	Encloses module info conform to norms	Paper adhesive	1 [pc]	25 [mm]	[62]

The considerations and calculations made in this research regarding the width and height dimensions of the edge sealants are crucial for the L-F module studied, which possesses different material properties and components compared to other gas-filled glazing products (NICE or TPedge). Various factors, including mechanical properties of the sealant, surface tension of the filler agent, glass sizes, and overall loads, influence the optimal width and height of the seals. For example, the mounting orientation (flat, tilted, or vertical) can significantly impact these factors in the long term, affecting module performance and costs. As the volume for the edge sealants was already given but considering the design structure of each component analysed in this research, it is therefore preferrable to define, for both primary and secondary sealant heights, a range rather than a single value. Therefore, a range of 2 to 3 [mm] over the total module perimeter is recommended, resulting in batch volumes per panel of 110 to 160 [cc] for the primary seal and 50 to 85 [cc] for the secondary seal.

Similar considerations apply to the seals' widths. The spacing left at the module's edge for PIB is 10 [mm], which is the minimum width applied in the glazing industry [55], while silicone width is 5 [mm]. These dimensions are based on the CB metrics, glass pane, and dimensions used in the glazing industry [63]. These widths can potentially be extended outwards or inward, depending on the specific requirements of the desired cell, formats, and module design.

The volume of the cell spacers changes according to the height of the edge seals, assumed to be in the interval 2-3 [mm]. Each cell spacer's area is computed based on the regular octagon formula $A = 2a^2 * (1 + \sqrt{2})$ (Source: *Cuemath*) with each of the four side lengths of 2 [mm], resulting in an area of 19 [mm^2]. With a thickness range of the spacers between 1.8-2.8 [mm], [3] and 50 spacers per panel, the total volume required for spacers is in the range of 35 to 55 [mm^3].

[3] The values result from the subtraction with the adhesive layer thickness (0.1÷0.2 [mm])

4.2.4.2 Module Spacing Assessment: Solar Cells/ Conductive Backsheet

The spacing at edges between cells and CB for the 120-cell version module is examined as follows. The CB dimensions over XYZ (W x L x H) direction are 1010 [mm] x 1746 [mm] x (0.3-0.4) [mm]. The module comprises 12 strings, each containing 10 solar cells, with six strings in the head and six in the tail of the panel, connected to the 3-point JB placed back-middle sided (see Figure 4.5).

Over the X-axis (short-straight edge), there are six cell strings. Considering the full dimension of a solar cell (166 [mm]) over this axis, and with a 2 [mm] spacing between adjacent cells, a total length of 1006 [mm] is occupied. Thus, a 2 [mm] gap is left at each solar cell-CB edge, which may be insufficient to accommodate edge spacers. It is a very small gap to possibly leave as a tolerance for the PIB injection and/or its potential reaction upon heating/cooling. Main metrics of the module edge and solar cells are drawn in Figure 4.11.

In the Y-axis (long-straight edge), there are 20 cells. Over this axis, cells are arranged with the half-cut side, with dimensions of 83 [mm/cell]. Further, with a spacing of 2 [mm] between cells, the total length occupied by cells over the long edge is 1696 [mm], leaving a 50 [mm] spacing for other purposes, such as accommodating metal traces for string interconnection up to the JB (see Figure 4.4).

Considering the above, it's advisable to maintain similar spacing between cells to ensure consistency in the module design, even for the 80-cell design. Additionally, there should be enough room to set an outer cell spacer at the solar cell edges to further reinforce the structure and accommodate different dimensions for the edge seals.

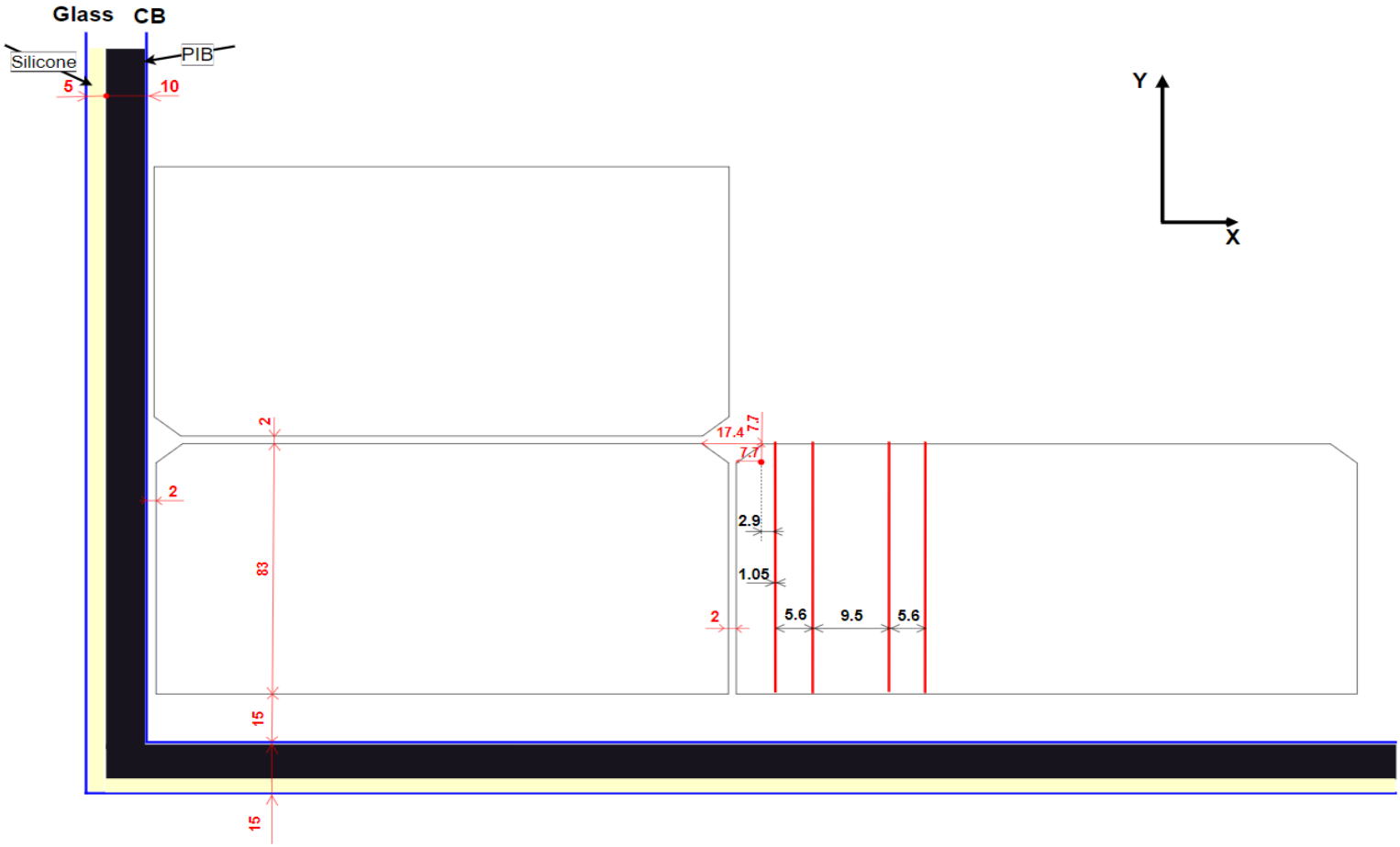

Figure 4.11 - Corner view drawing of the panel with the main metrics: the drawing is not in scale; only two pair of busbars are drawn for clearance. The X- and Y-axis are referred to as the short- and long-straight sides of the panel, respectively. The PIB and Silicone edge seals with dimensions are illustrated in black and yellow, respectively.

4.2.4.3 Solder Paste Extruded Volume

To compute the total extruded volume of the solder paste required for both cell-to-cell and string interconnections, the analysis is made by breaking the paste injected into different sections: **1.** under solar cell, **2.** between cell-to-cell, and **3.** string interconnections (bussing).

1. The paste dimension under each solar cell is 1 [mm] x 83 [mm] x 0.2 [mm] (W x L x H) formed of 9 [BB/polarity]. Over the entire 120-cell module, the total paste accounts for about 18 [cc].
2. Considering the spacing between adjacent solar cells and an additional 2 [mm] inner spacing at the solar cell edge for string interconnection, the total paste volume is 0.4 [cc].
3. The extruded paste volume required for string interconnections (busses) is computed over X and Y axes. In the X-direction, an estimation of 1000 [mm] is considered, resulting in 1.8 [cc] of solder paste. In the Y-direction, under the worst scenario, a 50 [mm] spacing is assumed, requiring 1 [cc]. The total solder paste required for strings interconnection accounts for 2.8 [cc] per panel. This volume also includes the metal paste length to go through the multilayer components (foils, glass) to reach the split JB.

The overall extruded paste volume per solar panel is calculated to be 22 [cc]. Wire lengths at the JB are computed based on dimensions, number of BB wires, and length to reach each section of the JB. Additionally, standard measures are used for cables and connectors during solar panel installations.

Next chapter focuses on the manufacturing of laminate-free modules, in relation to the product requirements and specifications outlined in this chapter.

5

The Process of Manufacturing Laminate-Free PV Modules

This chapter focuses on the manufacturing of laminate-free PV module Version 2. Initially, the chapter provides an illustration of the manufacturing process flow with a detailed description of the relative manufacturing steps for two different scales of production. Additionally, potential challenges and solutions involving adjusted and dedicated units tailored to the manufacture of the L-F module are investigated.

5.1 Assembly Steps and Manufacturing Workflow

The manufacturing layout for the L-F panel is designed to be flexible, allowing for possible integration or removal of machines from the line while maintaining a compact and low working footprint. Line flexibility is essential to accommodate future upgrades in component technologies and production volumes, as well as to facilitate easy module disassembly and repair. The processing steps for L-F panels are divided into five main block sections (Figure 5.0). Each block contains the necessary operations, starting from component loading and extending to testing and packaging, to facilitate the manufacturing of L-F modules.

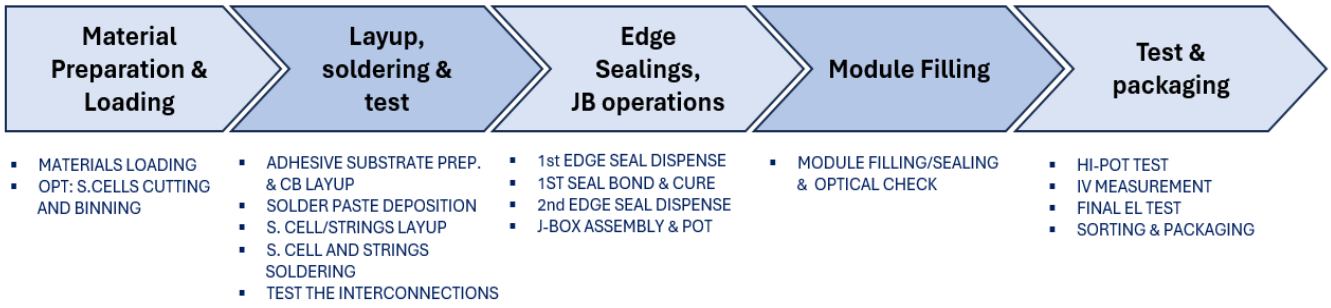

Figure 5.0 - Block sequence steps and process description for L-F module manufacturing.

The first step involves material preparation and loading. Hence, the CB, with integrated cell spacers and adhesive film, is fixed onto the rear glass. Following the assembly, metal paste is injected, and solar cells are accurately placed on the structure to be electrically interconnected via a soldering method. In the third step, the module is edge-sealed (primary and secondary seals) between the two glass panes, and the junction box is attached to the rear side. Module filling follows, and, similarly, to laminated manufacturing, testing, and packaging complete the final steps of the turnkey lines.

The study on the L-F module structure and its development, along with the related assembly operations, aims to establish an optimal and simplified process control sequence for the manufacturability of L-F solar modules. A block flow diagram is illustrated in Figure 5.1. After several iterations interchanging the sequence of processing steps and optional equipment within the line, the choice of this final configuration stems from a study on L-lines, interviews, inputs from various industrial and solar manufacturers, as well as guidance from supervisors.

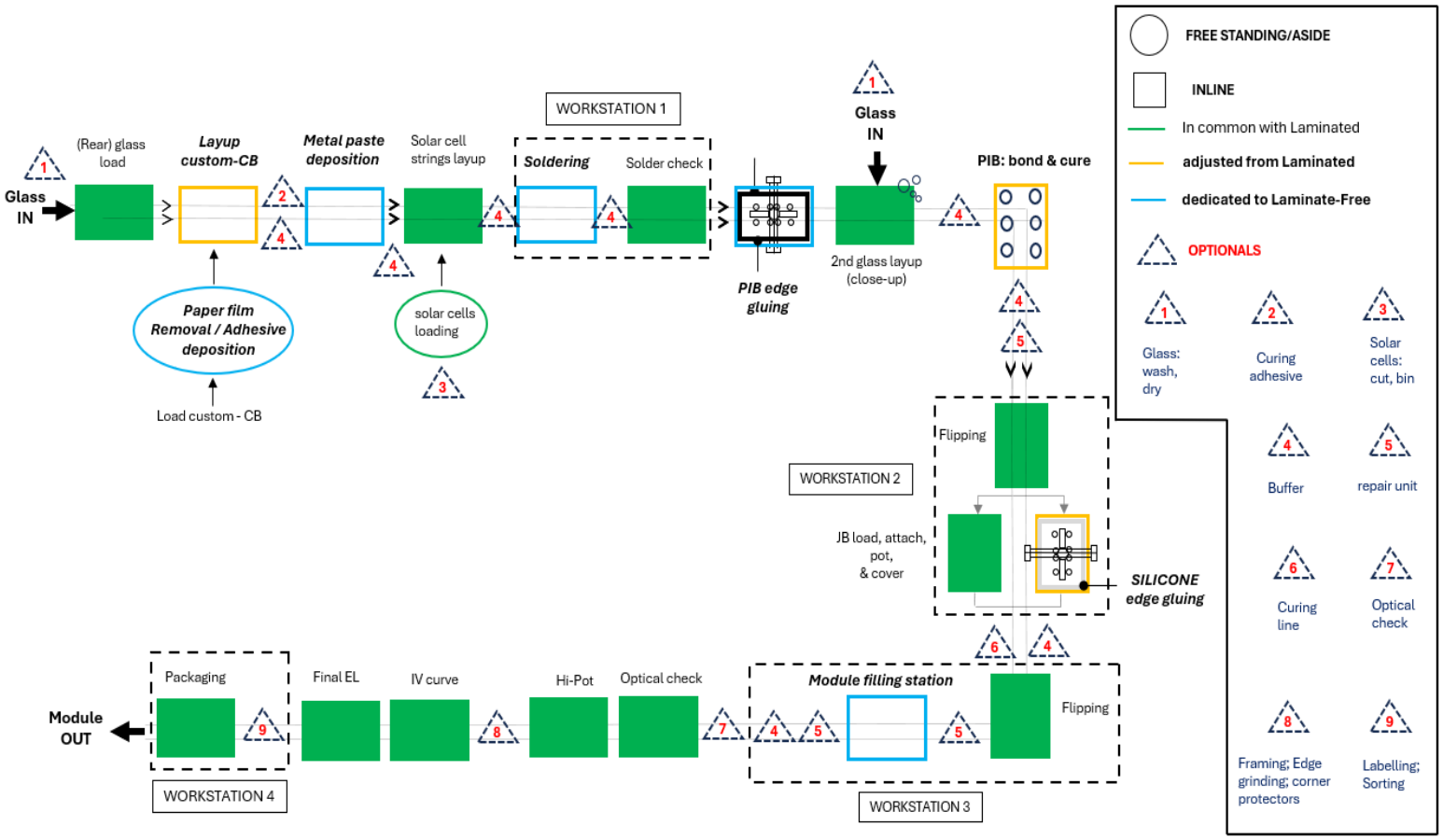

Figure 5.1 - General process flow diagram for L-F module manufacturing. The legend (upper-right) explains the settings and colour of each operation step. Process flow goes from upper-left, ending at the WORKSTATION 4.

The flow diagram is general and does not consider any scale of the line. It must be used as a visual reference for the processes required to manufacture Biosphere Solar product Version 2, examined in the previous chapter. This schematic of the process flow is employed with the new assembly technology using a ready-to-use and tailored CB for more scalable and improved throughputs compared to traditional stringing and soldering processes.

The green blocks represent operations common with the laminated lines, using, for instance, mainstream cell-to-cell stringing and bussing interconnection technology. Approximately 60% of the assembly processes can be reused from the L-lines (green blocks in Figure 5.1). These include glass loaders, solar cell layup, transport systems, motorized working stations with a flipping unit, testing systems, sorters, and palletizing. These operations mostly take place in the back end of the line.

To determine the optimized assembly layout, shortcuts in processing steps are adopted, for instance, through coupling or integrating operations and/or more efficient panel placement and mounting on a single workstation. From the process flow diagram drawn above, four workstations are present in the line. For instance, in WORKSTATION 2, the JB is fixed and potted while the same or a different toolset dispenses the silicone seal at the module edges. This may increase the line's throughput, equipment uptime, and operators' efficiency, these topics will be discussed in Chapter 6.

5.1.1 Process Flow Description

There are new assembly steps diverging from the traditional lines. Variations from the standard manufacturing imply that processing units must be either (partly) adjusted from already commercialized machinery in the solar industry or be dedicated equipment for L-F panel assembly. More precisely, the orange border blocks represent units deviating from the conventional lines using alternative interconnection techniques or assembly technology (e.g. conductive foils and/or adhesives), where no significant change in the control settings or mechanics of the equipment is required. Finally, blue borders indicate the dedicated units for L-F modules only, specific to the solar industry, where a substantial change in the equipment system is demanded. Alternatively, these may come from other manufacturing sectors such as insulating glass or electronic industry.

The manufacturing process begins with the loading of parts, including glass, solar cells, and CB. The patterned CB foil is securely affixed to the rear glass using a thin adhesive layer. The operation involves picking the sheet from its rack, removing the protective paper from its substrate, and accurately positioning it on the rear glass already on the transport belt. Alternatively, the deposition of adhesive can be integrated in the line, applied either on the CB substrate or rear glass, using methods such as spraying.

Prior to finalizing this design, various ideas and proposals were considered for the perforated CB design, including whether to apply adhesive only at the edge or throughout its surface. Considerations were also made regarding spacer assembly, such as whether to glue each spacer's substrate directly onto the rear glass using UV-cured adhesive or not. A later-developed concept suggested that these assembly operations might increase manufacturing costs for new machinery setups and further slowdown the production line speed. Embedding the spacers into the CB along with a thin adhesive layer deviates from standardization and may increase the final cost of the product. However, it is likely to reduce manufacturing costs and raise production outputs. The spacers are, for this study, already produced through moulding or milling and supplied in batches to be fixed into the CB, rather than being integrated into the line. These are complex and expensive machines whose purchase would increase the capital expenditure and enlarge the factory area (Expert Input: *member of Valoe*).

Additionally, gluing the overall CB substrate enhances module stability, avoids additional processing operations of gluing spacers on the rear side, and ensures accuracy in picking and positioning. Specifically, with this configuration, operations of loading, gluing, and placement of cell spacers on the rear glass support are therefore avoided.

The rear glass plate, with already three drilled holes for the JB placement, serves as a mechanical support. It is more advantageous to assemble it in a substrate configuration rather than from the front glass. The benefits of having a substrate configuration are related to the solder paste, which is more accurately injected into the grooves of the metal traces, present on the CB, rather than on the back-side ZEBRA cells' metallized paths. It avoids cell-front glass contacts (cell deterioration). However, in a superstrate assembly, a completely different assembly sequence would be required. The benefit of substrate assembly, however, is related to the avoidance of module flipping before JB attachment and the 2nd edge seal operation.

Once the conductive foil with spacers is affixed onto the rear plate, solder paste is metered and injected into the metallization traces of the CB. Solar cells are provided in batches of a half-cut format with either AA or BB orientation, as discussed in Chapter 4. Given the small gap between solar cells (2mm) and cell spacers (less than 0.5mm), an accurate and automated layup with P&P system is necessary to position every 10-20 half-cells onto the deposited paste [33]. Considering the low operating temperature of cell spacers, which ranges from 100°C to 150°C depending on the solder material used [44], [45], the interconnection of cells and strings is limited to low-T soldering techniques. Using low-T soldering offers benefits such as reduced energy consumption from the processing unit compared to high-T processing with stringers and bussing systems, although it may be costlier and limit market choices. It is recommended to use a solder check unit or an EL test to ensure the electrical integrity of the soldered cell strings. When the entire cell-module soldering has been checked, the panel is transported to the PIB gluing dispenser. Subsequently, the front plate is laid up to close the structure, after which the panel is ready to undergo edge bonding and curing by a cooling plate. Moving further, two horizontal turning units are integrated, one for flipping the module to the sunny side down and the second for the re-flipping of 180°. As silicone may be the common sealing agent, the secondary edge sealing, JB assembly, and potting processes can be aggregated together in the same workstation. After dispensing the silicone sealant and fixing the 3-point JB in the middle of the rear glass, the horizontal re-flipping is essential to facilitate the filling operation from the front glass nozzles. The Hi-Pot check, positioned before other testing operations, verifies the electrical isolation of the module due to the previous filling and soldering process, preventing any short circuits and checking for potential leaks. Other testing systems such as EL and IV curve measurement tests follow to guarantee high product quality.

Optional processes: Several optional processes can be integrated at any stage and line capacity. For example, disassembling the glass plate for repair by using the double glass repair manipulator, in L- lines, is typically done prior to entering the laminator. Here, the repair tool should be positioned after the PIB bond & cure and the module filling processes, as these may apply an undesired level of pressure and compromise the integrity of the glass sheets. Likewise, other optional processes such as framing, edge smoothing, and corner protectors are installed at the back end of the line. Similarly, the curing tunnel line, for high volume outputs, is after the silicone sealing and potting processes to guarantee a precise curing level and smooth process' flow. Next, the labelling process is incorporated in lines greater than 100-150 [MW] annual capacity due to the already high volume of modules carried through the line. Buffer systems, also installed in high-capacity lines (greater than 150MW), consist of

automatic drawers that temporarily stockpile PV modules, smoothing the flow of panels, avoiding bottlenecks. To replace the installation of costly multiple tools and/or potentially slow step processes, storage units may be necessary. See Figure 5.1 of possible operations requiring a buffer system (optional process N.4).

5.1.2 Scalability for Laminate-Free PV Modules' Manufacturing

Two production scales are considered, assuming a standard 300-325 [day/year] of production with a single working shift of 8 hours a day, as defined in Chapter 3. Firstly, a semi-automated (SA) line is compared to a small annual net output within the range of 10-20 [MW] of the L- lines. Small production lines are investigated for:

- Testing and transferring optimized cell and module production technologies.
- Exploring customizable options and formats, understanding line limitations, and making improvements.
- Facilitating the integration of more automated and newer solutions if larger production volumes are foreseen.
- Conducting experiments for solar panel prototyping and comparative tests using different recipes and raw materials.
- Minimizing and evaluating minimal manufacturing capital and operative expenditure costs for introduction into the market of startup companies.

The SA line is a cost-effective turnkey line that employs one basic equipment for each process and a low degree of automation. Only the most necessary automated toolsets are present, and they are not assisted by an operator. These tools pertain to operations requiring a certain level of assembly accuracy and tact time, such as paste deposition, soldering, and solar cell layup. Consequently, this does not lead to a drastic drop in the line speed and does not compromise the end-product integrity. It thus achieves the expected annual throughput, even though more labour force might be necessary. As will be evaluated in Chapter 6, up to 15 workers are needed.

Next to it, a Highly Automated (HA) line is compared with a 300 [MW] scale for L- modules' production. This line integrates more automated units and a greater amount of equipment per process, promising reduced labour force requirements, higher capacity, faster processing, and increased costs as well. This analysis aims to understand the potential of achieving a high annual throughput with a modular, flexible platform allowing for the highest level of semi- and fully automated solutions for L-F module production at a large scale. A plant capacity comparison of 300 [MW], although relatively small compared to the current gigawatt (GW) scale of installed manufacturing plants [64], provides a substantial indication of the differences in automation level and costs compared to the SA line. This scale is also a reasonable and viable size to be installed by a startup company, such as Biosphere Solar. Table 5.0 provides, for both lines, the assembly steps, their corresponding equipment, and the degree of automation.

Table 5.0 - Operation sequence with the relative description of the process for both the SA and HA lines. The level of automation of each process is indicated as **A:** auto, **Semi**, and **M**: manual. Similarly to Figure 5.1, the formatting colours express the comparison in process to the mainstream laminated plants **GREEN**: same operation, **ORANGE** adjusted unit, **BLUE**: L-F module dedicated unit. The table contains only the relevant processes for the manufacturing (optional units are not included).

N.	Process flow	SA line		HA line	
		Tool	Auto	Tool	Auto
1	(Rear) Glass loading on transport system	vacuum glass lifter	**Semi**	auto glass layup system	**A**
2	Pick and remove the protector film from the CB substrate / deposition method	manually/spraying/dispensing tool	**M/Semi**	manually/ spraying/dispensing toolset	**M/Semi**
	Align and place the CB on the back glass plate	CB layup unit	**Semi**	CB layup unit	**Semi**
3	Metal solder paste injection over PCB traces of the CB	conductive paste injector	**A**	conductive paste injector	**A**
4	Layup solar cell strings onto the deposited solder paste and between spacers of the tailor-CB	cell string layup system	**A**	cell string layup system	**A**
5	Soldering solar cell and strings (stringing and bussing)	low-T soldering machine	**A**	low-T soldering machine	**A**
6	Testing to check the outcome of soldering process	solder check unit	**Semi**	EL tester	**A**
7	Primary edge sealant deposition: PIB+ desiccant injection on one of the glass substrates	PIB injection machine + rotary table	**Semi**	auto PIB gluing machine	**A**
8	Picking the 2nd (front) glass from the pallet and lay it up on the structure (module close-up)	2nd glass lifter	**Semi**	2nd glass covering machine	**A**
9	Module bonding & cooling. (Edged or full panel)	clamping table or edge pressed with fans/coolers	**A**	cooling (and press) chamber	**A**
10	Horizontal module flipping of 180 ° (to sunny side down)	manually/turning table	**M/Semi**	180-degree turning unit	**A**
11	JB fixing (soldering or gluing) on the middle rear-side	glue dispenser for JB	**Semi**	JB soldering machine	**A**
12	Secondary edge seal deposition: silicone injection between glass panes	silicone dispenser	**Semi**	auto edge sealing machine	**A**
13	JB potting with glue (silicone)	dispenser unit	**Semi**	auto JB glue potting machine	**A**
14	JB closing box	worktable	**M**	JB closing machine	**A**
15	Horizontal module re-flipping of 180 ° (to sunny side up)	manually/turning table	**M/Semi**	turning table	**A**
16	Module filling, vacuum suction, and liquid fill injection. Remove air and fill with the liquid up. Sealing the two slits.	filling system	**Semi**	filling system	**Semi**
17	Optical check before proceeding to final testing and pack. Unit also used as a cleaning station	visual Inspection table 90°	**Semi**	line scanning machine	**A**
18	Hi-pot test to check electrical isolation after interconnections & filling	Hi-pot tester	**A**	Hi-pot tester	**A**
19	IV curve tracing to verify the quality of the module	sun simulator	**A**	sun simulator	**A**
20	Final EL test to check cells integrity before packaging	EL tester	**A**	EL tester	**A**
21	Set the label on the module according to previous test results	-	**-**	labelling machine	**A**
22	Sorting based on previous test results and labelled unit		**-**	sorter	**A**
23	Packaging station	worktable/bench	**M**	packaging station	**A**

Glass plates loading and module close-up (N.1 and N.8): The first glass plate is positioned on the transport system as a support for the entire assembly chain (N.1), and the second glass is loaded, positioned, and released gradually on top of the structure (N.8). Once the second glass is positioned, the PIB starts to bond between the two glass substrates.

For small lines, a glass handler, or a manipulator (Figure 5.2 (**left**)) is typically used for tasks such as loading the glass plates or unloading the finished panels by positioning them into a pallet at the end of the line. On the other hand, larger lines employ a fully automated glass loading system or glass covering machine. This is achieved with two glass pallet spaces for easy and non-stop operation (Figure 5.2 (**middle**)). A protective paper between the glasses is removed by a vacuum system, drawn into a recycling bin for easy waste management (Figure 5.2 (**right**)). The glass is automatically picked and centered on the motorized belt.

Figure 5.2 - Photographs of: Manipulator for glasses (**left**), automatic 2nd glass layup robot (**middle** and **right**). (Source: *Ecoprogetti – Catalogue, Sept. 2023*). Green contours: common to standard and L-F module lines.

Before or during the module curing process with the PIB agent, an operator performs a quick check and cleanup of the front glass for the unit's vacuum cups.

Custom-CB operations (N.2): It is assumed that the adhesive film comes already deposited on the total CB substrate area, in a ready-to-use state. Depending on the adhesive of selection, whether it is a silicone gel or a UV-cured adhesive, a possible curing unit may be followed for fast-curing. The curing equipment quickly hardens the adhesive layer substrate. Additionally, if an adhesive silicone gel is chosen as a sticking agent, care must be taken not to keep air trapped at the interface. The conductive sheet must be accurately placed on the carrier plate and aligned with the rear glass plate that transports it through the module build process. In both steps and line scales, the protective paper is removed, and the layup and fixing processes are performed by a machine and with the assistance of an operator, in a semi-automated mode. However, to reduce cycle time and ensure alignment accuracy, a robot arm equipped with multiple grabbing systems (e.g., vacuum cups) picks up the conductive foil from its rack. Then, an operator removes the paper, and the unit is precisely placed onto the glass plate via integrated cameras/laser system. The equipment performing this operation is considered an adjusted unit from traditional lines, as slight variations in coordinate positioning settings, time, and weight for the new material allow it to be performed by a glass or cell string layup system with vacuum or magnet grippers.

Solder paste deposition (N.3): After the conductive foil lay-up, the interconnection between the conductive metal sheet and BC cells is established by depositing low-T and possibly fast-curing conductive paste. As a technique example, metal paste injectors are available from various manufacturing industries, including electronics, automotive, aerospace, and other fields where very accurate soldering is demanded.

There is no specified solder paste material. The deposition equipment and solution need to match with the requirements of the fluid paste type, its properties, and metrics. Different application methods for the deposition can be applied with relative trade-offs. It ranges from dispensing, screen and stencil printing, roller coating, and spraying. Some methods are investigated in Section 5.2.2.

For both volume lines, precise control over the amount and placement of the thin paste lines is essential to be operated by a semi or fully automated system to achieve high-quality solder joints. The unit to adopt can be equipped with multiple nozzle syringes, under each paste volume area of 1 x 0.2 [mm] (W x H) over the 108 traces. The total extruded paste volume to dispense was computed in Chapter 4 to be approximately 20-25 [cc] per panel.

Layup solar cell strings (N.4): The thin and fragile ZEBRA cells are picked from the stack and placed at pre-programmed positions, making contacts on the top of the solder paste tracks by an automatic system such as a manipulator or robot arm, with very high accuracy to achieve a narrow gap between cells. In both lines, an automated and precise layup system is required (Figure 5.3). This is accomplished through a dedicated handling and vision system that checks the integrity of the cells, its orientation, and achieves precise alignment [65].

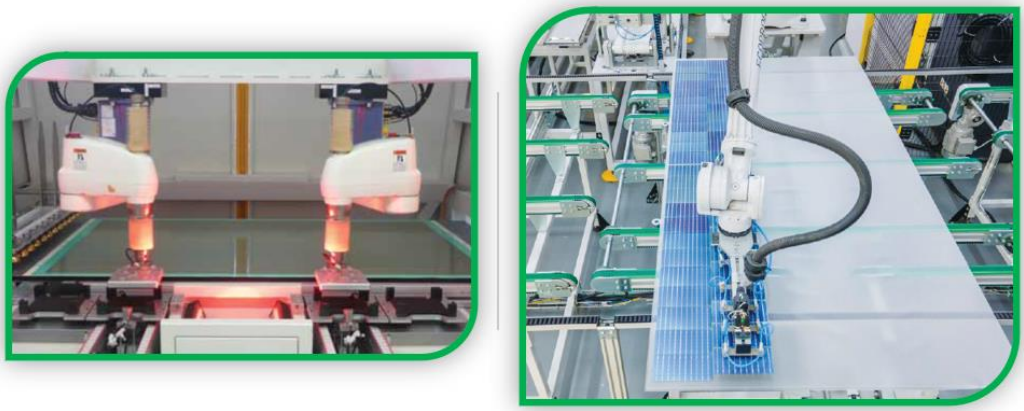

Figure 5.3 - Close-up view of automatic cell/string layup (via P&P) system: by cell (**left**) [24], and by string (**right**) [16]. Green contour: common to laminated lines.

Whereas in a traditional laminated plant, additional in-line stations and a returning position may be included for the assembly of conductive metal layers as well as encapsulant foils, for the L-F assembly, this does not occur, and the manufacturing moves forward to the cell strings soldering step.

Cell/string soldering (N.5): CB, along with the soldering paste, is a heat-activated substance, meaning that heat must be applied to perform the soldering process via a low-T soldering unit. Strings must be electrically interconnected to reach each of the three-part JB. They follow the traces on the circuited board and are soldered onto it, based on the JB disposition. Given the small paste and trace dimensions and considering this is one of the most sensitive and challenging operations that can compromise the panel yield and degradation, for both scales is suggested the adoption of a semi or fully automated unit(s) rather than a manual system(s). Low-T soldering methods typically operate between 100°C to 250-300°C. Each method relies on different techniques, including electromagnetic (heat) induction (with low-T solder alloys containing indium or bismuth), laser beams, and high-frequency mechanical vibrations (ultrasound), to generate heat directly in the solder joint (Expert Input: *member of Valoe*). This allows for precise control of temperature and minimizes heat exposure to surrounding components, such as cell spacers. Some of these methods, with related challenges, will be discussed in more detail in the last section.

After soldering, a checking unit, such as EL test, inspects and verifies the outcome of the cell and entire string interconnection before the module is closed and edge bonded, to facilitate repair.

In the edge sealing processes (N.7 and N.12), different assembly options exist. The panel can either be fixed on the belt or move with a (rotary) table, while glue injection heads can either be stationary or move straight along the panel edges.

PIB deposition (N. 7): As mentioned in Chapter 4, using hot melt PIB instead of butyl tape reels, the material can be heated and pumped out of large drums, eliminating the need to change tape, reducing manual labour, and increasing machine productivity. Regarding the equipment configuration, depending on the type of machine injection heads and their upper or lower position, they can be applied either to the front or rear glass substrate. A multi-purpose workstation with a pneumatic and vacuum-controlled lifter is beneficial for the SA line operations and for rotating capability. The manual tool can act as a cleaning station, support edge sealing of G/G modules, and eventually operate as an automatic conveyor for JB application. To enhance the automated line processing cycle, the upper (front) glass may be used to inject the 1st edge seal, rather than the rear glass. The plate is held by the automated upper suckers while the sealant is injected around the edges' perimeter substrate. Using the front plate enables this process to run almost simultaneously in the preceding step (N.6) while still under solder check, further boosting the line speed.

After the 1st seal deposition, the second glass plate is aligned and positioned on the structure. The module covering with the front glass must take place right after the injection of PIB to prevent it from curing before bonding. The cooling chamber or a workstation with a clamping system and coolers follows up for PIB bond and cure.

JB operations and secondary edge seal (WORKSTATION 2 – N.11 to N.14): As defined in Chapter 4, the JB is a standardized middle three-part junction box. The ribbons are fed through the perforated CB, holes in the back

glass, and interwoven on the back of the module. The connectors must extend from the 12 strings forming the panel via the solder paste traces. However, optimized processing of JB fixing, potting, and injecting the edge silicone seal can be achieved either sequentially with a single or multiple toolsets, or simultaneously. In the SA line, an operator loads and prepares the glue for the JB, attaching it to the rear glass with a semi-automatic silicone dispenser. Once attached, the machine meters and injects the silicone sealant, a common agent, at the module's edges. Upon completing both processes, the same working bench and dispenser can be used to pot the JB, and as a result, the boxes are manually covered. This approach saves costs and floor space compared to adding an extra motorized working station. Cycle times and the amount of sealant agent are computed in the next chapter.

In the HA production line, these operations could also be performed simultaneously with the aid of different automated toolsets. To achieve this, the panel must, in either case, remain stationary while injecting the edge sealant. The dispensing head(s) move along the XY axis while assembling the JB by gluing or soldering it by induction. If soldered, a reliable solder joint between ribbons and terminals must be ensured. Figure 5.4 shows visuals of both manual and automated JB assembly operations.

Figure 5.4 - Auto JB glueing (**left**), manual and auto JB potting (**middle** and **right**) [16]. Green contour: common to laminated lines.

One of the factors in the SA line is to be cost-effective; therefore, this research chooses to use a glued and potted JB for the cost-effective small line and a soldering station for the HA line.

Sealing against moisture vapor intrusion and long-term adhesion are two big challenges when attaching JBs. After the JB soldering, all the parts should be completely encapsulated by a potting material, which is generally made also of silicone sealant. In this process, the potting material is filled into each of the 3 small boxes, making sure the electronic wires inside, top surface of diodes and terminal base are all completely covered by silicone [66]. The overall potting amount per panel will be computed in Chapter 6, which results to be about 40 [cc].

Another issue in automation is not about assembling JB but the electrical cables connecting it. Cables are very difficult to control. When a JB is being loaded and picked up by the machine, there is no set place where cables could be, and this must be taken into consideration. That is one of the reasons why JB assembly should still be performed, even for fully automated lines, with a check by an operator (Expert Input: *member of Valoe*).

Eventually, if the silicone gel chosen for JB applications and 2nd edge seal requires longer curing times, a curing equipment is installed before the module re-flipping.

Module filling (N.16): Filling the panel with gas or liquid is not a standard practice in PV module manufacturing; hence, it is deemed a dedicated operation for assembling L-F modules. However, certain types of solar power systems, such as CSP systems, utilize liquids like oil or molten salt as part of their operation.

In specialized glazing applications such as dynamic glazing or smart windows, certain types of liquids may be used for specific functionalities such as light control or thermal management. However, gas filling is the predominant method used in the glazing industry. It is used to improve insulation properties and is typically performed after the unit has been bonded and pressed. This gas filling process, for instance, for household windows, may include two pre-drilled holes prior to glass processing into the glass panes, creating an outflow hole for air extraction and an inflow hole for filler injection. Alternatively, the filling can be performed by perforating across the single edge seal (usually at two opposite sides) and then sealed back with butyl tape. Similarly, this process can be applied to L-F panel manufacturing on one of the two glass plates. However, this operation requires careful consideration to ensure optimal nozzle positioning over the PV module, defining optimal

parameters for the process (operating temperature and pressures, cycle, etc.) based on the liquid selection properties, interference with other entities or parts, and constraints aimed at maintaining the structural integrity over time. Lastly, the performance of the seal of the two bores must be assessed.

As no scientific research has been conducted on the liquid filling on solar panels, it is therefore preferable, for both scales of lines, to initially adopt a semi-automated solution monitored by an operator.

Optical panel scanning (N.17): Panel scanning is an ideal solution for quickly checking the quality of the panel and can also be used as a cleaning station before the EL and IV tests. For high-throughput lines, an automated line scanning unit uses cameras from the front and back sides [67]. It is employed to detect defects and assess the module's quality after the flipping and filling operation, such as the presence of air bubbles. Additionally, it can also serve as a cleaning station before IV and final EL testing. Optionally, this process can also be performed in the SA line, utilizing a visual inspection table turned 90° [16].

Hence, the back end of line, including testing and palletizing, follows a similar process to that of the L-manufacturing lines.

The generic flow diagram represented at the beginning of this chapter (Figure 5.1) is unrelated to any automated solutions available in the industry; rather, it serves solely as a representative method for manufacturing L-F modules at any scale. In the next section, adjusted and dedicated assembly equipment will be explored and analyzed for each process.

5.2 Approaches for Adapted and Dedicated Process Equipment

Based on the generic flow diagram in Figure 5.1 and the operation sequences outlined in Table 5.0, the proposed solutions in this section are essential to build a complete manufacturing line for L-F solar modules and to be able to draw technical conclusions in comparison to laminate PV module plants. The relative technical and economic assessments will be presented in Chapters 6 and 7, providing a rationale for the choices made. The machine footprints refer to the dimensions in width, length, and height (W x L x H).

5.2.1 Conductive Backsheet Layup Systems

To select the customized conductive foil, grasp, hold it for paper removal, and position it precisely over the rear glass plate, various manipulators are repurposed from conventional manufacturing processes with adjusted settings, such as picking timescales and loads. They accomplish the operation on laminate modules in approximately 20 [s] and can work either manually or in a fully automatic mode. Adjusted machine options are discussed with the relative specifics, retrieved from [33], [67].

- **Curing Loading/Unloading Manipulator** (Figure 5.5 **(left)**): this equipment stacks the modules on the curing line for loading and unloading. To lay up the CB onto the glass plate, adjustments must be made to the multiple gripping systems, which can be either with suction cups or magnetics, trajectories in XY coordinates, and component weight. The equipment accomplishes the P&P, for a standard module, in maximum 20 [s] reaching a capacity of 2,800 pieces per day. The rated power is relatively low (4 kW) and high air consumption of 110 [L/min] (at 6-bar pressure). The overall dimensions are 3.2 [m] x 2.6 [m] x 4 [m] and it can work in a manual/automated mode [67].
- **Auto Sorter or Graduation Machine** (Figure 5.5 **(middle)**): This machine is for PV module handling, stacking, and unstacking. Parts comprise module and turnover ports accommodating up to 8 trays. Yet, the equipment may be reprogrammed without any significant redesign of the structure and cost, to undertake the CB layup. The tact-time for a standard module is 16-20 [s]. The rated power reaches 10 [kW] and 6-bar pressure for the compressor. The working area dimensions are 12 [m] x 3 [m] x 4 [m]. The broad equipment width results from the large number of pallets it can host and process. The machine can be set in manual or automated working mode [67].
- **Auto Glass Loader** (Figure 5.5 **(right)**): This manipulator with vacuum detection function is conventionally used to grab the glass and place it on the assembly line automatically. Similar performances are expected if a CB foil is grabbed by adjusting its spatial and loading parameters with either a vacuum or magnetic cups. The cycle including the paper gripping, for laminate panels, is achieved in 20 [s]. Similarly to the previous two machine types, the auto glass loader has a small, rated power and a large air consumption of 8.5 [kW] and 150

[L/min], respectively. The machine yield and uptime are greater than 95% with an overall working volume of dimension 7 [m] x 3.6 [m] x 1.8 [m] [33].

Figure 5.5 - Visual of market solutions potentially adopted to lay up the custom-CB for L-F modules: **(left)** curing loading/unloading manipulator [67], **(middle)** graduation machine [67], **(right)** auto glass loader [33]. Orange contour: readjusted from L-lines.

This adjusted process, besides the equipment selection, would require a start/stop operation and a manual paper removal as well as an accurate placement onto the rear glass. Consequently, the process tact time, for the custom-CB, will be longer than the conventional module assembly.

5.2.2 Methods for Metal Paste Deposition

Metal paste deposition systems, designed to accurately inject solder paste onto components or surfaces before soldering, are considered tailored units for L-F PV module assembly. They are commonly used in surface mount technology (SMT) assembly processes in the electronic industry, where solder paste is applied to the pads on the PCB before components are placed. These systems typically consist of a dispenser unit equipped with a syringe or cartridge containing the paste, along with mechanisms for controlling the injector heads. Programmable parameters, such as dispensing pressure, nozzle precision, and flow rate, are adjustable to achieve precise deposition. Some application methods, other than the classic dispensing, are worth exploring.

- **Jet dispenser** (Figure 5.6): Feeding paste out of a needle is the most common paste application method. This can be accomplished manually, by adopting small air pressure-driven dispenser units, or with automated dispenser systems for high volumes of production. Dispensing is suitable for heat exchanger plates of different types. Motor-driven precise screw dispensers (+/- 1% accuracy) is used instead of air pressure dispensers (+/- 5% accuracy) [49]. This technology fills a gap by shooting a small amount of paste to the substrate out of a print head with an attached syringe containing paste. The head can be mounted on an XY table as well as on any robot. The unit(s) may be equipped with multiple nozzle syringes to apply a paste volume, either contact or non-contact dispensing. By using the correct dispenser type, size, needle geometry, and diameter, application speeds up to 12 [m/min] can be achieved [49]. The dispenser type relies on the paste of selection.Given the range volume of the paste per panel (20-25 [cc]) and very high volume of production, a 1 [kg] cartridge offers an uptime of less than an hour. The diameter of the needle should match the width of the paste, of about 1 [mm]. For interconnection between strings, the dispenser head(s) need to consider a different and wider diameter than that of the cell-to-cell interconnection; therefore, the deposition time parameter should, for instance, be increased, keeping the machine flow rate steady, to achieve a wider deposition.

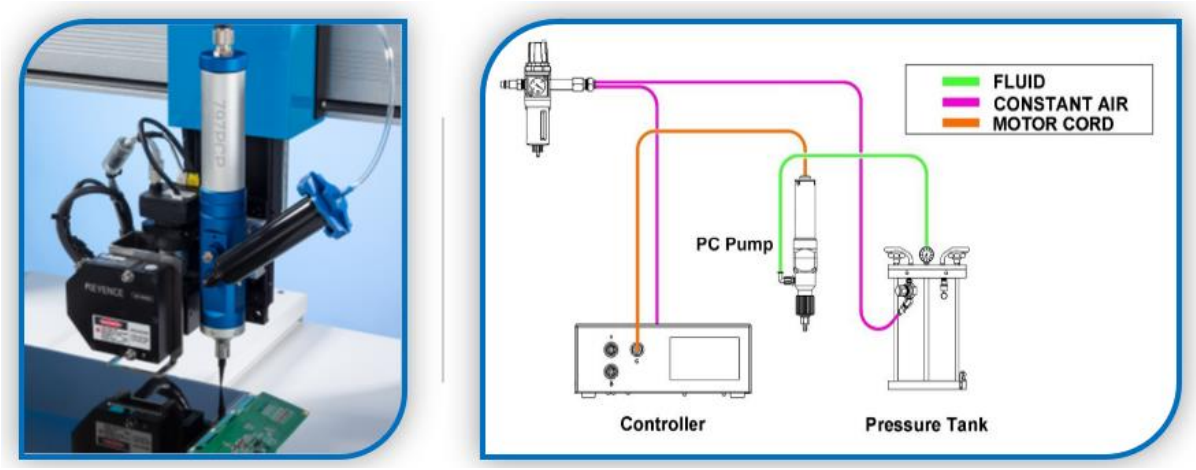

Figure 5.6 - Progressive cavity pump and injector head (**left**) [68], Schematic of a complete dispensing system (**right**) [69]. Blue border: dedicated to L-F module assembly.

The pump, handled by a controller unit, doses an exact volume of fluid allowing for continuous volumetric dispensing. The non-contact jet valve aids integration into robotic systems featuring fully adjustable parameters and properties for different fluid types (e.g., viscosities) and optimizes the process. The entire system is of a compact design of less than 1 [m^2] per system. An area of 1 [m^2] is assumed based on the specifications of each part [69]. Similarly, the total system rated power would be less than 1 [kW] and a maximum fluid pressure in the valve at 7 [bar] and 20 [L/min] [69].

- **Screen and stencil printer** (Figure 5.7): Automatic screen and stencil printers are specially designed to meet any product demand in the electronic industry for applications of solder paste and/or glue onto PCBs, under different substrates [70]. This method is suitable for flat components such as frames or hole plates where efficiency, production rate, and quality are of the highest importance. Screen printing is a paste application technique where a mesh is used to transfer the paste onto the component. A blade or squeegee pushes the paste through the open mesh area of the screen, which has been designed specifically for the component. Stencil printing is a technique using a laser-cut steel plate to transfer paste onto the component substrate. Similarly to screen printing, a blade pushes the paste through the laser-cut open area of the stencil, which has been designed specifically for the component. According to [49], thin paste layers down to 50 [µm] are possible with this method and structures as narrow as 0.3 [mm], but also up to 1 [mm]. Whereas printing material thickness, according to [70], ranges between 0.5-6 [mm]. This falls within the range for this study application as the paste thickness and width is 0.2 [mm] and 1 [mm], respectively.

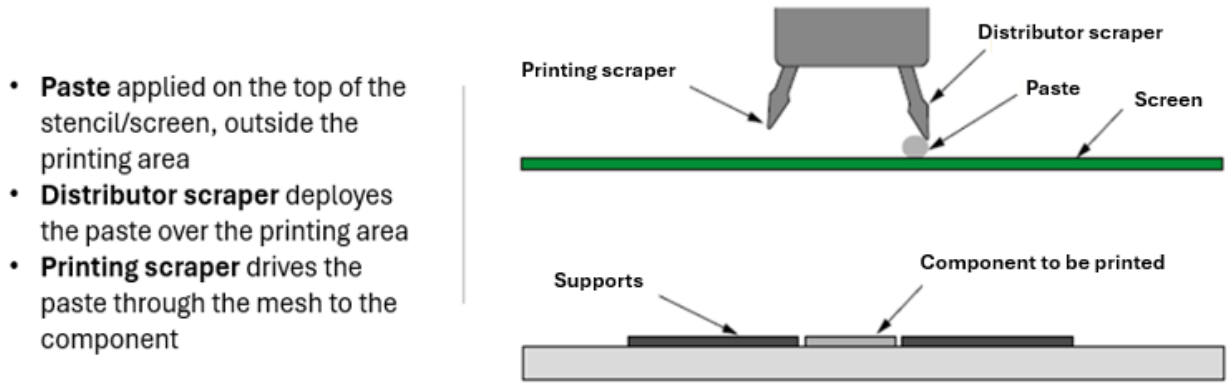

Figure 5.7 - Printing operation (**left**) and process setup (**right**) [49].

Performance is very fast, with cycle time of 12 [s] + printing time. Based on a printing area of 0.5 [m] x 0.5 [m] the machine rated power and air consumption are 2 [kW] and 15 [L/min]. The air supply and footprint are 5-6 [bar] and 1.3 x 1.7 x 1.6 [m] [70].

- **Spray coating:** Spraying is a technique in which a layer of metal paste is applied evenly across the surface of components. These machines are configured for a very broad range of spray coating and materials deposition substrates such as plastic, metal, and wood [71]. It is suitable for many different component types and

geometries. Applying the solder paste as a thin, even layer provides good bonding with substrates, improved part assembly, and reduced risk of erosion. The operation can be done both manually and with automated systems. These systems are usually formed of many component parts such as equipment robot manipulator & controller, metal spray equipment, chiller and heat exchanger, extractor and dust collector, power system. The dimension of the entire system may not be space-effective, exceeding 4 [m] x 3 [m] x 3 [m] volume area required for a 15 [kW] system [71].

Among the factors influencing the paste deposition methods, the particle grain size, for instance, is essential especially if the screen printing or spray coating methods are chosen. Thick grains may not be evenly deposited over the trace grooves or for small paste thicknesses. This, in turn, influences the quality and control over the soldered joints.

5.2.3 Soldering Methods

The 120 solar cells and 12 strings of the L-F module must be connected electrically to each other. Most manufacturers use an iron or IR soldering method. For thin and fragile solar cells, both methods have disadvantages related to the risk of breakage due to either cell contact or high-T heat up. As a result, mechanical stresses are induced in the solar cell [72].

Soldering systems, for this specific application of L-F module Version 2, should be designed to solder components at lower temperatures than traditional soldering of PV modules. This to prevent from compromising to heat-sensitive parts and peripherals.

Soldering systems are space efficient as they are often used in environments where floor space is limited. An estimated cycle time to solder a 120-cell module could range from less than a minute to dozens of minutes. This depends on various factors such as the number of solder joints, whether a local or total area is applied, the quality of the soldering result, the efficiency of the equipment, solder paste compatibility, automation, and system integration (Expert Input: *member of Ultraflexpower*).

Unlike the laminated module with CB, where soldering and encapsulation occur in the laminator over the entire foil surface, one barrier for L-F module manufacturing is that the electrical interconnections are likely to be soldered by local heat. Cells can be heated individually or in batches with heating times in the order of seconds, eliminating preheat times (such as in laminators) and reducing energy costs [73]. Additionally, the challenge is also in the flux formulas affecting metal-containing paste performance appropriate to this specific application aimed at good quality soldering, and the restricted residue flux where it can cause issues to surrounding areas. The rapid reflow[4] methods, which the paste does not spatter when heated as quickly as 0.25 [s] include laser, solder iron, hot bar, and heat induction [47]. For this study, a semi or fully automated construction is necessary, for both SA and HA lines. An overview of some methods and systems is presented.

- **Heat Induction System** (Figure 5.9 (**a**)): These types of inductors are formed by an induction heating power supply part in air and/or water-cooled configuration, the heat link controller, and the induction coil assembly. Power ratings are from 3 [kW] to 20 [MW] [73], providing the necessary non-contact local heat. Induction coils are unique and are developed per application process. There is no off-the-shelf solution for this process for the specific application of this research, as it is considered non-standard.

  The most important part of any induction heating system is the heating inductor, with a conversion efficiency of approximately 90% from input to output. Additional considerations for efficiency should be considered related to power transmission distance, the alloy heated, and induction heating coil design. The coil, for L-F module soldering, must be specifically designed, developed, and optimized to achieve optimal power, frequency, and design (Expert Input: *member of Ajax Tocco*).

  For this project, heating large surfaces homogeneously with induction is certainly challenging, with possible buckling happening. The presence of the cell spacers impedes this total surface heating solution. However, the advantage of large surface heating is for its homogeneous heat, less load for operators, fast warm-up time (energy-saving), and optical temperature control with accuracy +/- 1 degree. Induction heating can be used to heat the hot plate quickly indirectly with an induction coil (e.g., Al) but is an expensive solution (Expert Input: *member of Inductionheating*).

[4] Reflow soldering is used in electronics manufacturing to solder high-accuracy surface-mounted components to PCBs.

As said, for this L-F module design, it is hardly feasible to heat up all straight lines of the paste homogeneously at once. Lines are thin (small induction coil), so a high frequency is needed. The induction current chooses the path of least self-induction (impedance), due to the shape of the lines and the closed loops with different lengths. Whereby a prediction of uncontrollable induced currents resulting in hot spots and cold spots. What may be a solution is scanning with a relatively high frequency in the shape of a hairpin of for instance, 200 [mm] long. The coil must then scan the entire surface in lanes to allow the solder to flow locally (Expert Input: *member of Inductionheating*).

As far as the metal paste is concerned, a well-selected low melting point paste eliminates the need for a second or third reflow cycle due to the temperature-sensitive spacers. Consequently, this allows for a reduced reflow process per cycle and energy consumption. Low-T reflow profiles may enable the use of less expensive PCB substrates [48].

Low melt alloys/solder pastes containing bismuth (Bi) need to be considered. Due to this element, the solder joints are brittle, and this type is suitable if there is no mechanical stress on the joint. According to Table 4.0 in Chapter 4, a lead-free alloy with no Bi, has a melting point starting from 217 °C, therefore a reliable solder joint must have an intermetallic compound formation (IMC) layer between 1.3-4 [µm] (Expert Input: *member of TechonSystem)*. The IMC layer is determined by temperature and time. It is important for an adequate soak time in a curing process to minimize temperature differential without overheating the surface and peripheral parts. Approximately 85kW-seconds per kg of heated mass is required for a 120°C temperature rise. For 2 [kg] heated mass, which is two orders of magnitude greater than the total paste mass per panel for this study, the minimum recommended power supply rating would be 3.6 [kW] [73].

Based on prototype tests already performed on single cells, the soldering time can vary; for a single cell with 9-10 ribbons, soldering time ranges between 1 and 1.5 [s] (Expert Input: *member of Ultraflexpower*). For a 120-cell module, this is in the range of 120-180 [s]. Despite reaching precise temperature control, rapid heating, and energy-efficient process, to solder the full length of a PCB trace, the cell can still be easily overheated and bent. To check the feasibility of this process, a custom-designed coil is therefore unavoidable (Expert Input: *member of Ultraflexpower*).

The inductor heater needs to be sized and developed appropriately with multiple head designated coils. The coil design and quantity rely on the desired costs and speed to achieve. Two inductor units may work simultaneously on a single panel. Thanks to the symmetrical panel design, one inductor solders the top (six) and one unit works on the tail cell strings, hence halving the tact time. The chosen induction heating supply system has a power above the minimum of 3.6 [kW] and it is assumed to be between 5-10 [kW], with a 10 to 50 [kHz] (kilohertz) range. Its footprint does not exceed the half-meter volume dimension. A similar size can be assumed for the coil assembly and controller. Therefore, the volume occupied is roughly of 1[m^3]. If a SCARA robot is integrated, with a working area less than 1 [m^3] and a power consumption of 2.7 to 3.7 [kW] [74], the process features a total 13.7 [kW] system within a 2 [m^3] volume area. Figure 5.9 **(a)** shows images of the system's parts.

- **Laser Solder System** (Figure 5.9 (**b**)): Soldering by laser beam has also been broadly employed in the interconnection of electronic components and PCBs, especially when heat-sensitive components such as semiconductor sub-assemblies and plastics are present, inhibiting whole-body heating. Its special advantages of high precision on very small spots, under local, non-contact heating, and rapid cooling [75]. For certain specific applications, such as this study, laser soldering could be an attractive alternative, particularly for the ability to direct the energy beam accurately and precisely onto a target area with minimal heating of the surrounding parts. Additionally, by directing the heat to where it is required, the resultant temperature profile can often be controlled, hence reducing the mechanical stresses introduced [76].

  The heating principle differs between laser and iron-tip soldering. The first is surface heating, instantaneous heating time and suitable for detailed parts and applications. On the other hand, contact tip soldering is a heat transmission system, slow, suitable for large thermal capacity components, and with easy regulation (Input: *member of Japan Unix*)

  Temperature and thermal stress significantly affect the soldering performance and reliability of the solder joints. Surrounding materials can also alter the controlled laser temperature. Laser process parameters, including laser output power and output time, are the most significant factors. In particular, the scanning speed is the principal factor for the bonding strength during laser soldering [75]. As defined in Chapter 4, the grain morphology and size of the paste influence much the scanning speed of the laser, decreasing with wider

and coarser particle sizes. The laser power output, conversely, does increase proportionally [75]. An appropriate increase of laser output or time does contribute to the formation of a fine and uniform microstructure and homogenization. On the other hand, excessive power can result in the formation of void defects. These trade-offs are very challenging when it comes to soldering 120 delicate ZEBRA solar cells, without compromising the c-Si performance.

The recipe of high-performance heat transfer, a high absorption rate of the laser radiation at the solder spot is necessary, which is highest for short wavelengths. Laser soldering includes operations such as solder wire feeding with flux core, reflow soldering with solder paste, or a solder depot [77]. Diode lasers should meet the requirements of having at least 30 [W] power and a focus point smaller than 0.8 [mm]. An example of the laser soldering sequence of a pin between a PCB surface and, with a solder wire feeding tube (Figure 5.8), is summarized in three steps [77]:

1. **Pre-heating:** the solder wire enters the range of the laser beam. The direct radiating heats up the wire up close to melting temperature (solidus to liquidus), not over. If the laser beam hits the PCB outside the solder pad, the PCB surface may get damaged.
2. **Tin feeding:** the solder wire hits the solder spot and melts at the preheated solder pad and pin. If these are not sufficiently warm, the wire gets burned or bent and it does not melt properly.
3. **Hold time:** With a melted solder wire spread out, the shape of the solder spot starts to build up. Liquid solder has a significant lower absorption rate (it can act as a mirror). At this stage, the laser beam could be partially deflected and damage possible neighbouring components or plastic housing.

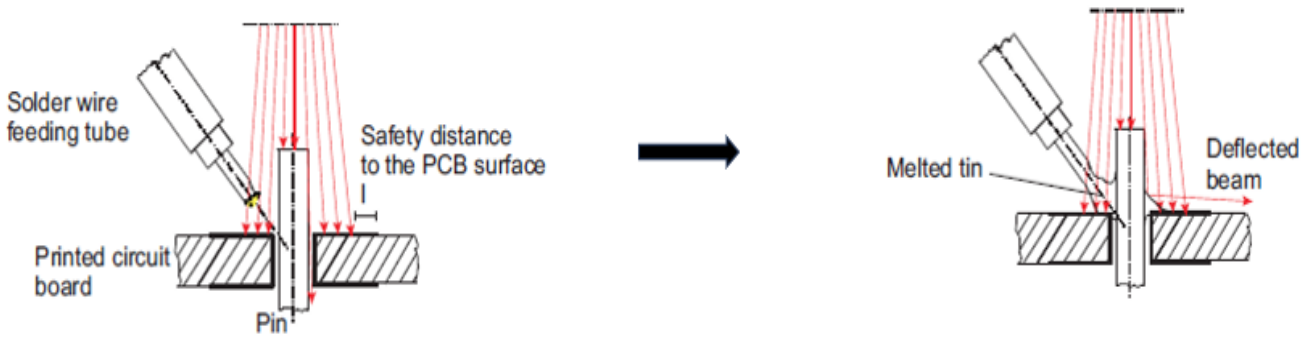

Figure 5.8 - Process sequence of the laser soldering with solder wire feeding with flux core [77].

Conventional systems are controlled by laser power instead of temperature. They are formed of a laser controller & oscillator, and a laser head [74]. Laser soldering head can be integrated into multiple-axis gantry robots. Figure 5.9 **(b)** illustrates the parts. A complete inline system can reach 2 [m^2] dimensions and less than 5 [kW] power [74], which can be employed for both SA and HA lines if these are considered inexpensive.

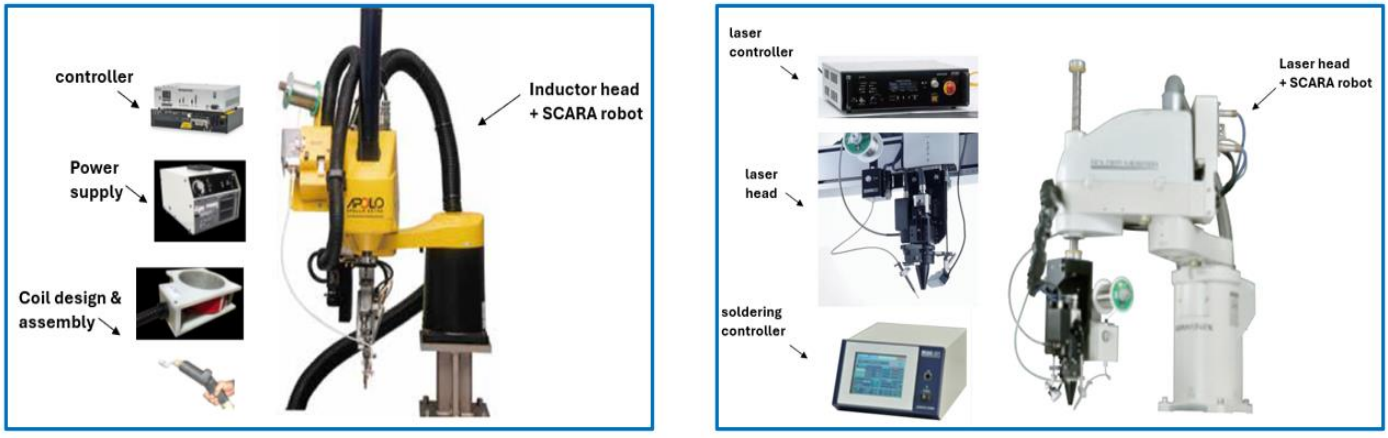

(a) **(b)**

Figure 5.9 - (a) Components of the heat induction soldering system [73] [74], **(b)** laser soldering system (Input: *member of Japan Unix*). Blue border: tailored to L-F module assembly.

High soldering quality needs a laser spot with precise (round) shape and constant intensity. Another challenge for this method in relation to this project study is that a laser must encounter different widths and trajectories

within the L-F module design, namely the wider dimensions of the paste over the 12 strings and those reaching the three-point JB.

If the laser soldering is performed correctly with precise control over the laser parameters, it may be possible to reach high-quality soldering in a short time and without causing harm. It is therefore crucial to ensure this process is carefully optimized to minimize heat exposure and ensure reliable electrical connection without degrading the performance or longevity of the module.

Similarly to the heat induction soldering, to further reduce the processing speed, a dual laser operation or multiple-joint soldering system on the two sections of the module could be performed concurrently.

- **ECA stringer:** ECA stringers are typically used in the manufacturing of electronic devices, LED lights, and semiconductor devices. The machine is an innovative cell interconnection technology standardized for solar panel manufacturing (Expert Input: *member of TeamTechnik*). It performs the metal deposition and cell/string interconnections at lower temperatures than the classic tabber and stringer, which uses non-contact IR light. This stringer is a good solution for ribbon interconnection using either FBC or BC cell metallization type without conductive backsheet technology. The embedded dispensing system of the ECA stringer precisely controls the flow of the conductive adhesive on substrates designed with a specific pattern. This programming determines the path that the dispensing "head" follows and controls parameters such as dispensing speed, pressure, and volume. In a standard module, thin conductive adhesive foil is printed on both sides of the cells. The ribbons are embedded in the machine and placed onto the ECA. Hence, the cell-ECA-ribbon interconnection, via low-temperature heat, is processed, and processing is cured under low temperature.

  For this study to have flexibility in manufacturing, an ECA stringer is offered to deposit the LTSP by printing, instead of ECA for trial-and-error (Expert Input: *member of TeamTechnik*), and make the interconnections, rather than individual dispenser and soldering systems. For cells and string interconnection, low-T heat is necessary, UV light, or chemical curing agents, undergoing a curing or drying process to solidify and bond to the surfaces. An example of an ECA stringer holds a maximum throughput of 3700 half-cells per hour (by string of 12), reaching an output of 30 [module/h]. This translates to a 2 [min/module] finished process. The machine's dimensions are 8 [m] x 2.3 [m] x 2.4 [m], with an average power consumption of 28 [kW] [78].

5.2.4 PIB Bonding and Curing

This stage is an important process to ensure that the first edge sealant is well bound between the glass plate substrates and to prevent any air bubbles or unwanted ingress agents. Holding the module under moderate pressure while cooling it is essential to achieve high-quality performance in the process. Solutions that may be adopted include:

- **Cooling Chamber** (Figure 5.10): Some processing units or integrated parts used in the L-module assembly are utilized without significant redesign for manufacturing L-F panels. For instance, the cooling chamber of large-capacity laminators, which is the last step on the unloading belt, can operate to let the PIB bond between the panes and cure the edges by cooling it. This system is vented and can quickly cool down the module using dedicated chillers or fans while gradually applying light pressure on it, allowing it to maintain a straight form, avoiding deformations. This plate is controlled by a programmable logic controller (PLC) system connected to the laminator and can easily be logged out of the control system and work autonomously (Expert Input: *member of Ecoprogetti Srl*).

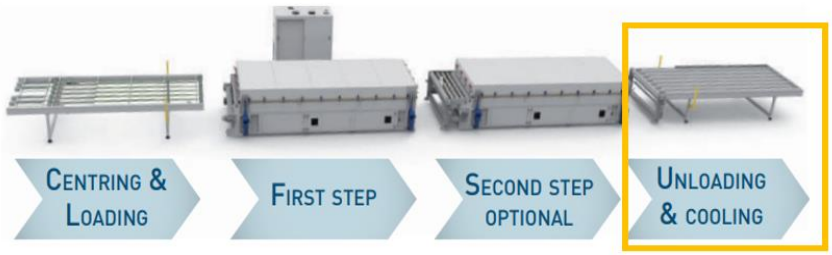

Fig. 5.10 - Visual of the entire laminator steps with a cooling press plate [16]. Orange border: adjusted from L-lines.

Its operating condition can be achieved by adjusting cooling temperature and pressure. The curing time must be accurately set for curing PIB from its processing temperature, which is in the range of 100-150°C, down to 25-35°C, and it is in the order of 1 minute [79]. This is relatively low compared to the 8-minute pressing and cooling for L-modules (under normal cure) [16]. The operating pressure, hydraulic or pneumatic, for complete PIB bonding with glass substrates are moderate and vary depending on factors such as specific PIB type used, cleanliness, glass substrate roughness, and method applied. The pressure can range from a few to tens of bar pressure, depending on the sizes and dimensions of components (Expert Input: *member of Kommerling*). This must align without compromising the module integrity. Press values to apply have not been investigated but the condition for pressure time and release is to stay within the agent curing time, of a minute. The challenge lies in determining the optimal values of cooling temperature rate and pressure for the machine, which depend on the PIB material type, and the selected dimensions. Additionally, it is essential to consider how these two parameters do change if dimensions larger or smaller than 10 x 3 [mm] PIB width and height are adopted. Very minimal pressures are preferred over having a longer curing time, to preserve the module integrity of thin and fragile inner components, an create a tight seal. Furthermore, the risk of overpressure on inner entities may be kept low thanks to the five pre-drilled slits on the glass panes, pushing the air out. This cooling plate could be used especially for the HA line in connection with automated loading and unloading belts. Since there is no available technical data on the adjusted equipment, the assumptions are based on the specifications of market-ready laminators. For a 3-plate and 5-plate laminator, the assumption is that each plate consumes 1/3 and 1/5 of the total electrical power, respectively. Hence, the electrical consumption of the cooling chamber is 9 [kW] for the 3-plate laminator and 18 [kW] for the 5-plate laminator [32]. The air consumption of a complete laminator machine is less than 1 [L/min] [32], and this value is used as a reference. The cooling chamber, depicted in Figure 5.10, essentially functions as an automated plate with dimensions approximating those of a transport system (conveyor). There are different plate sizes, ranging from large chambers of 11.5 [m] x 2.7 [m] accommodating multiple panels (up to 7), down to smaller dimensions of 2.8 [m] x 1.4 [m] x 1 [m] [33] (Expert input: *member of ConfirmWare*), which is the selected for this report. To save space and balance the stream of automated production lines, a double-stack cooling press can be used as an alternative to the single plate. The device has two plates stacked one upon another following the same principle as double-stack high-capacity laminators.

- **Clamping Table/Panel Press with (edge) Coolers:** The clamping system integrated into the process manages the required force and prevents shifting or breakage. It is operated by means of a foot pedal and recommended for unit manufacture using hotmelt sealants. When using this clamp table, the panel requires no extra fixing method but the integrated jaws that hold the glass firmly in place either during or after the sealing. Available sizes for this table are 2 x 1.5 [m] [121]. Alternatively, to the clamping table, a panel press table can be adopted. It uses a pneumatic press designed to aid the assembly of sealed units by pressing the two sheets of glass and PIB sealant together. The machine is featured by a moving platen with a pneumatic cylinder mounted on, and a fixed bed. No electrical power is required for the machine. The dimensions are compared to a transport system of dimension 2.8 [m] x 1.4 [m] x 1 [m] [33]. Fans or edge coolers are attached at the table or panel press edges to quickly reduce the PIB temperature down to 25-35°C. This system operates in manual mode, is very inexpensive, and therefore suitable for the SA production line.

5.2.5 Edge Gluing Dispensers

The dispensing of edge seals depends on the demanded output volumes and is carried out by a semi- or fully automated unit that extrudes and injects the adhesive agent around the four straight edges of the module. This applies to both sealants, PIB, and silicone. The difference between silicone gel and hot melt PIB machines is that the latter requires a feeding pump with a heated fluid section to bring the fluid up to its operating temperature and a heated follower plate with sealing [80].

In the SA line, a semi-automated unit is typically adopted with the assistance of an operator who dispenses the adhesive via a manual extrusion gun. A supportive rotary table or multifunctional table is required to support the panel. In HA lines, fully automated toolsets are chosen for the edge sealing processes. To address production issues while maintaining quality profiles and application speed, different equipment solutions are presented in the following sections.

Primary Edge Sealing: Equipment

To process the dispensing, the agent must be heated up to 140°C. The agent comes packaged in standard drum barrel sizes of 20 to 220 [kg]. Drum capacity and sealing agent amount are analyzed in Chapter 6. An overview of

potential sealing solutions with a description of the equipment applying PIB adhesive on a glass substrate is presented in the following sections.

- **PIB Heated Extruder and Injector** (Figure 5.11 (**a**)): This equipment can work in different modes. The feeding pump and heated fluid section can be equipped with a heated high-pressure material hose (minimum 3 [m] length) and a manual extrusion gun. Alternatively, a controlled volumetric metering unit with an automated valve provide reliable and repeatable precision in dosing. Optionally, for higher production volumes, a robot integrator is included to replace the operator, increasing the flow rate, reducing the cycle, and minimizing errors for metering and dispensing over the panel. A conveyor system must be tailored precisely to the application and components used to support the solar panel. This must include motorized loading, centering, and unloading [80]. The heated extruder consists of a feeding pump with a maximal working pressure between 300 and 400 [bar], a max inlet compressed air consumption of up to 650 [L/min] at 6 [bar] with a rated power of up to 6 [kW] (comprising a heated follower plate and heated hoses) [80]. The pump dimensions are compact, with a maximum of 0.8 [m] x 1[m] x 3.3 [m]. The shot metering unit system has a max flow rate of 2000 [cc/min] and can dose a volume between 3 to over 200 [cc] with a single shot. This falls within the PIB extruded volume of this study, with a range of 110÷160 [cc] per panel, enabling the accomplishment of a single-panel seal with one shot. Cycle times for edge seals are computed in Chapter 6. The metering system consumption and dimensions are 0.7 [kW] and 0.85 [m] x 0.25 [m] x 0.3 [m], respectively [80]. A standard supportive system, such as the multipurpose motorized belt, maintains a peak power and air consumption of 0.5 [kW] and 5 [L/min], respectively. The plate dimensions are 1.4 [m] x 2.3 [m] x 1 [m] [16] [81]. The overall working specifications for this process include a maximum power and air consumption of 7.5 [kW] and 655 [L/min]. An estimation of the working area needed is roughly 3 [m] x 3.5 [m] (W x L).

- **Auto PIB Gluing Machine** (Figure 5.11 (**b**)): The automated and tailor-made machine is designed to facilitate glass insertion and extraction, precise positioning using vacuum suction, and adhesive heads to meet specific requirements. The machine operates without the need for manual intervention under normal conditions. The glass is conveyed to the adhesive application using a synchronous belt, a lifting and transmission mechanism that is accurately positioned. The heads apply the heated PIB with desiccants to the four sides of the glass using servo motion and a control metering system. Based on the main component layout depicted in the bottom-right in Figure 5.11 **(b**), the processing steps of gluing are as follows [82]:

    i. Double glass loading on conveyor
    ii. Lifting upper or lower glass by air sucker
    iii. Glass sheet rotation
    iv. Dispense header moving forward and backward, keeping the distance with glass edge of desired length
    v. Gel injector heat and extrude the glue
    vi. Dispense header rotates with the glass edges

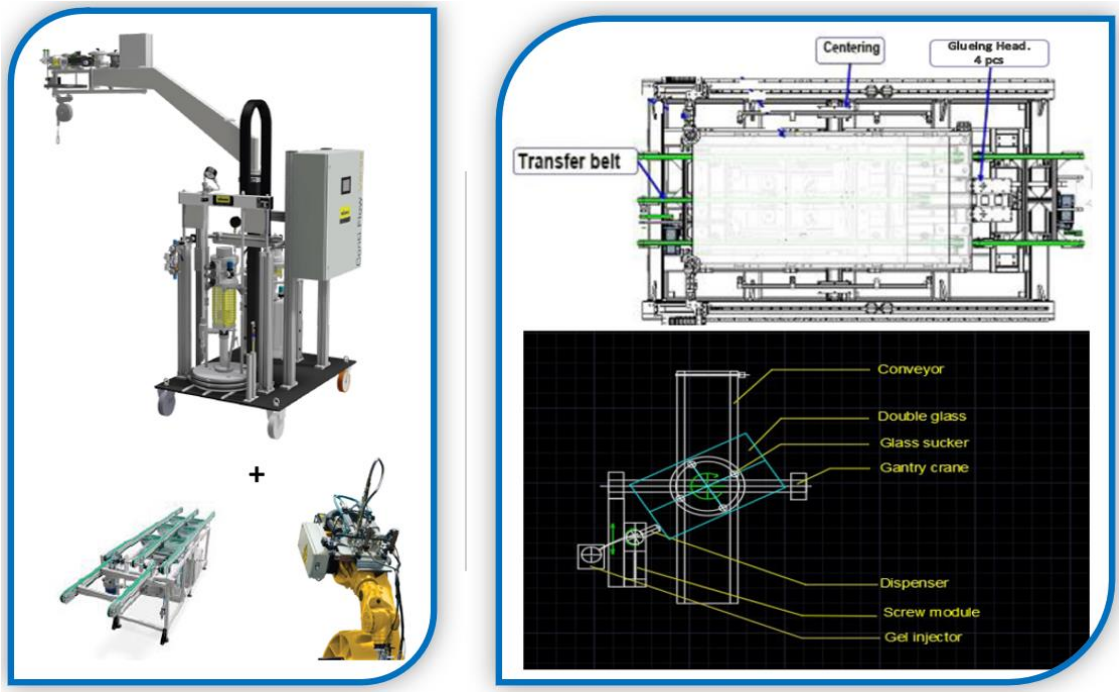

(a) **(b)**

Figure 5.11 -Schematic and visuals of PIB gluing machines: **(a)** PIB heated extruder and dispenser with the transport system and optionally a robot integrator [83], **(b)** Equipment internal structure with a conveyor belt, centering system, 4 gluing heads and up and down suckers for glass (**top-right**). Main componentry layout of the PIB dispenser (**bottom-right)** [82], [84]. Blue border: tailored to L-F module assembly.

The machine's rated power is at 10 [kW], and it consumes around 1400 [L/min]. It uses Compressed Dry Air (CDA) within 5 to 7 [bar] pressure. The machine footprint is 2.6 [m] x 3.8 [m] x 4.5 [m] [84].

The alignment and front positioning structures utilize a modular construction to be compatible with various wafer sizes, including the ZEBRA M6 half-cell. The adhesive system utilizes a double-barrel sealant to ensure uninterrupted provision. A PLC provides control over the operational and process parameters of both the adhesive machine and application platform, such as sealant pressure, temperature, trajectory formula, and flow rate.

Secondary Edge Sealing: Equipment

The silicone material is widely used for several PV assembly operations and applications such as frame sealing, rail bonding, JB attach and pot, optical coupling, thermal management, and PV encapsulation [85]. For small as well as large volume production, a list of potential solutions comprises:

- **Silicone Glue Dispenser** (Figure 5.12 (**a**)): A semi-automated extruder with an automated metering system. This includes drum and barrel pumps as well as pressure tanks. Similar to the PIB dispensing system in Figure 5.11 (**a**), a transport system is required, and for a fully automated mode, a robot integrator must be included [80]. This manual or semi-automated system, like the PIB extruder and injector, adopts the same parts without the heating fluid section and heated follower plate, but similar feeding pump and high-pressure material hose with a manual extrusion gun. Alternatively, a controlled metering unit with an automated valve system can be operated. Therefore, the technical specifications do not differ greatly from the PIB extruder and injector. Assumptions are 7.5 [kW] and 655 [L/min] for electrical and air characteristics. The working area is estimated to be roughly 3 [m] x 3.5 [m] (W x L) [80], [16].

- **Auto Edge Sealing/Taping Machine:** This equipment is generally used in L- plants that perform a complete tape edge bending process of the G/G module before entering the laminator. It prevents the melted fluid from overflowing at the module's edges, eliminating the occurrence of folds or bubbles after lamination. It is a swift process, taking no more than 20 [s/module]. With small adjustments in the injection heads, metering, and spatial coordinates, the unit also allows full edge sealing with silicone gel. This equipment's rated power and air consumption are 4.5 [kW] and 300 [L/min]. The footprint is 3.7 [m] x 2.5 [m] x 1.6 [m]. Its accuracy of +/- 1 [mm] is not enough to fulfil the requirements (of 0.4mm) tolerance for this study. Table 6.3 in Chapter 6 presents the accuracies and tolerances for the processing to comply with [33].

- **Glue Potting Manipulator** (Figure 5.12 (**b**)): Thanks to its servo belt structure and handheld programmer, this manipulator realizes automatic mobile glue potting in L- lines. Different trajectories and operating parameters of the manipulator can be edited with custom-defined processing to enable the edge silicone dispensing. The machine cycle time is +/- 20 [s/module] and over 99% uptime. Both electrical and air characteristics are optimal, with only 1.2 [kW] and 8 [L/min] of consumption. Similarly, its footprint is not large, at 3.1 [m] x 1.9 [m] x 2 [m] [33].
- ***Auto Glue Dispensing Machine for Frames*** (Figure 5.12 (**c**)): Together with the frame, also a layer of sealant is injected around the walls of the panel as a moisture barrier, made of silicone or a special tape. Typically, the framing process is divided into three steps:
    i. Loading frame
    ii. Automatic silicone dispensing into the rail frames
    iii. Frame assembly and tightening around the module

This system could solely perform silicone injection at glass edges without the need for a complete redesign of a fully customizable system. Some manufacturers prefer a single system, while others opt to install different machines in the line, each handling one of these three operations. For instance, in production lines such as those in [67] or [33], a framer dispensing machine is utilized solely for injecting silicone gel into frames. This machine accomplishes complete framing gluing within [20 s/module]. It features dimensions of 3.2 [m] x 2.9 [m] x 2 [m] and has power and air consumption properties of 2.5 [kW] and 160 [L/min], respectively [33].

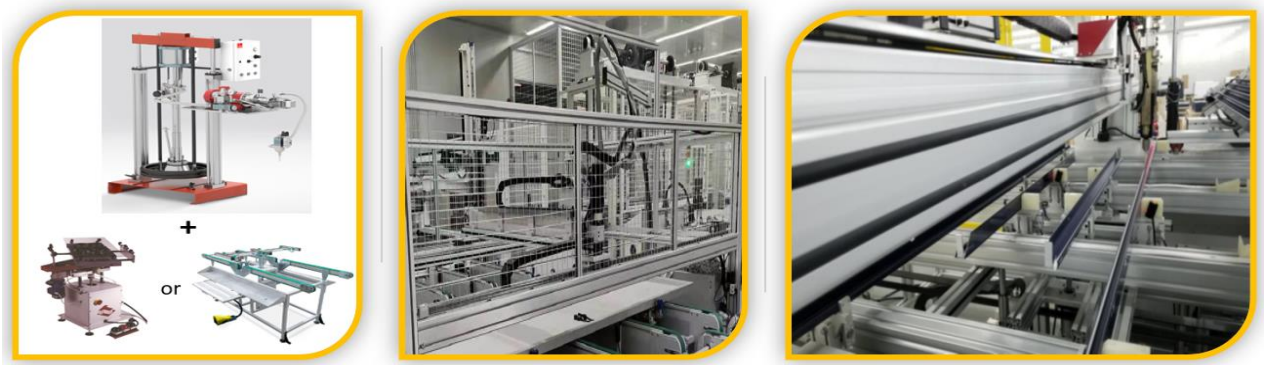

(a) **(b)** **(c)**

Figure 5.12 - Overview of potential toolset to operate the secondary edge sealing: **(a)** [86], [121] [16], **(b), (c)** [33]. Orange border: readjusted from L-lines.

The injection head of the framer machine moves straight forward or backward along the four panel edges while keeping the panel fixed on the conveyor. With multiple injector heads (two or four), the cycle can be further shortened.

5.2.6 Filling System

When analysing the line, one of the most important and challenging steps is the filling process and its sealing. Liquid-filled systems are widely used across various industries (food & beverages, pharmaceuticals, cosmetics, chemicals, automotive, and household). These systems are designed to accurately dispense liquid into a confined space at high speeds, ensuring efficiency and consistency in production. In this research, the inter-pane space is filled with a liquid following the conditions outlined in Chapter 4, considered as a new and thus non-standard process for the solar industry.

Various methods and apparatuses have been studied and suggested in the IG industry for replacing air with an insulating gas. In one method, air is gradually replaced with argon through an access port, in another, the inter-pane space is filled by drawing a vacuum before both panes are sealed to the spacer, and then gas is injected. In another, the bottom edge pane is partially assembled, spaced slightly offset to provide vertical openings for filling. Even a gas-tight conveyor belt can be used [87].

Similarly, a liquid-crystal vacuum filling system accomplishes the process via a “dropping method” in which the liquid crystal material is dropped directly onto one of the substrates, then aligned with the other substrate and the sealant dispensed on it, bonded under vacuum. Large inline filling machines for liquid crystal displays consist of a

vacuum & heating exhaust chamber, a filling and atmospheric pressure heating chamber. Up to 10^{-10} [bar] and 0.5 [MPa] (megapascal) are the values for high vacuum and filling pressures, respectively [122].

Defining conditions in this application, compared to other filling methods of other industries, is of fundamental importance to understand limitations and compromises amongst the different factors playing a role for the process itself and the entire production line.

One difficulty might be related to the realization and positioning of inlets/outlets hoses. For example, a gas filling machine can operate across the back of the profile via the frame or sealant. However, in this study, filling from the back or edge side comes with more downsides. The rear side filling means have already perforated not only the rear glass but also the adhesive substrate and CB layers. Further, it does not ensure and reach uniform distribution of the fluid between solar cells and the front glass. Filling through the edge is advantageous as the glass is not being perforated. However, unlike the single edge sealing in the glazing industry, for L-F module, this process will perforate both seals (PIB and silicone), increasing the panel's vulnerability to embrittlement due to the (liquid) filling, and the risk of leakage. Hence, the module's exposure to the external environment.

One possible solution is to fill the module from the front side, with two slits at the front sides of the panel. This method is already adopted in the IG industry, for example, in household windows, and the nozzles are already perforated prior to glass processing. These should not undermine the metal interconnections due to applied external forces. Hence, filling from the panel edges through the front glass plate is more beneficial. From Chapter 4, the cells-CB edge spacings available in the X and Y directions was 2 [mm] and 15 [mm], respectively. Positioning at the panel edges or corners is favourable as there is more spacing left as the central side of the panel may be the weakest. Furthermore, it is preferable the inlets and outlets are arranged at the corner and opposite sides, to reach higher performance of the process. In such a way, the air exhaust is extracted while the filler helps push air out from the other corner. It is more likely that an even distribution of the liquid throughout the corners, avoiding the risk of air-trapped or bubble formation. Further, the far positioning between the two nozzles can dampen the effect of swing pressure and de-pressure on solar cells, keeping the shear-stress low.

Another challenge is the pressure/de-pressure of operation. Unlike NICE technology that uses sensors for neutral gas-filled modules, pressure control inside the module is one of the key elements of the liquid-filled L-F technology. Indeed, on one hand, the forces applied to solar cells should be as small as possible to avoid cell breakage or undermining the soldered interconnection. On the other hand, the pressure cannot be too small otherwise complications may arise correlated with the air extraction and filling performance across the small cavities between cells, or at the module edges. Furthermore, a too slow filling especially for the HA line, would require various multiple tools and turn the manufacturing line cost to rise considerably. Filling pressure and air extraction de-pressuring is preferred with a gradual and accurate operation control. Vulnerable module parts should be filled in a way that is shear-sensitive and optimized for.

The filling pressure is very important but so is the accuracy in the operation. Filling accuracy relies on the type of system valves used. Pressure valves can be very fast and not so precise in the filling accuracy (+/-10%) while volumetric valves are slower but with very higher precision in tolerance and repeatability (+/- 1% filling accuracy) (Expert Input: *member of TechconSystem*). Volumetric valves would be a better fit over pressure valve systems as the inner PV module profile does not contain a smooth surface. Cell spacer heights do hamper the flow. This can conduct the filling machine to reach a pre-set value of the pressure within the module not completing the filling injection. Furthermore, a higher accuracy for the process is beneficial as there is no exact tolerance in volume to cover the area yet, as this is a new process which has not been explored before.

It is indeed known that in Argon-filled IG units, the gas concentration reaches a customary value up to 97% by volume and the exhaust port is then closed [87]. There is no need to adjust the filling time for gas-filled, smooth IG units as they are equipped with sensor that helps the gas volume, which is neither too little nor too much. Corner pieces are fitted to the two diagonal corners of the IG panel. The inlet hose is connected to the bottom corner piece and the sensor hose to the upper one. The gas inflows and the air inside are gradually pushed out, so when it is completely displaced, the sensor activates, and the filling automatically stops. The operation is fast, and the machine is of reduced size [87].

However, for the purposes in this report, continuous and constant dosing at variable back pressures with a volumetric valve and programmable suck-back function are the suggested parameters worth further investigation.

Another condition affecting the manufacturing is linked the dosing system. Dosing pumps and mixing heads need to fulfil the demanding and strict requirements of the fluid requirements suitable for this specific application. A

more mixed ratio and viscous fluid grades are more energy-consuming for the system heating mechanisms which also require longer dosing times. With increased viscosity, though, more precise control in the process can be achieved. Achieving reliable, and automatic filling from a few microliters to around 1 litre per second is possible, depending on the material used and process boundary conditions. Based on the mixing ratio and viscosity, the volume flow can range from 0.2 [mL/min] to 116 [L/min] with the smallest filling quantity of 0.1[mL] [120].

Barriers will also be experienced when sealing the filling nozzles. Adhesives, metal solder, glass, etc., can be used as sealing materials. Achieving a tight seal after the unit has been filled, either using a sealant agent such as butyl tape or through soldering, without inducing any electrical conductivity and leakage, is challenging to guarantee the long-term stability and performance of L-F modules. Depending on the sealant type and operation method, the overall process cycle may be prolonged, and an additional unit section within the same workstation may be needed.

An exact and comprehensive filling and sealing system cannot be determined for this application due to the lack of solid research and testing. To define specifications for a complete inline system, a large filling machine is selected as a reference from [88] and [89]. The unit features a 35 [kW] installed capacity, 550 [L/min] compressed air consumption, and a working area of 3 x 2 [m].

To conclude this chapter, adjusted and dedicated solutions illustrated are new processes for solar module manufacturing whose feasibility has not been studied and demonstrated yet for this specific application, especially concerning the filling process. Based on each process's trade-offs, decisions will be made for every unit in Chapter 6. The choice will be built on different key parameters, namely, cycle time, accuracy and repeatability errors, dimensions, energy consumption, and cost.

6

Technical Analysis: Manufacturing Processes, Comparisons, and Results

In this chapter, the identification and quantification of technical parameters for two scales of complete manufacturing L-F module lines are presented. This is achieved by evaluating differences in equipment requirements compared to laminated plants, as well as from processes investigation conducted in Chapter 5 for non-standard options and solutions. Technical results are derived from this analysis.

6.1 Line Processes for Laminated and Laminate Free Modules

This section presents a comprehensive assessment, including a list of assembly units and their key requirements. This enables us to evaluate and quantify differences in line parameters between L- and L-F production modules. The following three sub-chapters are divided into assembly operations common to both standard and L-F modules, exclusive to the L-module lines only, and readjusted as well as tailored to L-F module production.

6.1.1 Similarities in Assembly Operations

As noted in the preceding chapter, over 60% of the processes can be adapted from equipment utilized in the L-lines. Following the research conducted in Chapter 3 on the manufacturing of laminated panels and the sequence steps outlined in Chapter 5, with the reference to the green formats of Table 5.0 for L-F modules, a table can be constructed by selecting specific assembly tools which are common to both laminated and laminate-free modules. This selection is based on general research analysis and the level of details retrieved from current manufacturers. Yet, other similar available machines do exist in the market. Such equipment may have different technical characteristics and requirements. For this report, this sourced assembly machines are presented in Table 6.0, which serves as a reference to build up the production line for L-F modules and to draw technical conclusions.

Table 6.0 - Equipment requirements in common with 20 [MW] and 300 [MW] scale of L- lines: these units are used in the explored SA and HA production lines of L-F modules. Technical specifications for processes requiring multiple units. Rows split into two illustrate both the value per unit and the total value for that process.

20MW | SA line					300MW | HA line					
Tool | Reference	cycle time [s/module]	(TOTAL) power | air cons. [kW] | [L/min]	Labour	footprint [m x m x m] (LxWxH)	Tool | Reference	Sets	cycle time [s/module]	(TOTAL) power | air cons. [kW] | [L/min]	Labour	Footprint [m x m x m] (LxWxH)
Glass lifter [16]	40 - 60* [s/glass]	4 | 40	1	2.5x1x3.8	Auto Glass loader [33]	1	20 [s/glass]	8.5 | 150	-	7x3.6x1.8
Cell/string layup system [67]	42 **	19 | 200	-	4.7x2.8x2.5	cell/string layup system [67]	2	42 **	9.5 | 100	-	4.7x2.8x2.5
							21	19 | 200		9.4x5.6x5
Solder check unit [67]	25	2 | 12	1	3.2x2.9x1.9	EL tester [33]	1	20	4 | 12	1	3.2x2.9x0.9
Glass lifter [16]	40 - 60* [s/glass]	4 | 40	1	2.5x1x3.8	2nd glass covering machine [16]	1	20 [s/glass]	10 | 30	-	2.5x3.2x4
180° flipper [33]	20 - 30	0.5 | 250	1	3.6x1.9x1.5	180° flipper [33]	1	20	0.5 | 250	1	3.6x1.9x1.5
Glue dispenser for JB attach [33]	30 (10s/1pc JB)	0.8 | 8	1	0.7x0.6x0.6	Auto JB soldering machine [33]	1	20	20 | 400	-	3.4x1.8x2.1
Glue potter for JB [33]	30	1.5 | 10	1	1.1x0.9x1.2	Auto JB potting machine [16]	1	25	2 | 10	-	3.6x4.3x2.9
Worktable for JB closing [16]	30	0.5 | 3	1	2.3x1.4x1	JB closing machine [67]	1	16 - 20	20 | 500	-	4.2x2.3x1.9
180° flipper [33]	20	0.5 | 250	-	3.6x1.9x1.5	180° flipper [33]	1	20	0.5 | 250	-	3.6x1.9x1.5
Visual scanning 90°*** [16]	60 - 120*	1 | 5	1	3x2.3x2.5	Line scanning machine *** [67]	1	16	3 | 100 [33]	-	2.9x2.5x2.3 [33]
Hi-Pot tester [33]	40	3 | 5	1	3.2x1.8x1.4	Hi-Pot tester [33]	2	40	3 | 5	2	3.2x1.8x1.4
							20	6 | 10		6.4x3.6x2.8
IV tester [33]	20	3 | <1	1	2.4x1.6.x1.5 [16]	IV tester [33]	1	20	3 | <1	1	2.4x1.6x1.5 [16]
Final EL tester [67]	25	2 | 0.6	-	3.2x2.9x0.9 [33]	Final EL tester [67]	1	25	2 | 0.6	1	3.2x2.9x0.9 [33]
-	-	-	-	-	Labelling machine [33]	1	20	3.5 | 100	-	3.6x2.1x1.8
-	-	-	-	-	Sorting & packing island [16]	1	30	15 | 30	-	7.5x6x3
TOTAL	**7.5 - 9.5** [min]	**42** [kW] **825** [L/min]	**10** [worker]	**70** [m^2]		**17** [pcs]	**6.3 - 6.5** [min]	**115** [kW] **2050** [L/min]	**6** [worker]	**180** [m^2]

* cycle time estimated based on expert inputs and personal experience at the production site (Soltech) with process engineers

** one stringer picks and places one string of 20 cells in 7 seconds. The 120-cell module is performed in 42 [s]

*** optical scanning is an optional process, hence to arbitrarily be omitted from this table

As most of the operations require operator support, the labour force is nearly doubled for the SA line, with 10 operators. Some operations, however, require an automated layup system. For instance, the available cell/string layup systems, used for both lines, can grab up to 24 half-cells at a time [33]. Following the cell alignment in the configuration design explained in Chapter 4, a single-cell string is picked and placed by a six-axis robot to achieve high-precision layup. A multipurpose worktable, operated for manual operations in the SA line, comprises tasks such as module flipping of 180°, fixing and potting the JB, and injecting seals at the module's edges. Optional units, already discussed in Chapter 5, can be installed, and integrated at defined stages (see Figure 5.1).

Overall, for both scales, no single equipment exceeds 20 [kW] of power consumption, with limited footprints except for the auto glass loader, packaging & sorting island, which are 7 meters long. However, most of the fully automated units demand a great amount of compressed ai reaching a total value of 2000 [L/min].

6.1.2 Processes Exclusive to Manufacture Laminated Modules

Several assembly units exclusively utilized in L-plants include encapsulant foil cutters, stringers, and bussing stations, followed by laminators, and trimming machine. For G/G modules, the framing machine is also accounted for. Table 6.1 presents a list of toolset features for two production scales, based on the 20 [MW] (Figure 3.1) and 300 [MW] (Figure 3.2) lines detailed in Chapter 3. In the 20 [MW] line, each operation is processed by only one machine; hence, the number of sets is not displayed in the table. The last row of the table provides a summary, indicating the total value in main parameters for each tool.

Table 6.1 - Main technical specifications of equipment used exclusively in two different scales of L- plants. Rows split into two illustrate both the value per unit and the total value for that process. Last row provides the total value.

20MW					300MW					
Tool | Reference	cycle time [s/module]	(TOTAL) power | air cons. [kW] | [L/min]	Labour	footprint [m x m x m] (LxWxH)	Tool | Reference	set	cycle time [s/module]	(TOTAL) power | air cons. [kW] | [litre/min]	Labour	footprint [m x m x m] (LxWxH)
1st EVA positioning-worktable [16]		<1 | ≤1	1	2.5x2x1.6	Auto foil cutter [92]	1x	30 [s/foil]	5 | 9	-	6x2.5x2
IR stringer [90]	30	13.5 | 25	-	6.2x2x2.3	IR stringer [90]	4x	30	13.5 | 25 54 | 100	1	6.2x2x2.3 24.8x8x9.2
2nd EVA & backsheet cutter positioning – worktable | [92]	30	5 | ≤1	1	3.5x3.3x1.6	auto EVA & backsheet cutter with P&P [92]	2x	30 [s/foil]	5 | 9 10 | 18	-	5.9x4.5x2.2 11.8x9x4.4
Manual bussing station/ worktable [16]	120 - 180	≤1 | ≤1	2	2.5x2x1.6	Auto Bussing station [67]	1x	20	35 | 2000	-	5.6x5x2.6
Laminator [32]	240 - 400 ***	27 | ≤1	1	14x3.3x2.1	Auto taping (adhesive) machine [33]	1x	20	5 | 300	-	3.1x2x1.8
Manual trimming station /worktable [16]	40 - 60 *	≤1 | ≤1	1	2.5x2x1.6	Lead compression [33]	1x	20	7.5 | -	-	3.3x2x1.9
Frames silicone dispenser [91]	60	≤1 | ≤1	1	2.3x2.4x2.5	Laminator (double step) [32]	2x	72 - 120 **** 36 - 60	90 | ≤ 1 180 | ≤2	1	31x3.3x2.1 62x6.6x4.2
Inline horizontal framing machine [91]	60	5 | 3	1	2.7x3.8x1.4	Auto trimming machine [33]	1x	20	3 | 100	-	3.5x2.3x1.7
					Fully auto framing island [91]	1x	30	25 | 200	-	8.6x6.5x4
TOTAL	**10 - 15** [min]	**60** [kW] **35** [L/min]	**8** [worker]	**100** [m²] **		**14** [sets]	**5** [min]	**320** [kW] **2750** [L/min]	**2** [worker]	**835** [m²] **

* cycle time estimated based on expert inputs and personal experience at the production site (Soltech) with process engineer

** total footprint value expressed in [m²] and not [m³]

*** the laminator handles 9 - 15 [module/h] containing 3 module/cycle (or 3 plates)

**** the laminator handles 30 - 50 [module/h] containing 5x2 module/cycle (10 plate total in double-stack configuration)

Stringer and bussing units are dedicated to the mainstream interconnection technology for manufacturing exclusively laminated panels. However, with the new CB technology, cell and string interconnections are soldered via the heat generated during encapsulation in the laminator machine. This eliminates the need for costly and bulky stringers and automated bussing systems in the line.

The laminator consumes less than 1 [L/min] of air but a significant amount of electrical energy. Most of the power consumption of automated units comes from laminators, stringers, framing, and bussing machines. Additionally, trimming, framing, and bussing units are those with excessive air consumption. In small line scales, a three-plate laminator is utilized, while for higher outputs, 3 to 5-plate laminator(s) are installed in a double-step configuration [103].

Based on the data referenced in the table above, the total cycle time saved per module, by omitting these machines in L-F plants, is estimated to be, for each scale, of approximately 10-15 [min] and 5 [min], respectively. Regarding power consumption for both scales, when compared and summed up to values of Table 6.0, the total value in the last row (Table 6.1) accounts for up to 75% of the total power consumed by all assembly machineries of the line, which is seen as a gain for L-F module assembly. Particularly, only the share of the laminator(s) electrical consumption, for these two scales, can range between 20% and 50%, respectively.

In reference to the L-plants presented in Chapter 3, due to the avoidance of the lamination process, there is a significant reduction in the factory footprint and an increase in production line speed. To conclude, the laminator(s) alone for each line can account for up to 10% of the space occupied.

In addition to assembly equipment, transport systems conveying modules across the line must be included in this section analysis, exclusive to laminated plants. These systems range between 10 and 30 units for each line. It is important to understand the number of transport units needed, not only for their power consumed but also to gain a more detailed understanding of their cost share, which will be evaluated in Chapter 7.

Usually, when setting up a production line of small/medium capacity, especially for starting companies, it is preferable to work and control a few smaller units rather than one single and complex automated system. For example, stringers and bussing systems, which are not used for L-F module assembly, are essential parts of the laminated module's lines, difficult to run, and without skilled inline operators, bottlenecks and downtimes may likely rise in the production, slowing productivity (Expert Input: *member of Valoe*).

This first assessment does not include the non-standardized equipment required to manufacture L-F modules. Yet, these adjusted and dedicated new units, explored in Chapter 5, may offset, or even overtake the gain per panel just estimated. For instance, the edge sealing or filling system may request a considerable amount of electrical power or occupy more space in the line, as multiple toolsets may be needed to ramp up the total line throughput.

6.1.3 Re-Adapted and Dedicated Processes (non -standard) to Manufacture Laminate-Free Modules

All processes that deviate from the classic tabbing and stringing cell/module interconnection of L-plants in Chapter 3 are considered as readapted and/or dedicated processes. These, which were represented by the orange and blue format blocks illustrated in Table 5.0 (Chapter 5), comprises the following operations: layup custom-CB, solder paste deposition, cell strings soldering, module bonding and cooling, edge sealings, and module filling.

Based on the different options of application techniques explored in Section 5.2, the selection of a method and reasoning for the choice are now addressed. A summary table (6.2) with the selected solutions and their corresponding specifications is shown at the end of this sub-chapter.

CB substrate's paper removal and layup operation: As said, the adhesive film is assumed to be already deposited onto the CB substrate in a ready-to-use state with removable paper attached. Given the function of the three machines explored in Chapter 5, the cycle time to accomplish the loading and unloading in a traditional line is within 20 [s]. For this adjusted unit, an extra and larger 40 [s] is assumed for complete alignment and layup to achieve a higher accuracy grade. For each substrate paper removal operation, a range between 30 and 40 [s] is considered. For the two scales of lines, the curing loading/unloading machine is considered as it is a space-efficient and inexpensive option [67]. Two of these units are needed in the HA line. In the large-scale HA line, to avoid possible setbacks due to adhesive curing time, a curing equipment could be installed after the placement of the CB. The UV LED spot curing system encompasses an in-built power supply with a very reduced size [94].

Solder paste deposition tool: The screen and stencil process are very challenging for this application due to the long PCB traces and thin dimensions of the solder paste. These systems are standardly catered for flexible design within the electronic industry of printing area components less than 1 [m]. However, this technique may overtake the classic dispensing systems when it comes to efficiency, printing speed rate, and precision system [70].

Alternatively, by applying a spraying method for this study, an insulating foil may be needed when depositing the paste over the thin PCB traces as well as multiple gun heads. Additionally, to reach the desired paste height of 0.2 [mm], more than one spraying layer deposition would occur, increasing the process cycle further. Moreover, the spraying machine system occupies a large area. Therefore, the spraying method may also not be very appropriate for this study. The selected paste deposition method is the jet dispenser. With this system, application speed can range between 6 to 12 [m] per minute flow. A flow rate range between 10 to 12 [m/min] is assumed. Over the total panel length (approximately 95m) and the 108 traces, to finalize the process, between 8 and 9.5 [min] per panel are required. This is surely one of the slowest operations within the line. Given the symmetrical geometry of the module, with six strings in the head and six in the tail, a second unit is accounted to work simultaneously, cutting down the operation cycle to 4 to 5 [min] per panel. Two dispensers are needed for the SA line, reaching 3 to 4 [min/module] speed while ten units for the HA line to achieve a total process throughput of approximately 50 [s/module].

Soldering unit: Technically, by using a laser solder instead of an induction solder, the heat dissipation would probably be lower with shorter soldering times. It is therefore likely to yield better results, but it demands much more control over many important process parameters for both cell-to cell and strings soldering. This can lead to issues such as incomplete paste melting or laser beam deflection. Additionally, the laser method may bring to an easier and quicker local thermal breakdown of the module's components, such as burning of the peripheral CB or cell spacers deformation. Although its processing speed and thus installation for multiple components may be reduced in the HA line, the overall cost compared to a heat inductor system would probably still be higher. Furthermore, the focus point for laser soldering should be smaller than the 0.8 [mm] (the solder paste width of this project is 1[mm]). Indeed, this method would be more suitable for edge connectors with IBC cells, with the laser beam hitting the solder spot at the edges instead. Therefore, to similarly reach steady and reliable process, this study considers the heat inductor system as the soldering method. Based on the cycle time per cell discussed in Chapter 5, respectively one and three units are considered for the two scales.

Alternatively, an ECA stringer can be employed if a different assembly route is taken than the conductive backsheet. An ECA stringer would not work with the CB technology but rather with the classic ribbon interconnection via a conductive adhesive film, or a LTSP deposition. Additionally, interconnection with edge connectors "dog-bone" are also possible, but the machine would require an embedded or a separate unit containing the dog-bones for soldering. The advantages of the ECA stringer lie in its flexibility, allowing the use of either FBC or BC solar cells. Additionally, there is the benefit of having only one unit in the line, rather than the separate units for paste dispenser and soldering machine. However, the drawback is related to the difficulty of removing the adhesive layer from other entities for RRR and recycling purposes.

PIB edge sealing: In the small and cost-effective SA line, a semi-automated PIB heated extruder with a rotary table that moves along the edges is used (Figure 5.11 (**a**)). A tailor-made auto-gluing machine (Figure 5.11 (**b**)), in the HA line, performs the PIB injection over one of the two glass substrates held by up or down suckers. Dispensing the PIB over the front glass plate is more successful as it reduces the cycle time, enabling simultaneous operations. Drum capacities and cycle times will be assessed in Section 6.2.1.

PIB bonding and curing: To accomplish this operation, the SA line employs one manual clamping table with fans or cooler while in the HA line, two automated cooling chamber plates are necessary to reduce the cycle time down to 30-40 [s].

Second (Silicone) edge sealing: The choice of a semi-automated unit is for the SA line (Figure 5.12 (**a**)). It features a silicone glue dispenser and a stationary motorized worktable, enabling multiple processes to be carried out at one station with one inline worker. In the HA line, to reduce the process cycle and minimize dispensing errors by the operator, either a robot integrator or a re-adjusted manipulator system with single or multiple heads can be included. The adaption of either the edge sealing/taping machine or glue dispensing for frames are effective options. Among these last two options, the edge sealing/taping machine is the choice adopted as it consumes less air and power and is a less expensive option. Drum capacities and cycle times are assessed in Section 6.2.1.

Liquid filling system: Given that this process has not been investigated before for this type of application, the filling specifics are based on the assumptions made in Section 5.2.6. A continuous, slow and precise filling method is preferred, utilizing a volumetric pump. Consequently, a very low flow rate is considered. Recalling the

possible large range of volume flow from 0.2 [mL/min] to 116 [L/min] [120], a value of up to 1 [L/min] is chosen to comply with the conditions of slow filling. Both lines adopt the same type of unit, in a semi-automated mode. With a volume to fill between 1 to 1.5 [L], a complete filling takes 60 to 90 [s/module]. An extra 60 seconds is assumed for the sealing operation. As a result, respectively, one and two filling systems are employed for each scale of the line.

Motorized transport system: the conveyor system matching the dimensions of the cooling chamber plate (2.3 [m] x 1.4 [m] x 1 [m]), consumes 0.5 [kW] and 3 [L/min] [16]. It is used to support the system for conveying the panel through. Another transport system found, as a reference, is retrieved from [33], which automatically conveys panels across the line within 20 [s] and with plate dimensions of 2.3 [m] x 1.4 [m] x 1 [m]. This transfer unit serves multipurpose functions, including horizontal, longitudinal and bidirectional transportation, alignment station capabilities, pneumatic and manual folding, lifting as well as material rack support. For every process, the additional consumption of a transport system (0.5kW and 3 L/minute) is accounted for [16]. A complete overview with the toolsets and their corresponding specifications is shown in Table 6.2.

Table 6.2 - Re-adjusted and dedicated process specifics for two scale of L-F module lines: technical specifications for processes requiring multiple units. Rows split into two illustrate both the value per unit and the total value for that process. The separation marks (÷ and -) indicate both the range value.

SA line					HA line					
Tool | Reference	**cycle time** [s/module]	**(TOTAL) power | air cons.** [kW] | [L/min]	**labour**	**footprint** [m x m x m] (LxWxH)	**tool | reference**	**set**	**cycle time** [s/module]	**(TOTAL) power | air cons.** [kW] | [litre/min]	**labour**	**footprint** [m x m x m] (LxWxH)
Curing load/unload manipulator (CB operations) [67]	60 + (30 - 40) **	4 |110	1	3.2x2.6x4	**Curing load/unload manipulator (CB operations)** [67]	2	60 + (30 - 40) **	4 | 110	2	3.2x2.6x4
							30 + (15 - 20)	8 | 220		2x(3.2x2.6x 4)
Jet dispenser (paste deposition) [69], [49], [33]	480 - 570	1 | 20	-	(1x1) + (2.8x1.4) *	**Jet dispenser for metal paste** [69], [49], [33]	10	480 - 570	1 | 20	-	(1x1) + (2.8x1.4) *
	240 - 280 **(2 units)**	2 | 40		(2x2) + (2.8x1.4))			48 - 57	10 | 200		5x((1x1) + (2.8x1.4))
Heat Inductor (soldering) [73], [74], [33]	120 - 180	13.7 | -	-	(1x1) + (2.8x1.4) *	**Heat Inductor (soldering)** [73], [74], [33]	3	120 - 180	13.7 | -	-	(1x1) + (2.8x1.4) *
							40 - 60	55 | -		(4x4) + (11.2x5.6)
PIB heater & extruder (+ rotary table) [80], [33]	30 - 35	5.6 | 640	1	(0.8x1x3.3) + (2.8x1.4) *	**Auto PIB gluing machine** [84]	1	25 - 30	10 | 86	-	3.8x2.6x4.5
Clamping table with coolers [121]	60	<1 | <1	1	2x1.5	**Cooling chamber plate** [32], [33]	2	60	18 | 1	-	2.8x1.4 *
							30	36 | 2		5.6x2.8
Glue dispenser + transport system (silicone edge seal) [80], [16]	30	7.5 | 650	1	(3x3.5) + (2.8x1.4) *	**Auto (silicone) edge sealing/taping machine** [33]	1	25	4.5 | 300	-	3.7x2.5x1.6
Filling unit [88], [120]	120 - 150	35 | 550	1	(3x2) + (2.8x1.4) *	**Filling unit** [88], [120]	2	120 - 150	35 | 550	2	(3x2) + (2.8x1.4) *
							(60 - 75)	70 | 1100		2x((3x2) + (2.8x1.4))
TOTAL	**11 - 14** [min]	**68** [kW] | **2000** [L/min]	**6** [worker]	**55** [m^2]		**21** [set]	**4 - 5** [min]	**200** [kW] **1900** [L/min]	**4** [worker]	**180** [m^2]

* Transport system added to the assembly equipment working area from [33]

** The first term is the range in [s/sheet] that have been laid up on the rear glass. The second term is in [s/paper] removed from the CB substrate

When comparing the results of adjusted and dedicated process (Table 6.2) based on the application methods chosen, with the main technical specifics of equipment used exclusively in laminated plants (Table 6.1), it is found that:

- **CYCLE TIME:** There is no gain in cycle times as both results are nearly identical.
- **ELECTRICAL & AIR CONSUMPTION:** Similar power is consumed in the 20 [MW] laminated line and the SA line. However, the HA line's adjusted and dedicated machines can consume up to 30% less electrical power and compressed air (200 [kW] and 1900 [L/min]). In contrast, the compressed air needed in the SA line alone is 70% higher than that of traditional lines. This is mainly due to the filling, and the two edge sealing machines.
- **LABOUR:** Regarding the labour force, in the SA line, most of the assembly operations require an operator, while in the HA line labour is needed primarily for the filling and CB layup operations, with semi-automated machines. In transitioning from small to large scale L-F module production, labour force can, in the best scenario, be equal to laminate lines. At worst, it can even double when compared to the laminated plants in Chapter 3.
- **FLOOR SPACE:** The total floor area for readjusted and tailored units, for both small and large scales, is 55 [m^2] and 180 [m^2], respectively. When compared to the 100 [m^2] and 835 [m^2] (total space occupied by laminated equipment only, Table 6.1), this corresponds to a reduced production space area of up to 50 [m^2] and 655 [m^2], respectively. As result, a visible reduction in factory area occurs only in the large-scale line. A significant portion of the footprint area for the HA line is primarily due to the multiple units needed for dispensing the metal paste, soldering units, and ultimately, the filling systems. A more detailed analysis of the floor space required, compared to the laminated PV lines in Chapter 3 (Figure 3.1 and Figure 3.2) is evaluated in Section 6.2.2.2.

6.1.4 Alignment Systems: Tolerance and Accuracy in the Assembly

This sub-chapter presents an overview of accuracies to meet for the main and most critical assembly processes of the L-F module production, requiring high precision. Operations should satisfy the minimum tolerances in the assembly based on machine alignment systems and module design specifications in Chapter 4. A comparison of tolerances and adequacy to satisfy various processes of standard and L-F panel manufacturing is evaluated.

For the SA line, most operations are carried out on a transport system in manual or semi-automatic mode with the assistance of operators. Apart from processes requiring a certain level of accuracy, there is no proper alignment system connected to the assembly unit. However, for the HA line, every automated process should include a centering system with sensors or cameras, with exact tolerances for loading, aligning, and unloading.

Layup systems utilize optical inspection, with laser photodetection for string alignment and charged-coupled device (CCD) camera inspection for cell and string quality inspection. Alignment systems and tolerances to be satisfied for L-module assembly operations are presented in Table 6.3.

Table 6.3 - Main alignment systems of automated units for conventional and L-F module assembly. A comparison and accuracy are illustrated in the 3rd column. Design specifications for L-F components to comply with are listed in the rightmost column.

Unit/operation	Alignment system	Machine Tolerance in Accuracy [mm]		L-F design specs. [mm]
		L-	L-F	
Glass layup	Glass laser marker, XYZ centering (camera)	0.1 [84]	**satisfied**	**-**
EVA/backsheet foil cutter & layup	Auto cutter & centring system	EVA ±2; TPT:±1 [67]	**not required**	-
CB foil layup (auto layup machine)	Visual positioning system	± 0.8mm [33]	**satisfied**	2
Cell spacers layup within the CB foil	Already embedded into CBS	**not required**	-	0.20
Cell/string layup	Laser photodetection (string), CCD camera (cell & string inspection)	± 0.05 [38] ± 0.1 [34] ± 0.3 [67]	**Satisfied**	0.25
Solder paste dispenser [68]	Optical positioning and alignment	**not required**	± 0.01	0.5
Soldering unit [67]	Optical with laser	± 0.1	**satisfied**	0.5
Bussing system	Laser & CCD camera	≥ ±0.5mm [33]	Not required	
PIB dispenser	auto centring system	**not required**	±0.5 (width, height) ±0.2mm (corner) [84]	0.5
JB assembly & pot	Robot with camera	≥ ±0.5mm [67]	satisfied	-
Edge sealing/taping machine (for silicone)	Vision- and laser based	≥ ±1mm (tape)	**NOT satisfied**	0.4 (4%)
JB assembly and pot [67]	Auto centring system	±0.5 | 2-3% (pot)	**satisfied**	**-**
Filling operation [88], [120]	Pressure/volumetric sensor	**not required**	± (1% - 10%) (Expert input: *member of TechonSystem*)	0.25 [L] 5%

Stringers and soldering units employ optical cell alignment, with the requirement for cell positioning and string alignment accuracy to be within ±0.1mm [67]. For CB foil layup, from the product analysis in Chapter 4, edge spacing between solar cell-CB is 2 [mm]. The maximum allowed error for P&P is therefore 2 [mm]. Exceeding that dimension, the PIB sealant might risk being dropped over the solar cell edges, or the secondary sealant might overflow from the glass plates of the module, reducing its useful edge seal width. The accuracy in alignment for cell spacers in the perforated CB foil is recommended to be as small as possible, as the gap for each side of the octagonal cell spacer is 2 [mm]; therefore, a maximum tolerance of 0.20 [mm] was deemed sufficient. This accuracy is given even though the cell spacers come already embedded into the CB. The accuracy for cell/string layup considered by manufacturers ranges from ±0.05 to ±0.3 [mm] [42]. The accuracy for the paste dispenser is computed based on a trace width of 1.05 [mm] and the distance between two busbars of 5.6 [mm]. Therefore, the dispensing tolerance should not exceed 0.5 [mm] to ensure safety and avoid any risk of short-circuiting and current leakage. The PIB machine performs the sealing with +/- 0.5 [mm] precision width and +/- 0.2 [mm] and +/- 0.5 [mm] height on straight edges and at corners, respectively. The dispensing repetition accuracy is less than 1%, all values within the range requirements [84]. For accuracy in dispensing silicone edge seals, considering a max. 3 [mm] height for injection and possible shrinkage upon cooling/expansion upon heating, a tolerance of ±0.4 [mm] is deemed sufficient. This tolerance is in line with the 4% of shrinkage volume upon bonding and cooling for both sealants [57]. However, this tolerance cannot be met by any of the assembly solutions explored in Chapter 5. Lastly, for the filling process, general fluid machine accuracies can have a broad range (1% to 10%) of tolerance. As the filling volume area is not precise enough, an average value of 5% for the process in accuracy tolerance is deemed appropriate.

6.2 Criteria for Laminate-Free Modules' Manufacturing Line

Cycle times and production space are investigated for the two complete scales of lines. The section concludes with L-F module factory requirements.

6.2.1 Edge (Seals) Dispensing Operation: Drum Capacity and Cycle Time Analysis

A proper metering system is essential to ensure that adhesives are conveyed efficiently and without any air pockets. Depending on the material properties and processes to be finalized, the container drum size can be scaled accordingly. Standard mixing and dispensing systems for drum capacities are available in sizes ranging from 20 to 200 [L] [86]. Depending on the requirements for seals on the L-F panels, different container sizes and options are available for selection. A reserve barrel of 20 [L] might also be necessary to allow the feeding system to run continuously through an automatic switchover between pumps. This avoids downtime when changing plates without interruption or time pressure, in a so-called tandem form [86].

(a) **(b)**

Figure 6.0 - Drum and barrel pumps: double drum configuration (**a**), single drums sizes "from left to right: 1 to 20÷30 litre capacity" (**b**) [86].

To assess the scalability and durability of the barrel size, both line outputs are assumed based on the L-lines' throughput in Table 3.0 (Chapter 3). These account for 10 and 90 panels per hour, respectively. A single shift consists of 8 working hours. Hence, 80 and 720 panels per shift are produced, respectively.

❖ **1st Edge Seal: PIB & Desiccants**

The extruded PIB over one panel perimeter reaches a volume up to 160 [cc]. Considering the standard and available capacity of 20 [L], and a production of 80 panels per shift for the SA line, a drum change would occur every 1.5 shifts. However, looking at the HA line output volumes, this drum size would not be sufficient as one barrel would need to be changed every hour. On the other hand, for the HA line, based on the assumed productivity and considering the largest standard drum size available in the market of 200 [L], approximately 1240 panels can be edge-sealed with one barrel. This translates to a barrel change every 1.7 shifts. Details of drum sizes and related reserves for the 1st edge seal are provided in Table 6.4.

❖ **2nd Edge Seal: Silicone**

The silicone extruded volume computed ranges between 50 and 85 [cc] per panel. Assuming the same machine flow rate, this amount is nearly halved compared to the PIB volume, thus doubling the number of sealed panels with the same drum barrel size. For both SA and HA lines, a 20-liter and 200-liter drum would be changed every 3 shifts. However, if the same machine is used to pot the JB, a single barrel drum change time is reduced. The 24 [g] (8 g x 3) are being potted over the three-part JB. With a silicone density of is 1.1 [g/cc] [57], this results in 22 [cc] needed to completely pot a 3-point JB. The total amount of silicone now demanded for both edge dispensing and potting JB is 105 [cc] per panel. Under the assumptions made, a 20-liter drum barrel for the SA line would produce 190 panels and last 2.3 shifts. For the automated line, the maximum drum size of 200 [L] would last over 2.5 shifts. A reduction of drum size is preferred to achieve a smaller footprint and lower costs. Drum sizes and related reserves are presented in Table 6.4.

Table 6.4 - Estimated drum and barrel sizes for the 1st, 2nd edge sealant dispensers as well as for JB potting application, related to both SA and HA lines: The drum size + reserve columns represent, in litres, the capacity of the tandem form drum barrels formed of a primary barrel of variable size and a backup barrel of 20 [L] to avoid downtimes in the production.

Operation	Line type	
	SA	HA
	drum size + reserve [litre]	
Primary edge seal (PIB)	20 + 20	200 + 20
Secondary edge seal (silicone)	20 + 20	100+ 20
Secondary edge seal + JB pot	20+ 20	100+ 20

To compute the dispensing cycle for edge sealants, both the extruded volumes of the adhesives and the flow rate must be considered in continuous operation. From Chapter 4, the corresponding upper limit of extruded volumes for PIB and silicone were 160 and 85 [cc/panel], respectively. Based on these, the automatic piston metering volume of a small, semi-automated dispenser ranges from 3.5 to 254 [cc/shot] [86], which falls within the range of both edge seal volumes, if a single shot injection per panel is applied. Semi and fully automated meter and dispenser systems, such as *'DOPAG'* dispensers with gear, piston, or eccentric screw pumps, offer a wide range of flow rate speeds, from 0.3 up to a maximum of 6 [L/min] [86]. There is a broad difference in terms of flow rate ranges, and if enlarged production volumes and automation levels occur, a larger *DOPAG* unit would be integrated without any substantial change in the metering system.

Let us start by considering a slow flow rate of 0.7 [L/min]. Given the seal volumes mentioned earlier, with an assumed changeover of 1 second on every module's corner, and 10 to 15 seconds time for manual/automatic panel loading and unloading, the corresponding complete cycle times for dispensing PIB and silicone are smaller than 35 and 27 [s/panel], respectively. For higher speeds, such as 3 [L/min], the corresponding cycle times drop to 23 and 21 [s/panel]. In a semi-automatic unit, with the presence of an operator, it is reasonable to assume a slow flow rate, for instance, 0.7 [L/min], which is not likely to incur too many errors in dispensing. For the HA line, a fully automated unit should use a robot with injector head(s). Hence, a faster speed rate (3 [L/min] or more) can be expected to shorten the tact time. This refers to the time taken to complete a specific task or operation within a manufacturing process.

6.2.2 Manufacturing Line Assessment: Cycle Time and Production Space

Analysis of each process and the total lines' cycle time is investigated in these two sections, along with the production space of the factory. The operation sequence follows the process flow in Table 5.0. Each machine specification is taken from both the table of common machines with L-lines (Table 6.0) and that of re-adjusted and dedicated units for L-F module assembly (Table 6.2). By summing up these two tables, a complete manufacturing line sequence is resulted for L-F module production, enabling to investigate the line's cycle time and area required.

6.2.2.1 Processes and Line's Cycle Times

Cycle times of each machine are examined to identify bottlenecks for both scales. The slowest process, for the small-scale line, determines the total line's production speed, which is the paste dispensing operation, with the longest processing times. On the other hand, in the HA line, to verify bottlenecks, to ensure the process stream runs continuously within the line, the cycle time of each process should be levelled out through the integration of additional sets of working equipment and/or buffer systems. According to Table 6.0 and Table 6.2, several processes of the HA line require multiple units to increase that specific step throughput. More precisely, 2 manipulators for CB operations, 10 metal paste injectors, 3 soldering machines, and 2 units for cooling tables, filling machines, cell/string layup systems, and Hi-pot testers are necessary.

The conductive paste deposition, the cell/string soldering, and the filling process are the most challenging when manufacturing L-F modules. For these slow processes, the option is to adopt either additional units per station or a buffer system installed downstream and/or upstream. Technical factors and comparisons between these systems can assist in making the decision. For instance, opting to install a second cooling chamber plate may be more economically beneficial than implementing a buffer system. However, the former may require more electrical energy or occupy a larger area within the production space [33]. Processes with multiple units do work in parallel. In the graph in Figure 6.1, the process flow is visualized with parallel horizontal blue lines under the same operation number (in red). The upper limit value is considered for those processes where cycle time is expressed as a range, rather than a single value (e.g. inductor soldering). The line starts with the rear glass load and placement on the transport system (N.1). The CB pick up and substrate paper film removal (N.2) can already be performed when the rear glass plate is being loaded on the conveyor belt.

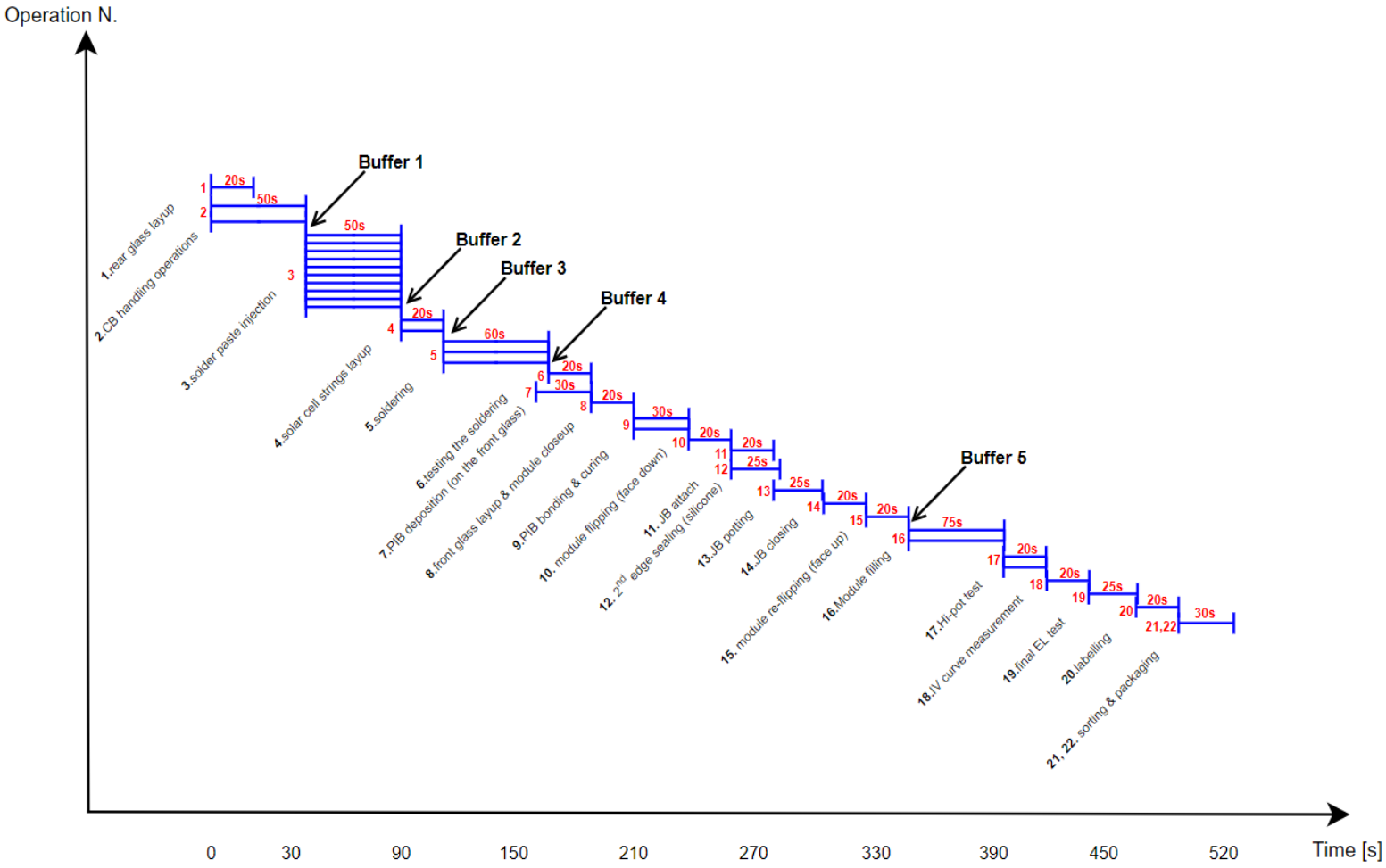

Figure 6.1 - Cycle times of manufacturing steps for a complete and optimized HA production line. The X-axis represents the processing times, while the Y-axis represents the operation number steps. Each blue line is indicated the operation number and the correspondent cycle time (in red). Parallel lines of the same operation denote the use of multiple tools, while vertical overlapping of the lines indicates simultaneous execution of more than one process. Additionally, five buffer systems are installed at different stages of the line.

To enhance the throughput of the HA line, the edge sealing processes can be approached differently.

Instead of applying the primary seal to the rear glass, it is proposed that the front glass plate is loaded onto the auto PIB extruder for edge dispensing (N.7). This operation can already occur during the soldering of cell strings (N.5). Specifically, the front plate is picked up by the 2nd glass covering machine, loaded, and released onto the auto PIB machine. While the front plate is in the auto PIB machine, and the soldering machines are still finalizing the interconnections on the rear glass profiles (end of N.5), the front glass is centered and held steady by the upper glass vacuum suckers of the PIB unit. Meanwhile, the injection head(s) dispense the sealant on the inner-pane substrate perimeter (N.7). Simultaneously, the rear glass undergoes inspection by the solder check unit (N.6). Once the PIB is dispensed and the rear glass is checked, the glass layup system picks the front glass and places it onto the fully inspected panel structure, ready to be moved to the PIB bonding and curing station (N.9). Overall, utilizing the front plate leads to approximately a one-minute reduction in cycle time.

Similarly, operations within WORKSTATION 2 (N.11 to N.14) can be overlapped to shorten the line's cycle time. Whether using semi or fully automated solutions, they can all allow simultaneous operations. After the module flipping (N.10), the first operation is the attachment of the 3-point JB on the back of the panel (N.11). This process can start simultaneously with the 2nd seal (N.2) with silicone at the module edges, ending up shortly after the attachment of the JB is completed (see cycle times in Figure 6.1). Therefore, the JB potting (N.13) can already start earlier when still dispensing silicone at the module's perimeter. No more concurrent operations take place in the line, other than still having multiple units working per process (filling process and Hi-pot test).

Another potential consideration is integrating the quick silicone edge sealing process (N.12) into the slower PIB bonding & curing process (N.10). While the panel is being cooled down to room temperature, the dispenser system activates at a pre-set temperature stage and completes both processes simultaneously. However, this manufacturing concept raises uncertainty regarding its viability, particularly about whether the silicone can be injected and in contact with the PIB while still heated, and the lapse time needed for both adhesives to properly bond and cure before the next step can take place.

To smoothen the flow of panels and dampen the stream of slower processes, five buffer (or storage) systems are installed. The first two are positioned before and after the paste deposition process, the second two are before and after the soldering process, and the last one before the filling process. The decision of two buffer systems, one up and another downstream the process, is due to the broad difference in the multiple units differing from one to the next process, generating possible disruptions in the flow. Each buffer dimension is 3.2 [m] x 1.8 [m] x 2.6 [m] (LxWxH) [33].

To define the total line speed and production capacity for both SA and HA lines based on the application methods adopted and presented in Table 6.2, the following considerations were made:

- **SA line:** almost all operations are carried out in succession. To fill up the cycle time in WORKSTATION 2, each quick process (JB attach, JB pot, 2nd edge sealing) is carried concurrently. By summing up all cycle times divided by the total number of operations, line speed is approximately 0.6-0.7 [module/min]
- **HA line:** Similar computation is made and, by subtracting all the concurrent operations, the 22 operations are completed into approximately 630-650 [s]. This is translated into a line speed of 1.7-2 [module/min].

To facilitate comparison, according to the specifications in Table 3.0, a laminated 300 [MW] line speed translates to the production of approximately 1.25 to 1.5 [module/min]. Consequently, this L-F module assembly line yields a slightly higher throughput. Considering the Biosphere Solar Version 2 module power rating of 390 [W] (Chapter 4), continuous production over 24/7 and 300/325 [day/year], the annual capacity output for the SA and HA lines ranges between 90-120 [MW] and 300-360 [MW], respectively.

6.2.2.2 Production Space of the Factory

The floor area layout is designed specifically for the HA line but is assessed for both scales. The working area for each machine is extracted from Table 6.0 and Table 6.2, and it adheres with the assembly flow outlined in Figure 5.1 (Chapter 5). The entire factory production area is depicted in a reduced-scale drawing in Figure 6.2.

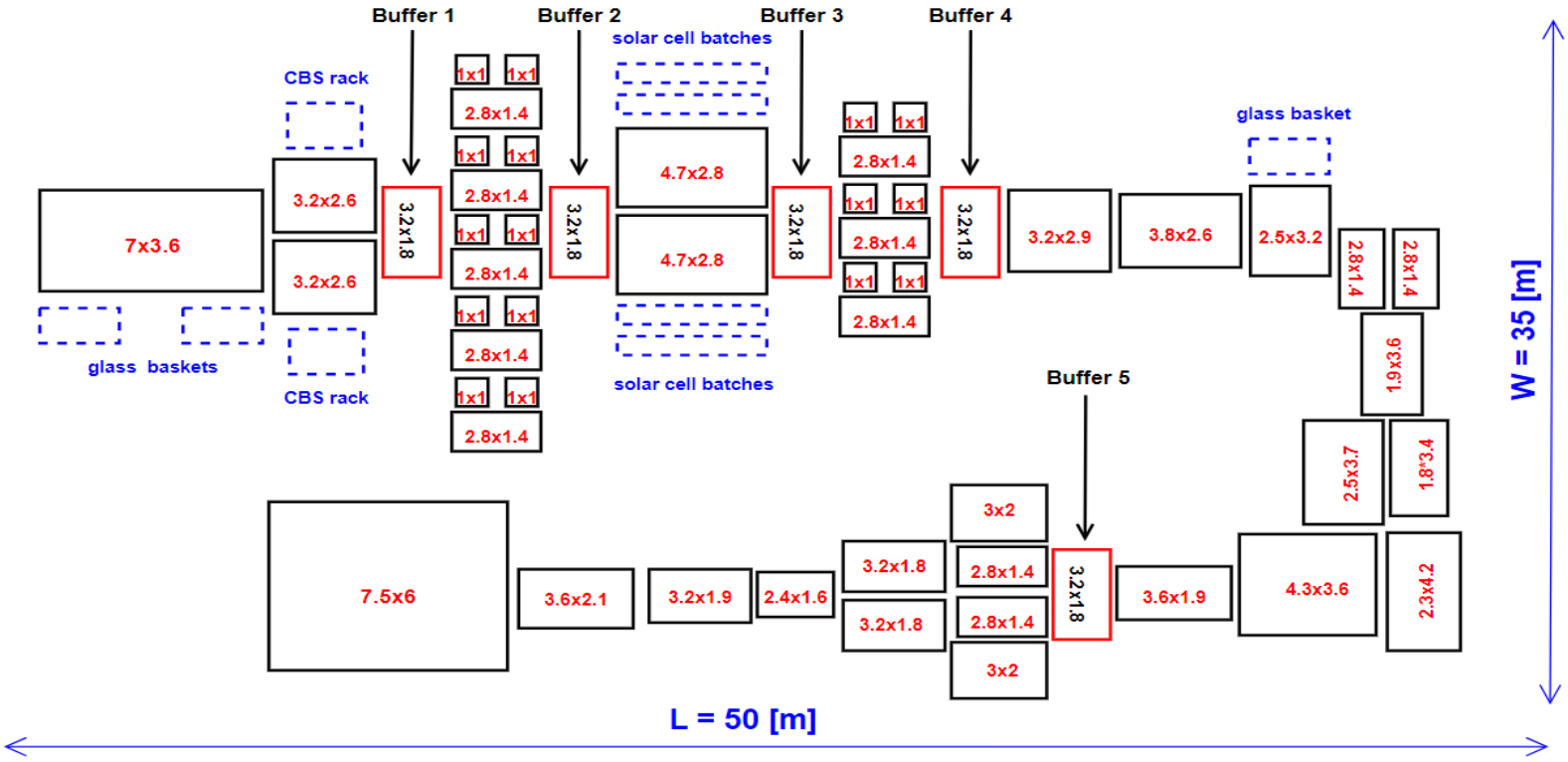

Figure 6.2 - Floor space dedicated to equipment of the HA production line. Dimensions of machines are indicated in the box and scaled in a reduced size. They account for width (W) and length (L) in meters. Five buffer system are integrated at a predefined stage indicated by the black arrows.

The actual values for floor length and width, including the five buffer systems, reach dimensions of 40 [m] and 25 [m]. An additional 10 [m] x 10 [m] was allocated for loading/unloading conveyors, various carriages, and loading of raw materials. The total HA production line area reaches 1750 [m^2]. The height of the L-F factory is not considered. The highest unit is 4 [m] (2^{nd} glass covering machine) and, assuming an extra 3 [m] for various installations, the total factory height can reach a minimum of 7 [m]. Under the same assumption of 10x10 [m^2] as extra safety space, an estimation of the footprint for the SA line resulted to be 690 [m^2]. A summary table comparing computed working areas with laminated plants in Chapter 3 is presented in Table 6.5.

Table 6.5 - Factory footprint comparison based on the two capacity lines for L- and L-F factory types.

PV FACTORY TYPE	Production line working area (L*W) [m^2]	
Laminated [16]	20 [MW]	300 [MW]
	750 (50 x 15)	**3300** (94 x 35)
Laminate-free	SA line	HA line
	690 (34.5 x20)	**1750** (50m x 35m)

As indicated in Table 6.5, the reduction in factory footprint is notably significant only for the HA line, amounting to half of the value in comparison to the 300 [MW] laminated plant. If optional units are integrated into the automated line, the factory footprint would experience an increased area. However, the installation of a curing line would lead to a substantial increase, expanding to 22 [m] x 3.5 [m] [33].

6.2.3 Factory Requirements for Laminate-Free Module's Production

A summary table containing the main factory requirements for L-F module production is presented in Table 6.6.

Table 6.6 - Parameters and plant requirements for L-F module's production.

Plant Parameters	SA line	HA line
Automation Level	55%	95%
Module type	half-cell, double glass, frameless, laminate-free	
Solar cells [42]	120 mono c-Si half-cells, Bifacial M6 ZEBRA IBC (24.4%, 6.67Wp)	
Production speed (throughput)	35-40 Module/H	100-120 Module/H
Annual production capacity (300/325-day production)	90-120 MW (3 shift/day)	300-360 MW (3 shift/day)
Labour required (Per shift)	13-15 [worker/shift]	8-10 [worker/shift]
Production space (equipment only)	690 [m^2]	1750 [m^2]
Power supply requirement	380-400 V, 50 Hz, 3 phase 5 wires	
Rated power for assembly equipment	110 [kW]	315 [kW]
Air and pressure supply	2800 [L/min] 6-7 [bar]	3900 [L/min] 6-7 [bar]
Water	little needed	
Temperature and humidity level	~25 °C 50-70 %	

The automation level was determined from Table 5.0 in Chapter 5. Specifically, the manual, semi-automated, and fully automated processes were converted to 0%, 50%, and 100% share, respectively, and then divided by the total number of assembly steps. This resulted in automation levels of 55% and 95% for the respective lines. The specifications such as power/air consumption, labour force, and production space were derived by summing up the total values from Tables 6.0 and Table 6.2. The pressure supply value was determined based on the highest value found among all equipment. In reference to the specifications in Figure 3.1 and Figure 3.2 for the two laminated scales, it was found that for the HA line only, there was a visible reduction in both power and air consumption up to 20-30%. Similarly, the floor area gain is notable only for the HA line, with a factory space reduced by up to 50%. Number of operators required L-F module manufacturing is greater than that for laminated lines. At best, the labour workforce size can be equal.

In conclusion, the technical results indicate that the manufacturing of L-F modules can demonstrates competitiveness with standard laminate lines. This competitiveness is particularly evident for the HA line scale, where, under similar annual production capacities, both the production space and power consumption are notably lower compared to conventional plants. However, this efficiency improvement may come at the expense of requiring an increased number of inline workers. Nonetheless, to form a comprehensive understanding and draw more complete conclusions, it is essential to also address the economic aspects of manufacturing.

7

Cost Analysis and Economic Results

In 2017, one of the first studies presented at the 33rd European PV Solar Energy conference demonstrated that with L-F solar module production, the Total Cost of Operation (TCO) could be reduced [97]. However, the study focused on potential cost savings without conducting an in-depth analysis of the options for manufacturing processes to achieve these results. One of the objectives of this thesis is to build a more detailed understanding of how cost reduction in manufacturing processes can be achieved. This chapter contains an economic analysis, divided into Capital Expenditure and Operating Expenditure (CapEx, OpEx), making a distinction between the two different scales of lines, with the economic results derived as a conclusion in comparison to traditional lines.

7.1 Capital Costs of PV Manufacturing Plants

When it comes to starting a PV module manufacturing business, the setup costs are a major barrier to entry. The overall cost of establishing a manufacturing plant depends on the scope of the project, size, and type of the facility. These capital or startup costs consider the necessary equipment and machining tools, infrastructure, and other facility-related expenses that can be capitalized. This section examines the assembly equipment and facility infrastructure cost for the developed SA and HA lines, comparing them with laminate solar plants. The reason for specifically choosing to analyze assembly equipment and facility infrastructure costs is because these are the main factors that differentiate an L-F plant from the traditional L-plant. They are generally among the main CapEx to address when setting up a production line.

7.1.1 Investment for Installing Equipment

One of the main cost considerations is the investment for installing assembly machineries needed to start a manufacturing business. These include equipment costs incurred of the two scales of lines for: complete laminate plants, exclusive for L-plants only, and a complete investment for L-F plants.

7.1.1.1 Equipment Costs: Laminated PV Module Plants

The overall cost for setting up assembly equipment for exemplary two scales of laminate PV module plants is illustrated in Figure 7.0. The relative machine costs are classified into pre-lamination, laminating, and post-lamination stages.

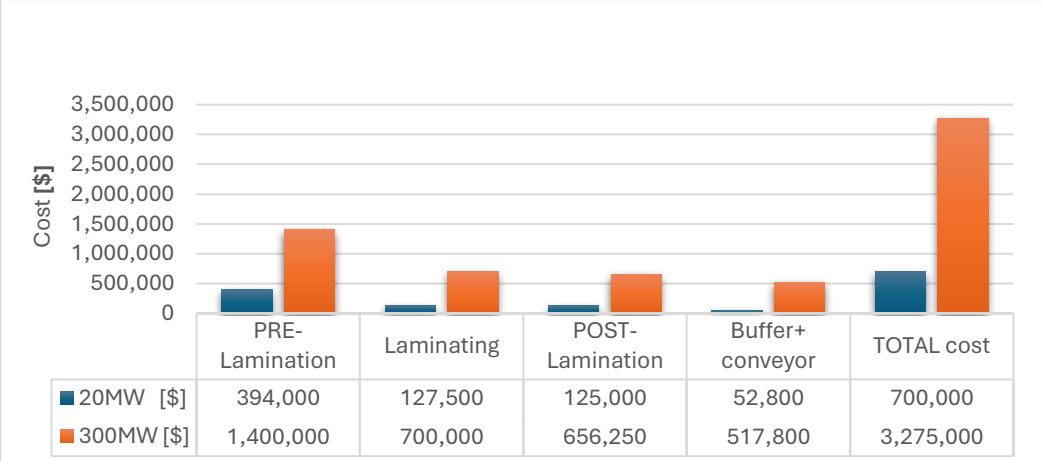

Figure 7.0 - Investment cost for installed equipment of two PV laminated line scales (20MW and 300MW) [67], [33].

Referring to the last column, to start a fully scaled 20 [MW] and 300 [MW] annual capacity plants, a purchase of $700,000 and $3.3 million is expected for the production machinery, respectively. The 20 [MW] line subtotal costs refer to the complete production line (Figure 3.1) of Chapter 3. It comprises the following toolsets [33], [67]:

- **Pre-Lamination**: glass loader, cell stringer, layup machine, EVA/back sheet foil cutter
- **Laminating:** laminator (1set)
- **Post-Lamination:** framer silicone dispenser, glue dispenser for JB, IV tester, EL tester, Hi-pot testing unit
- **Transport system (conveyors & shuttles)**: 24 sets

The cost of each stage and equipment of the 300 [MW] scale is provided from [33], which includes two double-step laminators and 95 sets of accessories between buffers and conveyors. Most of the line expenditure is attributed to the stringers, bussing, and laminator machines, with the latter constituting up to 20% of the total line cost, for both scales. Two high-capacity laminators of the HA line scale equal the entire cost of the SA line's machineries, at $700,000.

To delineate the cost differences between the complete line and toolsets used exclusively in laminated plants, a price list and the number of sets are presented in Table 7.0. These mainly include encapsulant foil cutters, tabber & stringers, laminators, trimming, and, if G/G modules are adopted, also the framing machines.

Table 7.0 - Price list of assembly equipment used in laminated PV module plants only for a 20 [MW] and 300 [MW] scales. The 3rd column indicates the automation level, expressed as: **A**= automated, **Semi**= semi-automated. The line type is split into set (pieces/process) and sub-total cost. These, in turn, are both referred to the 20MW and 300MW scales.

[Reference]	Equipment type	Auto	Unit cost [$]	Line type			
				Set [pcs/process]		Sub-Total cost [$]	
				20MW	300MW	20MW	300MW
[67]	Transport system	-	2,200	12	33	26,400	73,000
[33]	Encapsulant foil cutter & layup	A	26,000	1	-	26,000	-
	Encapsulant foil cutter, P&P system	A	85,000	-	1	-	85,000
[31]	Tabber and stringer	A	150,000	1	-	150,000	
[33]	High speed MBB Stringer	A	305,000	-	2	-	610,000
[67]	Auto Bussing station	A	160,000	-	1	-	160,000
[33]	Lead compression	A	61,000	-	1	-	61,000
[67]	Laminator	A	127,500	1	-	127,500	-
[33]	Laminator	A	348,800	-	2	-	700,000
[67]	Trimming machine	A	27,500	1	1	27,500	27,500
[67]	Framer dispensing machine	Semi	6,300	1	-	6,300	-
[33]	Auto dispensing tool for frames	A	55,200	-	1	-	55,200
[67]	Framer assembling machine	Semi	58,000	1	-	58,000	-
[67]	Auto framing machine	A	84,300	-	1	-	84,300
					TOTAL [$]	**420,000**	**1,850,000**

The first element (row) in Table 7.0 refers to all the transport systems costs. These include conveyors or shuttle systems for all the assembly units, including loading and unloading belts. In the 20 [MW] scale, it also includes manual bussing and trimming bench stations.

Quantities and prices are determined from the conventional G/B manufacturing lines, discussed in Chapter 3 for any type, formats, and metallization contact of cell modules.

Classic IR stringers and bussing stations for the laminated lines are estimated as units not used for L-F module assembly. The most expensive (from Table 7.0) and the least space-efficient (from Figure 6.1) units are laminators followed by high-speed stringers, making up most of the production equipment cost. All unit costs of laminate plants only ("TOTAL" row in Table 7.0) account for up to 60% of the total line's equipment cost (last column to the right in Figure 7.0)

7.1.1.2 Equipment Cost: Laminate-Free PV Module Plants

A budget price list for process equipment required for two complete L-F scale of lines is presented in Table 7.1. As a safety margin for pricing, the machine investment is rounded between half and twice the potential equipment cost.

Table 7.1 - Equipment pricelist for L-F module manufacturing for SA and HA lines respectively: The table is divided into precure & bond, cure & bond, and post-cure & bond stages. Colour formatting in **GREEN**, **ORANGE**, **BLUE** represent toolsets in common to laminated, adjusted from laminated, and dedicated for L-F panel manufacturing. The automation level is indicated as: **A:** auto, **Semi**, and **M**: manual. Correspondent sub-total costs are in the last table rows. The total project cost is in the very last table row. The equipment cost is computed based on a 50% up to 200% range of its unit value.

No	Equipment type / [reference]	Auto Level	Unit cost range [$]	SA Set [pcs/process]	HA Set [pcs/process]	SA Sub-Total cost [$]	HA Sub-Total cost [$]
1	Glass loader [67]	Semi	8,500 - 34,000	1	-	8,500 - 34,000	-
	Glass layup system [33]	A	18,000 - 73,000	-	1	-	18,000 - 73,000
2	CB layup machine (manipulator load/unload) [67]	Semi/ A	7,000 - 28,000	1	2	7,000 - 28,000	14,000 - 56,000
3	Dispenser for solder paste (Expert Quote: *Member of TechconSystem)*	A	20,000 - 40,000	2	10	40,000 - 80,000	200,000 - 400,000
4	Solar cell/string layup system [33]	A	22,000 - 87,000	1	2	22,000 - 87,000	44,000 - 174,000
5	Heat inductor soldering unit (Expert Quote: *member of Ultraflexpower*)	A	40,000 - 80,000	1	3	40,000 - 80,000	120,000 - 240,000
6	Solder check unit [67]	Semi	2,300 - 9,000	1	-	2,300 - 9,000	-
	EL tester [33]	A	9,500 - 38,000	-	1	-	9,500 - 38,000
7	Heated Extruder for PIB dispensing *(Expert Quote: Reoo technologies)*	Semi	17,500 - 70,000	1	-	17,500 - 70,000	-
	Power Lift and Turn Rotary Table [121]	-	2,300 - 9,000	1	-	2,300 - 9,000	-
	Auto PIB dispensing station [95]	A	30,000 - 120,000	-	1	-	30,000 - 120,000
8	Glass loader [67]	Semi	8,500 - 34,000	1	-	8,500 - 34,000	-
	2nd glass covering machine [67]		16,800 - 67,000	-	1	-	16,800 - 67,000
				Total (PRE - bond & cure)		**145,000 - 420,000**	**450,000 - 1,170,000**
9	Clamping table with chillers (Expert Quote: *Thermoseal Group*) [121]	M	800 – 3,800	1	-	800 - 3,800	-
	Cooling chamber plate (from laminator) [67]	A	20,000 - 40,000	-	2	-	40,000 - 80,000
				Total (bond & cure)		**800 - 3,800**	**40,000 - 80,000**
10	180-degree flipper [67]	A	2,700 - 11,000	-	1	-	2,700 - 11,000
11	Extruder for SILICONE injection [80]	M	12,500 - 50,000	1	-	12,500 - 50,000	-
	Power Lift and Turn Rotary Table (Expert Quote: *Thermoseal Group*) [121]	M	2,400 - 9,800			2,400 - 9,800	
	Auto edge sealing machine (SILICONE injection) [33]	A	23,000 - 90,000	-	1	-	23,000 - 90,000
12	Glue dispenser for J-Box [33]	Semi	2,200 - 8,800	1	-	2,200 - 8,800	-
	J-Box soldering machine [67]	A	28,000 - 116,000	-	1	-	28,000 - 116,000
13	(JB) glue potting manipulator [33]	A	4,800 - 19,000	1	1	4,800 - 19,000	4,800 - 19,000
14	JB closing machine [33]	A	19,000 - 76,000	-	1	-	19,000 - 76,000
15	180-degree flipper [67]	A	2,700 - 11,000	-	1	-	2,700 - 11,000
16	Filling machine (Expert Quote: *member of procure-net*)	Semi	25,000 - 50,000	1	2	25,000 - 50,000	50,000 - 100,000
17	Visual check 90° [33]	Semi	5,000 - 20,000	1	-	5,000 - 20,000	-
	Line scanning machine [67]	A	13,000 - 50,000	-	1	-	13,000 - 50,000
18	Hi-Pot tester [67]	Semi	5,300 - 21,000	1	2	5,300 - 21,000	10,600 - 42,000
19	Solar simulator [67]	A	27,000 - 106,000	1	1	27,000 - 106,000	27,000 - 106,000
20	Final EL tester [33]	A	9,500 - 38,000	1	1	9,500 - 38,000	9,500 - 38,000
21	Auto Labelling machine [33]	A	18,000 - 73,000	-	1	-	18,000 - 73,000
22	Auto Sorter and packing [33]	A	51,000 - 204,000	-	1	-	51,000 - 204,000

					Total (POST-bond & cure)	**94,000 - 322,000**	**260,000 - 935,000**
	CONVEYOR (bench/roller table, shuttle, belt, etc.) [67]	Semi/A	1,100 - 4,400	20	55	22,000 - 88,000	60,000 - 240,000
	BUFFER [33]	A	8,500 - 34,000	-	5	-	42,000 - 170,000
					Total: BUFFER + CONVEYOR	**22,000 - 88,000**	**102,000 - 410,000**

Sub-Total (in common with traditional plants)	95,000 - 377,000	275,000 - 1,100,000
Sub-Total (adjusted from traditional plants)	140,000 - 350,000	400,000 - 860,000
Sub-Total (dedicated for laminate-free plants)	7,800 – 32,000	77,000 - 225,000
PROJECT TOTAL [$]	**265,000 - 850,000**	**855,000 - 2,550,000**

General repair units, as well as optional equipment, can be integrated at any position of the line, facilitating module disassembly. The units and associated costs, in [$], are retrieved from [67], [33] and include a repair removal machine ($9,000 to $37,000) and a glazing repair machine ($17,000 to $66,000). Prices for optional equipment include **Curing (manipulator + line):** $30,000 to $120,000; **Corner protector wrapping machine:** $20,000 to $80,000; **Edge chamfering machine:** $6,500 to $26,000; **Centring unit:** $800 to $3,200; **Auto framing machine:** $42,000 to $168,000.

Due to the lack of market availability for some adjusted and dedicated (customized) units, their budget prices were derived from a range value proposed by manufacturers and considerations made from traditional PV module equipment costs:

- **Cooling chamber plate:** A rough estimation of cost was derived from the total laminator cost divided by the number of plates contained. A 3-step laminator comprises 3 plates, and the cooling and chamber plate cost make up 1/3 of the total laminator cost, even though the most expensive section is the core, the heated chambers.
- **Dispenser for solder paste:** The cost for a rotary solder paste valve, pump, and controller unit is about $5,000. For a complete system, customized design options and integrated automation, the price can increase further (Expert Quote: *member of TechconSystem*). A range of $20,000 to $40,000 per unit is assumed.
- **Soldering machine:** For a complete standard and manual process, the cost is approximately $10,000. The custom design, engineering, and process development cost for this application doubles the investment to $20,000. An embedded automated solution further increases the budget (Expert Quote: *member of Ultraflexpower*). A rough budget assumed for this report is in the range from $40,000 to $80,000 per unit.

The number of buffer systems was already defined in Chapter 6, while the number of conveyors is counted based on the number of equipment present and an additional 15 sets (in the HA line) for loading/unloading. Additionally, UV-curing equipment may be necessary to ramp up the curing time of the UV-curing adhesive at the backsheet/glass interface, with a unit cost of $2,000 [96].

When analyzing Table 7.1, even when considering twice the machine costs for non-standard equipment, besides the auto PIB dispenser, there is no investment exceeding $100,000 per unit. Even with the installation of ten paste jet dispensers, when considering the upper limit range, their total cost can still be nearly half the price of one high-capacity laminator, which is about $350,000. With these broad range assumptions for costs, the SA line still maintains a comparable upper limit cost compared to the laminated 20 [MW] scale, which is about $700,000 (Figure 7.0). However, based on the results of the technical analysis in Chapter 6, the SA line should be compared to a similar line capacity producing 100 [MW] panels per year. Hence, the capital cost would be considerably lower, and the technical specifications of the line may outweigh those for laminated 20 [MW] scale as well. Regarding the HA line costs, there is still room (20-30%) for investment to reach the $3.3 million of the traditional 300 [MW] scale. This cost gain, in quantity terms, can be equated to either setting up a completely new SA line or purchasing a single high-capacity laminator.

7.1.2 Costs for the Working Space Infrastructure

The facility lease/purchase cost for launching a manufacturing plant largely depends on the size and location of the facility. In terms of site selection, according to [109], land prices may fluctuate from $55,000 up to $800,000 per acre, varying by region. While the facility building cost may range from $200 to $250 per square meter. Besides building costs, the result is that the facility cost for the SA line is similar to the 20 [MW] scale cost. Whereas the great saving for the investment in infrastructure is for the HA line, with up to a 50% reduction in building cost. These cost insights are depicted in Table 7.2.

Table 7.2 - Overview of the capital costs related to the facility building by plant type and scale. Parameters, presented in the leftmost column, include area required, infrastructure cost, and total cost for each type and scale of PV module plant.

Parameters	Plant type & scale			
	Laminated		Laminate-Free	
	20MW	300MW	SA	HA
Area required **[m^2]**	750	3300	690	1750
Infrastructure cost **[€/m^2]**	250	250	250	250
TOTAL building cost **[$]**	190,000	830,000	170,000	437,000

7.2 Operational Costs of PV Manufacturing Plants

Variable costs (or “cash” costs) are generally compiled at the conclusion of each accounting period. They include the cost of materials to be converted into a product, any other consumable materials, all direct manufacturing labour costs, and consumption for utilities and equipment maintenance. In this section, the main costs of the module components, labour, and energy consumption for machineries are investigated for both production plant types.

7.2.1 Material and Component Costs for a PV module

When budgeting costs for launching and operating a solar manufacturing business, it is paramount to factor in the costs for materials and components. Costs of raw materials used in producing a single solar panel vary considerably by type and technology. This, in turn, is influenced by the number of panels being purchased as well as their exact specifications. According to [97], the material that detains the highest costs for laminate G/B module is solar cells, accounting for up to 50% of the total cost, followed by glass, frames, foils, seals, and other components. To quantity the material cost per panel, a summary table highlights the main material and component costs for a laminate G/B panel (Table 7.3).

Table 7.3 - Template of Bill of Material (BoM) for a laminate G/B solar panel. Dimensions refer to LxWxH. The first four rows illustrate the specifics of the panel and number of working hours. Module's components are numbered from N.1 to N.15 and the last column on the right indicates the cost of each material based on its quantity employed per single panel [67].

Calculate on Panel		550W,	2279 x 1134 x 35 [mm^3]			
Working shift		8 [hour/day]				
Output		380 [pcs/h] / 500 [MW] line				
Solar cell, 182 half-cut		144 [pcs]				
	N.	**Name**	**Dimension/Specifics**	**Q.ty Per panel**	**Unit cost [$]**	**Per panel [$]**
Main Raw Material / Component	1	Solar cell	182 x182 [mm^2]	72 [pcs]	0.69	50
	2	EVA film	2273 x 1128 [mm^2]	2 [pcs]	2.80	5.6
	3	Backsheet	2273 x 1128 [mm^2]	1 [pc]	3.50	3.5
	4	PV glass	2273 x 1128 [mm^2]	1 [pc]	9.13	9.2
	5	Aluminium frame	2279 x 1134 x 35 [mm^3]	1 [pair]	7.12	7.2
	6	Soldering ribbon	0.23 x 9 [cm^2]	0.3 [kg]	12.5	3.8
	7	Bus bar	0.23 x 6 [cm^2]	0.15 [kg]	12.5	1.9
	8	Junction Box	PV-JB001	1 [pc]	6	6
	9	Silicone gel		0.2 [kg]	3.2	0.65
	10	Sealing gel		0.1 [kg]	3.5	0.4
	11	Double faced tape		0.3 [m]	0.01	0.003
	12	Transp. Adhesive tape		2 [m]	0.02	0.04
	13	Soldering flux		0.3 [kg]	0.06	0.02
	14	Alcohol		0.25 [kg]	0.04	0.01
	15	Carton box		0.04 [pc]	4	0.16
Water and electricity, artificial, powerhouse, equipment depreciation				1	0.6	0.6
				TOTAL	**[$]**	**88.5**

The cost for 144 half-cut cells of a G/B laminate panel results in $0.16/W. Most of the cost is due to the solar cells, but the highest unit cost results from the BBs and soldering ribbon, followed by PV glass and aluminium frame. Similarly, an estimation of the main material and component costs for a single L-F panel production is presented in Table 7.4.

Table 7.4 - BoM for a laminate-free, glass-glass and liquid-filled solar panel Version 2 of Biosphere Solar. Dimensions refer to W x L x H. The first four rows illustrate the specifics of the panel and number of working hours. The module's components are numbered from N.1 to N.15, and the last column on the right indicates the cost of each material based on its quantity employed per single panel. Values for unit costs are not expressed as a range but were considered only the highest value based on each sourced material and variable quantity to purchase.

Calculate on Panel		390W, 1040 x 1776 x 4 [mm]				
Working shift		8 [hour/day]				
Output per shift		40÷120 [pcs/h] / 40 [MW] ÷ 120 [MW] line				
Solar cell, 182 half-cut		120 [pcs]				
	N.	**Name**	**Dimension/Specifics**	**Q.ty Per panel**	**Unit cost**	**Per panel [$]**
Main Raw Material / Component	1	Solar cell [123]	166 x 83 x 0.16 [mm^3]	120 [pcs]	0.3 [$/W]	117
	2	PV glass (Expert Quote: *AGC glass*)	1040 x 1776 x 4 [mm^3]	2 [pcs]	11.5 [$/m^2$]	41.4
	3	Cell spacer (Input Quote: *Biosphere Solar*)	~1000 [mm^2]	50 [pcs]	18 [$/m^2$]	0.02
	4	Conductive paste (Input: R*otec*)	1 x 0.83 x 0.2 [mm^3]/ 1BB cell	0.02[5] [kg]	100 [$/kg]	2.2
	5	CB foil [67]	1010 x 1746 x 0.4 [mm^3]	1 [pc]	35 [$/sheet]	35
		Metal ink for traces (Expert Quote: *copprint*)	108 x 850 x 1.05 [mm^3] x 0.02 [mm] (H)	0.002 [kg]	700 [$/kg]	1.4
	6	Glue adhesive film (CB/glass) (Expert Quote: E*llsworth adhesives*)	1010 x 1746 x 0.2 [mm^3]	0.35 [cc]	300 [$/L]	0.1
	7	Filler (dielectric liquid) [98]	1010 x 1746 x (0.7÷1) [mm^3]	1÷1.5 [L]	15 [$/L]	23
	8	PIB & desiccants [99]	10 x 5532 x 3 [mm^3]	0.17 [kg]	200 [$/kg]	34
	9	Silicone gel (edge seal) (Expert Quote: O*ttochemie*)	5 x 5572 x 3 [mm^3]	0.08 [kg]	13 [$/L]	1.05
	10	Silicone gel (JB seal & pot) (Expert Quote: O*ttochemie*)	-	0.18 [kg]	13 [$/L]	2.35
	11	Junction box (3-split points) (Input Quote: *Biosphere Solar)*	7.2 x 25 [cm^2]	3 [pcs]	14 [$/3pcs]	14
	12	MC4 connectors [124]	5.9[mm] x 4 [mm^2]	2 [pcs]	1.5 [$/2pcs]	1.5
	13	Cables [125]	1200[mm] x 4[mm^2]	2 [pcs]	7.4 [$/m]	9
	14	Label [62]	25 [mm]	1 [pc]	0.30 [$/pc]	0.30
	15	Packing [67]	2300 x 1200 x 1000 [mm^3]	0.04 [pc]	4 [$/pc]	0.16
		Water and electricity, artificial, powerhouse, equipment depreciation		1	0.6	0.6
			TOTAL		**[$]**	**285**

The cost of module materials and parts is considered based on the highest value of each sourced material and component, taking into account purchases ranging from small to large quantity volumes of production forecast. Most of the prices for materials were derived from quotes and input from current manufacturers in different fields of application. Without lamination, it is preferrable to use ARC glass to enhance the optical performance of L-F modules, which result in higher price for the glass compared to a non-ARC glass. The theoretical price for the conductive sheet foil was assumed to be up to 10 times more expensive than a standard backsheet foil, retrieved from [67]. Its effective value may even be higher considering the manufacturing cost for the cell spacers integration. Similarly, a comparative cost analysis of IBC solar cells was obtained from [123], given the lack of public information available for the ZEBRA IBC technology. From Table 7.4, the cost for 120 half-cut cells of a G/G laminate-free panel results to be 0.75 [$/W], up to 4-5 times more expensive than the standard panel concept in Table 7.3. While costs for junction boxes, glass, silicone gel, etc., are not deviating much for the two concepts, the cost of IBC solar cells, conductive sheet, pastes, liquids, and adhesives can have a very high value for unit costs. The small quantities needed per panel keep their cost still low even though solar cell and PV glass still contribute to the greatest share of costs. However, saving on the frame, encapsulant, backsheet foil, and soldering materials will not likely offset the high and variable cost of dedicated elements of L-F solar modules.

7.2.2 Cost for: Labour Force and Energy Consumption for Running Equipment

Besides the component costs of a PV module, other important factors of variable costs are the labour and energy used by processing equipment.

[5] It accounts the total solder paste per panel needed calculated in Chapter 4 (under cells, between cells, to bus to the JB)

It is important to account for the cost of employees to ensure that the production site runs efficiently. The labour cost varies based on the size, scope of the plant, and level of training. For instance, in large-scale plants where the toolsets may be oversized and more difficult to operate, a higher level of skilled technicians and engineers is required to oversee the day-to-day production operations. This could necessitate additional financial resources.

The total labour force to examine is compared to the main line specifics for different PV module manufacturers of Table 3.0 (in Chapter 3), which varies from company to company. In the best-case scenario, the minimum number of in-line workers, for the two different laminate line scales is 8 and 6 whereas for the of L-F scales, a comprehensive range of in-line workers per working shift is 13-15 and 8-10, respectively (Table 6.6). Besides the monthly wage cost of an inline operator, based on the number of operators required, the L-F scales may require, in the worst case, twice the investment for all direct manufacturing labour.

To quantity the cost of running equipment, the rated power and compressed air for the production line types is:

Table 7.5 – Overview of the equipment consumption (power and air), indicated in the left column, by plant type and scale (right columns).

Parameters	Line type			
	Laminated [16]		Laminate-Free	
	20MW	300MW	SA	HA
Electrical power **[kW]**	150	470	110	315
Air compressed **[L/min]**	900	6300	2800	3900

According to these amounts, the negativity of the SA line is related to its highly intensive use of compressed air, while the HA line holds a gain over both electrical energy and air consumption, up to 30% saving. If an average electrical rate for the facility in the European zone in 2023 is 0.4 [$/kWh] [126], indicative values of energy costs for the SA and HA line machineries, operating for a working shift of 8 [hours/day], are $350 and $1000, respectively. The main cost for the laminated lines is related to running the laminator, mainly in the large line, with a rated power of 180 [kW], which is almost half of the total power consumed by the HA line. This translates to a cost of $500 per 8-hour shift.

To conclude the economic chapter, the capital costs in manufacturing give promising results, mainly for the costs associated with the infrastructure building and installation of equipment in the large-scale HA line. This is offset by a larger operational cost, mainly by the materials constituting the laminate-free panel, which can be up to five times more expensive than a laminate panel, and in minor proportion, to the number of operators needed to run the manufacturing lines.

8

Conclusions and Future Outlook

8.1 Conclusions

This thesis provides an initial insight into the manufacturing of L-F solar modules on a large scale. Lamination, despite its benefits, also presents a major limitation for manufacturing and disassembly, making it considerably difficult for circularity within the solar industry. The aim was to explore the boundaries and address the challenges encountered when manufacturing this innovative solar module design. To evaluate these challenges, a comparative analysis is conducted with respect to traditional and mature laminated PV manufacturing lines to identify potential benefits and drawbacks. To address scalability in manufacturing, the approach used two different levels of automation: semi-automated and highly automated lines.

To answer the initial research questions, it is essential to first become acquainted with the product and processes involved. This was addressed through a literature review on the mainstream technology of c-Si PV module concepts and how general processes of manufacturing laminated panels can be conducted. An innovative assembly technology is also viewed as an alternative method to the classic tabbing and stringing approach, via conductive backsheet technology. Next, it was vital to understand the design of L-F modules in development by Biosphere Solar, how to relate the panel architecture to the processing, and how large-scale manufacturing affects the panel architecture. For instance, the solar cell orientation or cell spacer designs were investigated to bring benefits to the processing, in terms of assembly time and total costs.

RQ1: *What are the barriers encountered in the manufacturing of L-F modules using BC solar cell technology?*

The Challenges lie in investigating non-standardized processes that must be integrated in the classic PV manufacturing lines to replace the laminator machines, as well as assembly units for encapsulants and backsheet foils. Adjusted and dedicated units tailored specifically for this application are therefore required. The most difficulties in the assembly are encountered for the metal paste deposition, soldering, and filling operations. One constraint in manufacturing, in terms of line flexibility, is due to the electrical interconnection process, which could determine the characteristics of the manufacturing sequences. This is a barrier for manufacturing related to the constraints in the product design (heat-sensitive cell spacers, unproven long-term stability for conductive backsheet technology), diverging from the standard laminated panels. Consequently, the LTSP deposition and soldering systems limit the flexibility in the application methods used. Additional and to a lesser extent, barriers regard the CB layup, primary and secondary edge sealing processes. Care must be taken when selecting the suitable materials investigated (liquids, adhesives, etc.), as these can impact on the application method to adopt and related boundaries in the processing and factory layout.

RQ2: *How can these challenges be effectively addressed and what trade-offs exist in both product architecture and manufacturing processes?*

The application methods selected for the most critical and challenging assembly operations are: **i.** Jet dispenser for the metal paste deposition, **ii.** Heat induction system for the cell string soldering and, **iii.** liquid filling system.

i. This paste deposition method should be corrected based on the conductive paste properties such as type, size of the grains, as well as the flux category selected, all of which define the quality of the solder paste. Programmable parameters, such as nozzle precision and needle geometry, as well as flow rate, need to be adjusted based on the different dimensions and trajectories of the patterned CB traces. For instance, for interconnection between strings, the dispenser parameters need to consider a wider diameter than that of the cell-to-cell interconnection. A single dispenser unit would take less than 10 minutes to finalize the deposition over the 108 panel traces. Therefore, the process should be optimized with improvements in the dispensing cycle time, such as employing multiple nozzle syringes and/or dual units working on the two symmetrical parts of the panel.

ii. The electrical interconnection, via heat induction soldering, is accomplished not on a large surface, but by non-contact local heat. Despite the high conversion efficiency of inductors and rapid heating, it is hardly feasible to heat up all thin and straight lines containing the paste homogeneously at once (possible buckling may occur). Soldering the full length of the thin lines, despite precise temperature control, can easily cause local overheating and bending of solar cells. Cells can be heated individually or in batches, eliminating pre-heat times. Therefore, the inductor heater needs to be appropriately dimensioned and developed for this application to achieve high-efficiency unit and process. In particular, multiple custom-designed coils that scan the surface by batches are necessary, specifically designed to achieve optimal power, frequency, and design. Adequate heating up and soaking time are important to avoid the formation of IMC by minimizing temperature difference and without local overheating. Most importantly, the flux formulas of the metal-containing paste and the restricted residue flux must be appropriate for this specific application to achieve quality in soldering and avoid additional reflow cycles due to heat-sensitive components. Two inductor units can work simultaneously on a single panel, halving the tact time.

iii. Filling and sealing the module is the most challenging operation. Different factors play a role and could pose barriers. One difficulty could be the realization and positioning of the two inlet/outlet hoses for air extraction and liquid injection to achieve a reliable, low-stress, and uniform distribution across the overall inter-pane space. The suggested arrangement is on the front side and at opposite diagonals. Other boundaries are related to the filling pressure and accuracy in the operation. Too small pressures may generate complications with air extraction (bubble formation or trapped air), filling quality (unevenness across cavities), and increased manufacturing costs. On the other hand, high pressures can undermine the internal components. Likewise, accuracy lies in the type of valve used. Pressure valves can be fast but not very precise in filling, while volumetric valves are slower but have higher precision. Slower but with higher accuracy is preferable for this application considering the not smooth inner volume (cell spacer heights hampering the flux), sensitive components present, and no exact tolerance in volume area defined. A range value for tolerance in accuracy was assumed within ± (1% - 10%). All these inputs and the process control are rigorously related to the strict requirements of the fluid properties (e.g., viscosity) selected for this specific application. For instance, the dosing and mixing system relies on the viscosity grade of the fluid. High viscosity fluids are more energy-consuming for the system heating mechanisms and require longer dosing times. On the other hand, more viscous fluids can achieve more precise control in the process. This parameter must be carefully tuned as it is crucial to maximize light transmission. In this report, continuous and constant dosing at variable back pressures with a volumetric valve and programmable suck-back function are the suggested parameters worth further investigation. Lastly, achieving a liquid-tight seal after filling without inducing any electrical conductivity and leakage is challenging for the long-term stability and performance of these modules. Depending on the sealant type (metal solder, glass, butyl tape, etc.) and operation method, the total process cycle time is extended, and an integrated unit section for sealing may possibly be needed.

All these dedicated processes impact the panel performance and the line layout. The number of units to be installed in the HA line for the paste dispenser, soldering, and filling systems are 10, 3, and 2 respectively. Particularly, the filling process is the most crucial barrier, both technically and economically. This research study assumed that filling does not influence any other process, but at some stage, an effect is expected, which remains an open question for this thesis. The process needs further elaboration. Likewise, the paste deposition and solder methods explored are non-standard for this application, and further study is necessary.

RQ3: *What are the technical as well as economic implications of manufacturing of L-F modules at large-scale in comparison with the conventional laminated PV modules' production lines?*

Based on the methods used for the non-standard assembly processes, the derived manufacturing line specifications and layout reveal promising results. The study demonstrates the competitiveness of manufacturing this innovative PV module architecture with its potential for scalability. Upon closer inspection, the equipment's energy consumption and working space can offer significant competitiveness, especially for the highly automated large line, resulting in a positive outlook and, under best-case conditions, up to a 30% energy saving (between electrical and air consumption) and up to a 50% reduction in assembly space can be achieved. This is due to the compact machine work area and their limited power usage, with the absence of the laminator. However, an increased value in air supply for the semi-automated line scale is seen as a drawback. The capital costs are also promising and can potentially outcompete laminate lines. This primarily concerns the HA line scale which can offer up to a 30% gain for equipment costs and up to a 50% gain for building infrastructure costs. At worst, it is equal to laminated plants. It is important to note that the main factors exacerbating the mitigated capital expenditure (equipment and infrastructure investments) are the operational costs associated with the module materials required to form a PV product, which can be up to 4-5 times higher than for a standard laminated panel.

Additionally, the required manpower force may be similar to laminate PV lines and, at worst, demand up to twice more investment for all direct manufacturing labour.

Concerning the module material cost, optimizing the cell architecture and module layout concurrently can impact module output and total costs. For example, optimizing the number of contact points between rear cells and conductive components of the module can improve both cell and module efficiency, affecting manufacturing processes such as cycle time, consumption, and thus costs. An important parameter influencing module performance is the thickness of the conductive layer; the costs of the metal paste, sheet (e.g., copper), and the processes used to create specific design patterns can increase with increasing layer thickness. However, resistive losses in the module will be reduced with increasing layer thickness. As a consequence, a technical vs economic optimum should be met [24]. Issues are also related to the weight of glass/glass filled L-F panels and uncertainties concerning the long-term stability of cells, internal components, and edge sealants. Development in design and manufacturing should emerge in response to the above problems.

The major gain, however, does not come solely from the technical and economic (capital costs) landscape analyzed but from the higher likelihood than laminated panels to achieve greater goals in terms of circularity, with easier disassembly and recyclability of solar products, enabling extraction of high-valued module constituents at a likely lower cost than the current recycled modules. This, consequently, in relation to the technical and economic competitiveness explored, could lead to even higher gains when also including the potential ecological benefits these modules could deliver.

Nevertheless, whether liquid-filled, L-F panels are an economic alternative to conventional panels today is an open question. It is probable that a single liquid-filled panel can be assembled for the same cost as assembling many similar PV modules in a conventional approach, with the costs of solar cells, filling agent, and custom conductive backsheet remaining high. The panel, similar to emerging technologies such as thin and powerful back-contact ZEBRA cells as well as conductive backsheets, is still categorized as a niche product until it gains more traction in the PV market. Until then, this results in an expensive product for the solar industry. The high production cost and the yet unproven long-term reliability compared to laminated panels can be offset in the long run by their high value recyclability. The absence of long-term studies to ensure the reliability of this alternative design to laminated panels is noteworthy. Nevertheless, there is a positive confidence in the lifespan of L-F modules, particularly due the potential advancement of encapsulation strategies aimed at reducing degradation rates, along with the implementation of recovery methods contributing to the circular economy [100].

Further research and development should be undertaken to validate and refine the accuracy of the results achieved in this study. Deeper product-process research must be conducted to better understand the level of difficulty in these identified and explored barriers, mainly associated to the non-standardized processes, such as dispensing, soldering, and module filling. The latter is a very novel process in the solar industry, never studied before at any production scale. Without thorough product-process research and testing, there is no precise definition of the system type, its components, and parameters to be selected.

8.2 Future Outlook

Research on manufacturing L-F PV modules is innovative and previously unexplored. This report serves as an opening for future study and as a potential reference for setting up a PV production line. To successfully overcome encountered challenges and optimize manufacturing lines for PV modules in the future, the following research pathways should be pursued.

At the product level:

- A reliable adhesive material at the CB/rear glass interface with short lead and curing times.
- Proper selection of each module component and material, compatible with entities in contact with. More focus is on crucial materials such as solder pastes and liquid fillers. Regarding the latter, it is essential to conduct experiments or simulations to determine the precise type of fluid (e.g., silicone oils or synthetic esters) by blending viscosity and refractive properties to best suits the specific setup and requirements. Additionally, factors such as compatibility with panel materials should be considered to optimize light transmission at the lowest cost.
- Lowering the material cost of the end-product to comply with potential entry market requirements for L-F modules.

- Re-analysis of edge seal materials and their dimensioning under different liquid fillers to minimize module degradation over time. Barriers with sensors for moisture detection could optionally be integrated. According to the study from [108], the width of the PIB primary seal was 8 [mm] while the width of the secondary, silicone seal varied between 10 [mm] and 12 [mm], which differs from the metrics given for this study project. Similarly, for both durability and appearance considerations, the dual silicone/PIB seals could alternatively be backed by stiffer seals including aluminium.
- Product and process improvements and milestones must be demonstrated over time, such as panel rigidity, encapsulation, efficiency, degradation, and thermal management.

At the process level:

- Enhanced flexibility is necessary to explore alternative module components and assembly methods beyond the adoption of conductive backsheets for module interconnection, all while maintaining low manufacturing costs. One major challenge lies in the electrical interconnection of cells and modules. For instance, it is essential to have the option to use either front-back contact or back-contact solar cells by employing different interconnection methods than the innovative CB and evaluating the associated trade-offs. This includes considering the use of a standard stringer machine with embedded cell spacer parts and ribbon-based connections for electrical connections. Alternatively, employing an edge connector integrated into an ECA stringer with paste deposition or printing the ECA foil and applying low-temperature solder throughout the panel. Similarly, flexibility in the adoption of different IBC cell architectures is crucial for understanding the consequences reflected in manufacturing. For instance, it is important to determine which deposition and soldering methods could be advantageous in that case. Understanding the benefits and drawbacks in manufacturing when using classic tabbing & stringing versus edge connectors assembly is also essential.
- Consider incorporating additional processes that align closer to those used in traditional panel manufacturing, with new equipment models designed to have a reduced technical as well as economic impact on manufacturing.
- Explore methods for integrating in-line disassembly stations to implement repair/refurbishment strategies within the assembly line investigated. Additionally, consider assessing lines of different scales than those explored in this study.
- The inner frame is a core part of L-F modules, a distinguished and indispensable component for scalability. It is therefore equally important to investigate their integration into production line in terms of their manufacturing via milling or moulding process as well as its assembly into the PV module.
- If edge-tailed junction boxes become the mainstream choice in the PV market at more affordable unit prices than today, there will be an opportunity to build a tailor-made and integrated junction box (JB) with module filling becoming more realizable (Expert input: *member of Valoe*). The same openings might be used for the filling. The fluid agent should be able to be dispensed through one clip and sealed straight after. This would be more feasible if the filling agent is in liquid form. On the contrary, sealing gas-tight from the JB is not standard at all. Furthermore, ensuring proper sealing of the module on both sides, for the inflow bore for injection and outflow bore air extraction, may be very challenging. The benefit is that JB attachment, potting, and closing, as well as filling and sealing operations, can be performed within the same workstation, resulting in a more compact manufacturing layout.
- Process speed and quality milestones will have to be set later to demonstrate the capabilities of the technology and newly module architecture (such as minimal and maximum processing time, overlap steps for PIB and silicone) to ensure a uniform deposition of the sealants and thus quality output of the product while maximizing throughput. Each module will have to be closely inspected for edge seal uniformity, PIB and silicone overlapping, and overall manufacturing quality.

References

[1] J. A. Tsanakas, A. van der Heide, T. Radavičius, J. Denafas, E. Lemaire, K. Wang, J. Poortmans, E. Voroshazi, *Towards a circular supply chain for PV modules: Review of today's challenges in PV recycling, refurbishment, and recertification* (**2019**), DOI: 10.1002/pip.3193

[2] R. Deng, Y. Zhuo, Y. Shen, *"Recent progress in silicon photovoltaic module recycling processes"*, Resources, Conservation & Recycling 187 (**2022**) 106612

[3] E. El-Khawad, D. Bartkowiak, K. Kümmerer, *Improving the end-of-life management of solar panels in Germany*, Renewable and Sustainable Energy Reviews 168 (**2022**) 112678

[4] Solar Mag, *Maxeon Solar Cells: An Illustrative Guide to Sunpower's Branded Solar Cell Technology* (**2022**), https://solarmagazine.com/solar-panels/maxeon-solar-cells/

[5] SU.RE.CO, Sustainability & Resilience, (**2021**), https://www.su-re.co/post/linear-recycling-and-circular-economy

[6] M. Woodhouse, B. Smith, A. Ramdas, R. Margolis, Crystalline Silicon Photovoltaic Module Manufacturing Costs and Sustainable Pricing: 1H **2018** Benchmark and Cost Reduction Road Map, National Renewable Energy Laboratory (NREL), https://www.nrel.gov/docs/fy19osti/72134.pdf

[7] K. Hartman, *Final Technical Report*, OSTI.GOV (**2019**), DOI: https://doi.org/10.2172/1494794

[8] ECOPROGETTI srl, *What is the raw material that composes a photovoltaic module?* (**2014**), https://ecoprogetti.com/the-structure-of-photovoltaic-module/

[9] SINO VOLTAICS, *Double Glass Solar Panels: Design and Advantages*, https://sinovoltaics.com/learning-center/solar-panels/double-glass-solar-panels/

[10] H. Schoot, P. Maccario, R. Kopecek, *Back-Contact's Move to the Front*, DSM Advanced Solar (**2020**)

[11] ISSOL ARCHITECTURE-BIPV, *issol.eu*, http://www.issol.eu/wp-content/cache/page_enhanced/www.issol.eu/_index.html_gzip

[12] SONNENSTROM FABRIK, DRIVER OF INNOVATION FOR Glass/Glass solar modules (2024), https://www.sonnenstromfabrik.com/en/glass-glass/

[13] A. Sinha D. B. Sulas-Kern, M. Owen-Bellini, L.Spinella, S. Ulicna, S. A. Palaez, S. Johnston, L. T. Schelhas, *Glass/Glass photovoltaic module reliability and degradation: a review,* J. Phys. D: Appl. Phys.(**2021***),* 54 413002, DOI: https://doi.org/10.1088/1361-6463/ac1462

[14] *MATERIAL STRUCTURE OF PHOTOVOLTAIC MODULES*, https://www.raytron.co/material-structure-of-photovoltaic-modules/

[15] XINOLOGY, Photovoltaic EVA Encapsulation Film Production line, http://www.xinology.com/Glass-Processing-Equipments-Supplies-Consumables/glass-photovoltaic/photovoltaic-encapsulation-EVA-film-production-line/overview/introduction.html

[16] ECOPROGETTI srl, SPECIALIST IN PHOTOVOLTAIC PRODUCTION PROCESS, Catalogue (**2023**), https://ecoprogetti.com/

[17] S. K. Kurinec, Silicon Solar Photovoltaics: *Slow Ascent to Exponential Growth, Women in Engineering and Science* (WES) (**2022**), pp. 221-243, DOI: 10.1007/978-3-030-91546-9_15

[18] R. Kopecek, J. Libal, J. Lossen, V. D. Mihailetchi, H. Chu, C. Peter, F. Buchholz, E. Wefringhaus, A. Halm, J. Ma, L. Jianda, G.Y onggang, Q. Xiaoyong, W. Xiang, D. Peng, in *Photovoltaic Specialists Conference (PVSC), 47th IEEE **(2020)*** (pp.1008-1012), DOI: 10.1109/PVSC45281.2020.9300503

[19] M. Spath, P. C. de Jong, I. J. Bennett, T. P. Visser, J. Bakker, *A NOVEL MODULE ASSEMBLY LINE USING BACK CONTACT SOLAR CELLS, (**2008**)* 33rd IEEE Photovolatic Specialists Conference (PVSC), DOI: 10.1109/pvsc.2008.4922528

[20] M. K. Mat Desa, S. Sapeai, A. W. Azhari, K. Sopian, M. Y. Sulaiman, N. Amin, S.H. Zaidi, Silicon back contact solar cell configuration: A pathway towards higher efficiency, Renewable and Sustainable Energy Reviews 60, (**2016**), pp. 1516-1532, DOI: https://doi.org/10.1016/j.rser.2016.03.004

[21] D. Shangguan, FLEXTRONICS, *Advanced Technology Group - Solar PV Module Assembly* (**2011**)

[22] A. Barin, L. Hirvonen, M. Osborne, *FuturaSun brings European n-type mono IBC 'ZEBRA' panel technology to market* (**2020**), https://solar-media.s3.amazonaws.com/assets/Pubs/Webinars/FuturaSun/FuturaSun-Zebra-PV%20Tech%20webinar%20-%20Slides%20191120.pdf

[23] D. J. Tyler, *17-Joining of wearable electronic components*, Joining Textiles (**2013**), pp. 507-535, DOI: https://doi.org/10.1533/9780857093967.4.507

[24] P. de Jong, *Achievements and challenges in crystalline silicon back-contact module technology,* Energy Research Centre of the Netherlands (ECN), Petten, The Netherlands

[25] N. Chen, *Development of High-efficiency and Sustainable Back Contact Solar Cells*, Ph.D. thesis, Delft University of Technology, The Netherlands (**2023**), DOI: 10.4233/uuid:28cb2308-d63e-44ec-b785-326c0c4d12c5

[26] M. Hutchins, Weekend read: As simple as IBC (**2023**), https://www.pv-magazine-australia.com/2023/03/25/weekend-read-as-simple-as-ibc/

[27] ISC Module Technology- Research for a sunny future, (ISC Konstanz), https://isc-konstanz.de/en/isc-module-technology/

[28] F. Gerardus, H. van Duijnhoven, R. Janssen, I. Bennett, *Electro-Conductive Backsheet For Solar Cell Modules* (**2019**), https://patentimages.storage.googleapis.com/1c/2f/de/96ac3c47cfcdc1/WO2019076913A1.pdf

[29] S. Xie, *What is MWT Back Contact Technology for solar panels?* (**2023**), https://www.linkedin.com/pulse/what-mwt-back-contact-technology-solar-panels-shelly-xie/

[30] M. Mahajan, *Developing Modular Interconnection Techniques for Disassemblable PV Modules*, Master's Thesis (**2023**), Delft University of Technology, The Netherlands. https://www.biosphere.solar/wp-content/uploads/2024/02/Mihir_Mahajan_MSc_Thesis__Development_of_Modular_Interconnection_Techniques_for_Disassemblable_PV_Modules.pdf

[31] Ooitech.solar, *Solar Panel Production Line,* https://www.ooitech.solar/Solar-Panel-Module-Production-Line/Manufacturing-Solar-Panels-5MW-30MW-Semi-Automatic-Solar-Panel-Production-Lines-Solar-Panel-Making-Machine-r-41.html

[32] ECOPROGETTI srl SPECIALIST IN PHOTOVOLTAIC PRODUCTION PROCESS, Datasheet laminators, https://ecoprogetti.com/products/laminators/

[33] ConfirmWare Technology Co., Ltd., *300MW PV Module Production Line* (**2023**), (Internal document)

[34] ECOPROGETTI srl SPECIALIST IN PHOTOVOLTAIC PRODUCTION PROCESS, Datasheet glass layup system (ECOLAYUP 100), https://ecoprogetti.com/wp-content/uploads/2016/11/Datasheet_ECOLAYUP-100.pdf

[35] Abloomax LLC, Solar Panel Production Lines, https://www.abloomax.com/solar-panel-production-lines

[36] *mondragon-assembly.com*, https://www.mondragon-assembly.com/solar-automation-solutions/turnkey-lines-for-pv-module-manufacturing/

[37] ConfirmWare Technology Co., Ltd., *Turnkey Solar Panel Production Lines*, https://en.confirmware.com/product-category/solar-panel-production-line/

[38] T. Mebmer, F. Demiralp, A. Halm, "*Low-cost semi-automated assembly unit for small size back contact modules and low-cost interconnection approach"*, 6th Workshop on Metallization and Interconnection for Crystalline Silicon Solar Cells, International Solar Energy Research Center - ISC Konstanz (**2016**)

[39] A. K. Shnatmann, F. Schoden, E. S. Hellkamp, in "*Sustainable PV Module Design—Review of State-of-the-Art Encapsulation Methods"*, Institute for Technical Energy Systems (ITES), Sustainability **2022**, 14(16), 9971, https://doi.org/10.3390/su14169971

[40] A. Halm, *Zebra manual interconnection guide, ISC research for a sunny future,* International Solar Energy Research Center (ISC Konstanz).

[41] AGC Solar Glass, Factsheet SunMax Premium Range, https://www.agc-solar.com/product-solutions/

[42] SPIC Solar, datasheet ZEBRA IBC M6 Cell.

[43] Omnexus, The material selection platform: *Comprehensive Guide on Acrylonitrile Butadiene Styrene (ABS),* https://omnexus.specialchem.com/selection-guide/acrylonitrile-butadiene-styrene-abs-plastic

[44] Tensile Behavior of Acrylonitrile Butadiene Styrene at Different Temperatures". In: *Advances in Polymer Technology* 2020 (**2020**), pp. 1–10. issn: 0730-6679. doi: 10.1155/2020/8946591

[45] Anand B. Balaji et al., "Natural and synthetic biocompatible and biodegradable polymers". In "*Biodegradable and Biocompatible Polymer Composites"*. Ed. by Navinchandra Gopal Shimpi. Woodhead Publishing Series in Composites Science and Engineering. Woodhead Publishing, 2018, pp. 3–32. isbn: 978-0-08-100970-3. doi: https://doi.org/10.1016/B978-0-08-100970-3.00001-8

[46] MASTERBOND, ADHESIVES | SEALANTS | COATINGS, *UV Curable Systems*, https://www.masterbond.com/products/uv-curable-systems?matchtype=p&network=g&device=c&adposition=&keyword=uv%20glue&gad_source=1&gclid=CjwKCAiArfauBhApEiwAeoB7qOAVq954eZV82-ClrtyRd88wdcTfnk-nqk7SSoFV9xJkvPKbTOv9khoCuDAQAvD_BwE

[47] Nordson EFD, *Solder Selection Guide*, https://www.nordson.com/en/divisions/efd/resources/solder-selection-guide

[48] MacDermid Alpha, ELECTRONIC SOLUTIONS, Technical bulletin & Datasheet: *ALPHA CVP-520 SOLDER PASTE*, *Low Melting point, No-Clean, Lead-Free, Zero Halogen*.

[49] Hoganas, *Filler metals | Processing | Application development*, Technical Handbook (**2023**).

[50] P.-C. Hsiao, A. Lennon, *Backsheet Metallization of IBC Silicon Solar Cells*, The School of Photovoltaics and renewable Energy Engineering.

[51] SYSTEM SOLUTIONS FOR THE SOLAR INDUSTRY, *Adhesives and Sealants for Photovoltaic and Solar Thermal Applications*, (kommerlinguk.com)

[52] Sika, SEALING AND BONDING IN FACADES THE COMPETENCE COMPENDIUM, https://nor.sika.com/dam/dms/global-industry/l/BRO-Facade-Systems-Specification-Guide-en.pdf

[53] Kömmerling, *Thermoplastic Spacer (Warm Edge System),* Datasheet: Ködispace 4SG.

[54] E. Saint-Sernin, R. Einhaus, K. Bamberg, P. Panno, in "*INDUSTRIALISATION OF APOLLON SOLAR'S NICE MODULE TECHNOLOGY",* (Apollon Solar, Vincent Industrie).

[55] M. Molinaro, *How Edge Sealants Can Improve Performance in Crystalline Modules,* ASI, ADHESIVES & SEALANTS INDUSTRY (**2023**), https://www.adhesivesmag.com/articles/100246-how-edge-sealants-can-improve-performance-in-crystalline-modules

[56] TRAXLE, Inova Solar, PV PANELS RENOVATION AND REPAIR: *Advantages of silicone gel encapsulant,* https://www.solar-trackers.com/silicone-gel-technology/polysiloxane-advantages

[57] OTTOCHEMIE, *The neutral-curing 1-component silicone sealant and adhesive for industrial purposes*, Technical Datasheet: Novasil®S 56

[58] S. S. Joshi, A. S. Dhoble, *Experimental investigation of solar photovoltaic thermal system using water, coconut oil and silicone oil as spectrum filters*, J Braz. Soc. Mech. Sci. Eng. 39, 3227-3236, (**2017**), DOI: 10.1007/s40430-017-0802-0

[59] Y. Wang, Z. Fang, L. Zhu, Q. Huang, Y. Zhang, Z. Zhang, *The performance of silicon solar cells operated in liquids*, Applied Energy 86, 7-8 (**2009**) pp.1037-1042, DOI: https://doi.org/10.1016/j.apenergy.2008.08.020

[60] MIVOLT, *LIQUID IMMERSION COOLING, DFK Dielectric Liquid*, Technical Brochure.

[61] Gelest, *SILICONE FLUIDS: STABLE, INERT MEDIA, Engineering, and design properties for: heat transfer, mechanical, lubrification, smart fluid, dielectric and optical applications*, Property Profile Guide, www.gelest.com

[62] Wind & Sun, *Labels for Solar PV Systems*, https://www.windandsun.co.uk/collections/labels-for-solar-pv-systems

[63] TECHNOFORM, *Insulating glass performance at its best*, https://www.technoform.com/en/solutions/insulating-glass-edge-bond/hybrid-warm-edge-spacers

[64] Clean energy technology observatory. European commission. Photovoltaics in the EU, *Status report on technology development, trends, value chains and markets* (**2022**), DOI: https://doi.org/10.2760/812610

[65] M. Späth, P. C. de Jong, I. J. Bennett, T. P. Visser, J. Bakker, A.J. Verschoor, *FIRST EXPERIMENTS ON MODULE ASSEMBLY LINE USING BACK-CONTACT SOLAR CELLS,* (ECN-Solar Energy, TTA-Eurotron).

[66] TE connectivity, *Solarlok PV BAR Junction Box Assemblies*. Application Specification. 114-137167, (**2019**) Rev. E2

[67] REOO Technology Co., Ltd., *Customized Solar Panel Production Line 500MW Capacity, 99% Automation*, Specifications and Quote: V20230909 (**2023**), (Internal document).

[68] Nordson EFD, Technical datasheet: *797PCP Series Progressive Cavity Pump; Volumetric dispensing for industry-leading process control* (Internal document).

[69] TECHCON SYSTEM, Technical Datasheet:*TS8100 Series, Progressive Cavity Pump* (Internal document).

[70] EKRA Screen printing technologies, 1) *EKRA-X4-Brochure*, 2) *EKRA-X6-Brochure* https://qysurplus.com/wp-content/uploads/2023/02/EKRA-X4-Brochure.pdf and https://islandsmt.com/wp-content/uploads/2017/05/X6_13_05_09_E.pdf

[71] *Metallization, thermal spray solutions,* https://www.metallisation.com/wp-content/uploads/2020/11/Met-Cell-Equipment-Spec-Email.pdf

[72] H. Schmidhuber, S. Klappert, J. Stollhof, G. Erfurt, M. Eberspacher, R. Preu, (Fraunhofer ISE, Fraunhofer IPT, TRUMPF Laser GmbH + Co. KG, Deutshe Solar AG, Solar Factory GmbH), *"LASER SOLDERING – A TECHNOLOGY FOR BETTER CONTACTS?",* in *20th European Photovoltaic Solar Energy Conference (2005), Barcelona, Spain*, https://publica-rest.fraunhofer.de/server/api/core/bitstreams/f5957b4a-1ab5-4d39-84c9-ed4e4d2e360e/content

[73] Ajax TOCCO, Technical Brochures: "*Induction Heating, For Electric Motor Manufacturing Applications and Power Supply TOCCOtron AC 5kW, 10kW",* (**2020**), (Internal documents).

[74] APOLLO SEIKO, *Product Catalog 2023-2024*, https://www.selecs.de/wp-content/uploads/2024/02/2023-2024-Apollo-Seiko-Product-Catalog.pdf

[75] Z. Yang, L. Li, W. Chen, X. Jiang, Y. Liu, *Numerical and experimental study on laser soldering process of SnAgCu lead-free solder*, Materials Chemistry and Physics 273 (**2021**) 125046, DOI: http://dx.doi.org/10.1016/j.matchemphys.2021.125046

[76] P.M. Beckett, A. R. Fleming, J. M. Gilbert, D. G. Whitehead, *The laser in manufacture - its use in the soldering of electronic assemblies,* Sage Journals 21, 1 (**1999**), DOI: https://doi.org/10.1177/014233129902100101

[77] WOLF, Brochure: *Laser Soldering with High-Power Diode Laser*, https://www.orion-industry.com/robot_laser/Brochure%20Laser%20Soldering.pdf

[78] Teamtechnik_Solar, Technical Datasheet: Stringer TT4000 i8 ECA. *Advanced adhesive technology for high-performance crystalline solar cells* (Internal document).

[79] XINOLOGY, *Hot Melt Butyl IG Sealant – Features & Spec,* (Model: HMB), http://www.xinology.com/Glass-Processing-Equipments-Supplies-Consumables/glass-sealing/hot-melt-butyl-ig-sealant/features-spec.html

[80] WAGNER REINHARDT-TECHNIK, TECHVICE, SOLUTIONS & CONSULTANCY, Reference: MM - 06 November **2023** - Budget quote nr.: 23.042 (Internal document).

[81] ECOPROGETTI srl, *Ecomultistation*, https://ecoprogetti.com/product/eco-multistation/

[82] Abloomax LLC, *the processing step of PIB gluing for double glass solar panel*, (**2023**), (Internal document).

[83] WAGNER REINHARDT-TECHNIK, Brochure: *Counti Flow series – Gear Metering systems. One system – Individual applications*, (**2023**), (Internal document).

[84] Abloomax LLC, *Double Glass Solar Panel PIB Gluing Machine*, (**2023**), (Internal document).

[85] J. Thompson, M. Putzer, N. Gonsior, C. Miller, S*ilicone Encapsulation Enhances Durability, Efficiency, and Enables New PV Cell and Modules Technologies*, National Renewable Energy Laboratory (NREL), Silicone Encapsulation Enhances Durability, Efficiency, and Enables New PV Cell and Modules Technologiesv (nrel.gov)

[86] Meter Mix, Hilger & Kern group, *METER – MIX -DISPENSE, DOPAG: 1K glue Line SOLUTIONS FOR APPLICATION OF 1K ADHESIVES AND SEALANTS*, (**2023**), (Internal document).

[87] P. Trpkovski, *Method for filling insulated glass units with insulating gas,* United States Patent: 6158483 (**2000**), https://patentimages.storage.googleapis.com/44/c4/e5/49a7408c2eb8c0/US6158483.pdf

[88] ROMACO, *Oftalmica liquid filling machine,* https://www.romaco.com/products/product-details/oftalmica?gad_source=1&gclid=Cj0KCQjw-r-vBhC-ARIsAGgUO2CHBJ_FZV2Zmg6x5UssQ-X2zjdeLcH1Ospjy4Kq6trTUn_JAUl-Pl8aAu44EALw_wcB

[89] WE grid products, Technical datasheet: *SF_6 gas solutions* https://www.wika.com/media/Data-sheets/SF6-gas/Service-Equipment/ds_sp6317_en_co.pdf

[90] Teamtechnik Solar, *Brochure & Datasheet: STRINGER TT2100* i8 (Internal document).

[91] ECOPROGETTI srl SPECIALIST IN PHOTOVOLTAIC PRODUCTION PROCESS, Datasheet framing machines, https://ecoprogetti.com/products/trimming-framing/

[92] ECOPROGETTI srl SPECIALIST IN PHOTOVOLTAIC PRODUCTION PROCESS, Datasheet cutting machines, https://ecoprogetti.com/products/cutting-machines/

[93] teamtechnik_Solar, *STRINGER TT2100 i8*, https://www.teamtechnik.com/en/new-energy/stringer-systems/solar-stringer-tt2100-i8

[94] UViTRON INTERNATIONAL, *SkyBeam UV LED Curing System: Brochure*

[95] ABLOOMAX LLC, For and on behalf of REOO IMPORT & EXPORT CO. LIMITED: *Quotation PIB Gluing Machine* (**2023**), (Internal Document).

[96] UVITRON INTERNATIONAL, *Skybeam UV cure equipment*, QUOTE:8416, https://www.uvitron.com/products/uv-spot-systems/skybeam/

[97] M. Mitag, U. Einer, T. Neff, (ISE Fraunhofer, Bystronic glass), "*TPEDGE: PROGRESS ON COST-EFFICIENT AND DURABLE EDGE-SEALED PV MODULES"*, in 33th European PV Solar Energy Conference and Exhibition (**2017**), Amsterdam, The Netherlands.

[98] MIVOLT, *LIQUID IMMERSION COOLING, DFK Dielectric Liquid* (**2023**), Quotation (Internal Document).

[99] Polysobutylene, https://amp.chemicalbook.com/ChemicalProductProperty_EN_CB8147859.htm

[100] A. K. Schnatmann, F. Schoden, E. Schwenzfeier-Hellkamp, *Sustainable PV Module Design—Review of State-of-the-Art Encapsulation Methods, Sustainability* (**2022**), 14(16), 9971, DOI: https://doi.org/10.3390/su14169971

[101] XINOLOGY, *Solar Module Production Line: Solar Module Laminating & Inspection*, Solar Module Production Line - Features & Specs - Solar Module Laminating & Inspection (xinology.com)

[102] E. Saint-Sernin, R. Einhaus, K. Bamberg, P. Panno, *INDUSTRIALISATION OF APOLLON SOLAR'S NICE MODULE TECHNOLOGY,* (Apollon Solar, Vincent Industrie).

[103] S. Ellis, L. Maple, T. Shimpi, G. Tamizhmani, W. Sampath, A. Pavgi, K. L. Barth, *Demonstration of Non-lamination encapsulation techniques for thin film solar modules,* 47th IEEE Photovoltaic Specialists Conference (PVSC) (**2020**), DOI: 10.1109/PVSC45281.2020.9300665

[104] ECOPROGETTI srl SPECIALIST IN PHOTOVOLTAIC PRODUCTION PROCESS, Gel *content kit: monitor the lamination process*, https://ecoprogetti.com/product/gel-content-kit/

[105] K. Agroui, *Indoor and Outdoor Characterizations of Photovoltaic Module Based on Multicrystalline Solar Cells*, Silicon Technology Development Unit (UDTS), Energy Procedia 18 (**2012**) pp. 857 – 866.

[106] J. Dupuis, E. Saint-Sernin, K. Bamberg, R. Einhaus, E. Pilat, A. Vachez, D. Bussery, *IEC CERTIFICATION AND EXTENDED AGEING TEST OF NICE MODULES,* (Apollon Solar, Cea-Ines, Vincent Industrie).

[107] R. Einhaus, F. Madon, J. Degoulange, K. Wambach, J. Denafas, F. R. Lorenzo, S. C. Abalde, T. D. Garcia, A. Bollar, *Recycling and Reuse potential of NICE PV-Modules*, Apollon Solar & UAB Soli Teck R&D.

[108] M. Cwyl, R. Michalczyk, S. Wierzbicki, *Polyisobutylene and Silicone in Warm Edge Glazing Systems – Evaluation of Long-Term Performance*, Materials **2021**, 14, 3594, DOI: https://doi.org/10.3390/ma14133594

[109] H. Sheykin, FINMODELSLAB, Sun-Powered Mission: Startup Costs for Solar Panel Production (**2023**), https://finmodelslab.com/blogs/startup-costs/solar-panel-manufacturing-startup-costs

[110] IRENA, IEA-PVPS, **2016**, *End-of-life management: solar photovoltaic panels*.

[111] ITRPV, 2021. International technology roadmap for photovoltaic (ITRPV) **2020** results.

[112] ITRPV, 2019. International technology roadmap for photovoltaic (ITRPV) **2018** results.

[113] EUROTRON. *PV-MODULE Technology*, https://www.eurotron.com/technology/

[114] SolarReviews (**2023**), https://www.solarreviews.com/blog/maxeon-solar-panels-expert-review

[115] EUROTRON. *PV-MODULE Equipment,* https://eurotron.com/pv-module-equipment/

[116] Valoe's PV Modules, https://valoe.com/solar-modules

[117] DXC Technology, *The circular economy: What it is, why it matters now, and how it can help your organization,* https://dxc.com/uk/en/cp/intelligence_delivered/perspectives/blogs/the-circular-economy-what-it-is-why-it-matters-now-and-how-it-can-help-your-organisation

[118] Slocable Products (*Split Junction Box for Solar Panel, PV cable assembly),* https://www.slocable.com.cn/products/

[119] STAUBLI, *Original MC4 Renewable Energy | Solar Photovoltaics,* https://www.staubli.com/content/dam/spot/SOL-MC4-11014112-en.pdf

[120] ViscoTec, *FILLING PUMPS,* https://www.viscotec.de/en/products/filling-pumps/

[121] THERMOSEAL GROUP, *Machinery & Parts,* https://www.thermosealgroup.com/products/machinery-parts

[122] Ayumi Industry, *LC filling equipment* http://www.ayumi-ind.co.jp/en/products/vacuum_equipment/ekisyoutyuunyuusouti/

[123] SOLAR MAGAZINE, *IBC Solar Cells: Definition, Benefits, vs. Similar Techs,* https://solarmagazine.com/solar-panels/ibc-solar-cells/

[124] Sunstore, *MC4 type solar connectors,* https://www.sunstore.co.uk/product/mc4-solar-connectors-male-female/

[125] Westech, https://westech-pv.com/Solar-cable-4mm-and-6mm-red-black-meter-length

[126] EUROSTAT **2023**, https://ec.europa.eu/eurostat/cache/infographs/energy_prices/enprices.html?geos=&product=6000&consumer=HOUSEHOLD&consoms=KWH_LT1000&unit=KWH&taxs=I_TAX,X_TAX,X_VAT&nrg_prc=NETC,NRG_SUP,OTH,TAX_CAP,TAX_ENV,TAX_NUC,TAX_RNW,VAT&currency=EUR&language=EN&detail=0&component=0&order=DESC&dataset=nrg_pc_204&time=2023-S1&modalOption=0&chartOption=0&precision=1&modalOpen=0&modal=0&modalLineOption=0

A

Appendix A: Insights on Laminators

The laminator is used for vacuuming, heating, encapsulating, pressing, and curing assembled solar modules. When the encapsulant film melts under vacuum, it starts to flow freely, filling all spaces inside the PV panel. As a result, all composite materials are firmly encapsulated and bonded into one cohesive body. This feature protects the cells, holding them in place and ensuring the panel's longevity [15].

During the lamination process, sheets of encapsulant polymerize by transitioning from a solid to a liquid state and then, with the rise in temperature and pressure, into a gel. This gel must set correctly and with adequate quality to ensure that the layers of the module remain sealed over time, thereby securing the module's lifetime [104]. The encapsulant film must shrink when heated in the initial laminating chambers as well as in the final step of the cooling press. Achieving a low shrinkage rate prevents the risk of damage to solar cells. However, if the shrinkage rate is too slow, it can lead to poor production capacity. Therefore, finding an optimum speed against the shrinkage rate is crucial [15].

Polymeric layers comprise either thermoplastic or thermosetting polymers. Thermoplastics become pliable and mouldable above specific temperatures and solidify upon cooling, while thermosetting polymers form irreversible chemical bonds during the curing process. Thermosetting materials do not melt but decompose and do not reform after cooling [28]. The solar module encapsulant agents, upon heating, are initially thermoplastic and then turn thermoset during the curing process.

Laminator solutions can be configured differently according to solar module types and production volumes, in terms of curing size, single or multiple stages, and the presence of belts and/or buffers.

The laminating cycle, including heating, vacuum, curing, and cooling stages, is identical regardless of the laminator capacity. The degree of automation differs in the loading and unloading belt. Semi-automated machines require manual operation, resulting in most of the downtime [101]. Fully automated laminators have inlet and outlet conveyors as well as a high-temperature-resistant belt within the laminating area. The automated laminating cycle is monitored by an operator who can interact with the controlled PLC interface to achieve industrial automation. A user-friendly HMI touch display simplifies parameter settings. The cycle is classified based on curing time, which can be ultrafast, fast, or normal, on the encapsulant material used as well as on solar module architectures for instance squared, prismatic, double glass, transparent backsheet and flexible modules. [16]. Laminating stages and module productivity are presented in Figure A1.

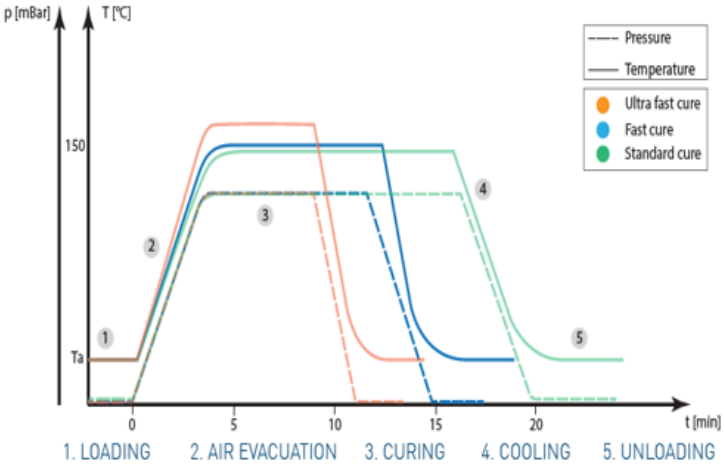

Modules/cycle	EVA 20'	EVA 15'	EVA 12'	POE 13'
3	9 mod/h	12 mod/h	15 mod/h	14 mod/h
4	12 mod/h	16 mod/h	20 mod/h	19 mod/h
5	15 mod/h	20 mod/h	25 mod/h	23 mod/h
3x2	18 mod/h	24 mod/h	30 mod/h	28 mod/h
4x2	24 mod/h	32 mod/h	40 mod/h	37 mod/h
5x2	30 mod/h	40 mod/h	50 mod/h	46 mod/h

Figure A1 - (**left**) Laminating cycles per step and curing times, (**right**) laminator productivities based on encapsulant type, [16].

Under standard curing, the heating plate temperature is set at 130°C, with a vacuum and press time of 12 [min]. For fast curing processes, the heating plate temperature is increased to 145°C, with vacuum and pressing, and

cooling time between 13-17 [min] [15]. To minimize the melting time of the lamination process, new fast-curing encapsulants that crosslink must be discovered.

Small and medium-sized laminators, with three or a maximum of four heating plates, are usually employed in production lines up to 100 [MW] capacity. Each plate is divided into three controllable zones heated with a uniformity of ± 2°C by electrical elements and complete with loading and unloading belts. Temperatures in each zone are independent to ensure a uniform gel content over the complete module surface [16].

High-capacity laminators typically contain five heating plates, accommodating five modules per cycle (batch). The cycle is divided into pumping and curing time to double the production capacity. Each level may also be stacked on top of each other, reducing space and increasing line throughput. According to Figure A1 the highest laminator capacity, with the use of EVA 12', reaches a production speed of 50 [module/h]. An overview of the different type of laminators is visualized in Figure A2.

Figure A2 - Visuals of laminator typologies and sizes. (*Adjusted from* [16]).

More and more laminated solar modules in G/G configuration are emerging. This is encouraged by the fact that the two glass sheets, when going through the three-chamber lamination process, have unrivalled strength. This time-consuming lamination process grants G/G modules the best protection against moisture, delamination, and bubble formation [12].

B

Appendix B: The Production Line of NICE Solar Modules

NICE module technology was introduced to overcome limitations of the state-of-the-art module encapsulation technology based on EVA lamination and to reduce the production costs of PV modules. From a production standpoint, this technology presents a simplified module assembly process since it allows for a complete inline operation that can be fully automated [102].

The pilot line depicted in Figure B1 was developed, manufactured, and put into operation at the beginning of 2008 by APOLLON SOLAR's partner VINCENT INDUSTRIES. This equipment will serve to validate the industrial feasibility of this technology. The line incorporates all necessary automated production stations without automatic loading and sorting [102].

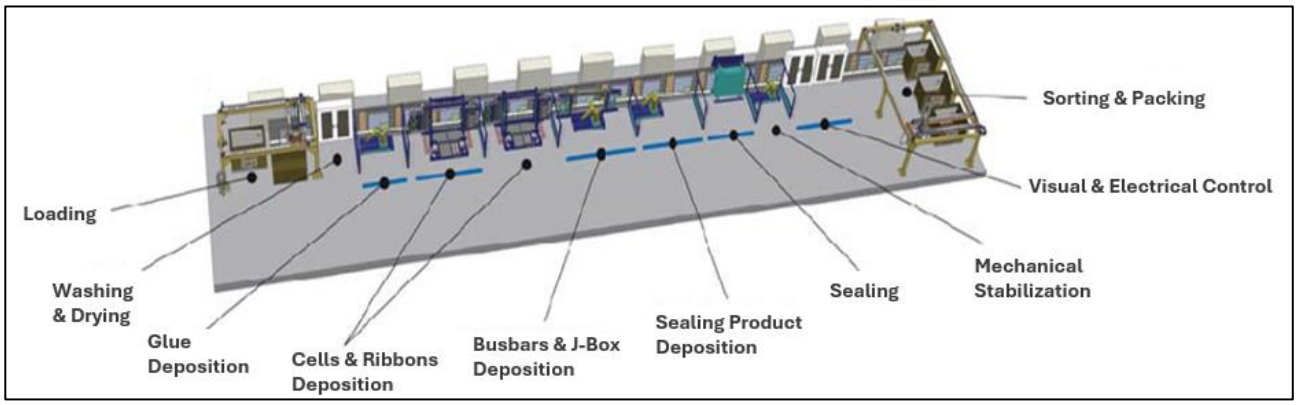

Figure B1 - Schematic drawing of a NICE production line: underlined units by blue bar form the operational pilot line, process flow is from left to right [102].

The first step consists of depositing the PIB material on the rear sheet, which comes ready to use. This refers to the metal sheet with the electrical insulating layer already deposited. The PIB sealing unit has two nozzles, one for the deposition of gluing stripes (for fixing cells, ribbons, busbars, and external connectors), and the other for the sealing line on the module perimeter. The different module components are automatically positioned by the robots. Front and rear glass sheets are transported into the pressing unit. Pressure control inside the module must be gradually and accurately applied, which is one of the key elements of the NICE technology. Indeed, on one hand, the forces applied to solar cells should be minimized to avoid cell breakage. The optimization of this internal under-pressure has been achieved through electroluminescence imaging and thermal cycling tests. Apart from pressing the module components together, the operation also involves flooding the module with neutral gas [102].

Important parts, such as the organic sealing material, have been further developed. A typical NICE module features at least a 10 [mm] wide sealing line, which is potentially sufficient to ensure humidity tightness for more than 30 years [102]. Three operators per shift for a 45 [MW/year] line. Due to its compactness, the required floor space is drastically reduced by a factor of 5 compared to a state-of-the-art module assembly line [102]. This prototype equipment demonstrated the feasibility of the process, with production costs and module parts costing less than 0.30 [€/W] [106].

Acknowledgements

First and foremost, I would like to thank my academic supervisor, Dr. Patrizio Manganiello, for guiding me through tasks, providing stimulating feedback, keeping my work on track. Again, my sincerest gratitude for your assistance, effort, and discussion of the progress of the academic research since the acceptance of the project proposal.

Special thanks go to the academic supervisor and leader of the IDE faculty, Prof. Ruud Balkenende, for accepting the supervision of this project. Always critical in tackling topics from a manufacturing perspective, providing insights into new challenges and concepts.

Thank you both for teaching me how to be concise and consistent, putting arguments into perspective while maintaining focus on the research objective.

My acknowledgement extends to the company supervisor and founder of Biosphere Solar, Siemen Brinksma, for his support and guidance throughout the project's duration, always available and open to discussing uncertainties on topics from both industrial and scientific perspectives. A big thank you to all Biosphere Team members for always being welcoming and respectful to each other.

I have consistently been given the freedom to pursue topics I deemed relevant within this thesis project experience, without pressure, and steered in the right direction when needed, learning how to overcome barriers, resulting in greater efficiency and performance.

The credit goes to all the input and support received from expert inputs of several companies, through meetings and feedback, giving me the chance to delve into topics and recommendations that I would hardly have accomplished through literature research or onsite experience.

It goes without saying that family, friends, and other close individuals have also indirectly contributed to bringing this academic journey to an end, and I am immeasurably thankful to all of you.

Antonio Pacifico
Delft, April 2024